UNIVERSIDADE FEDERAL DO PARANÁ

JOSÉ AUGUSTO POCHAPSKI

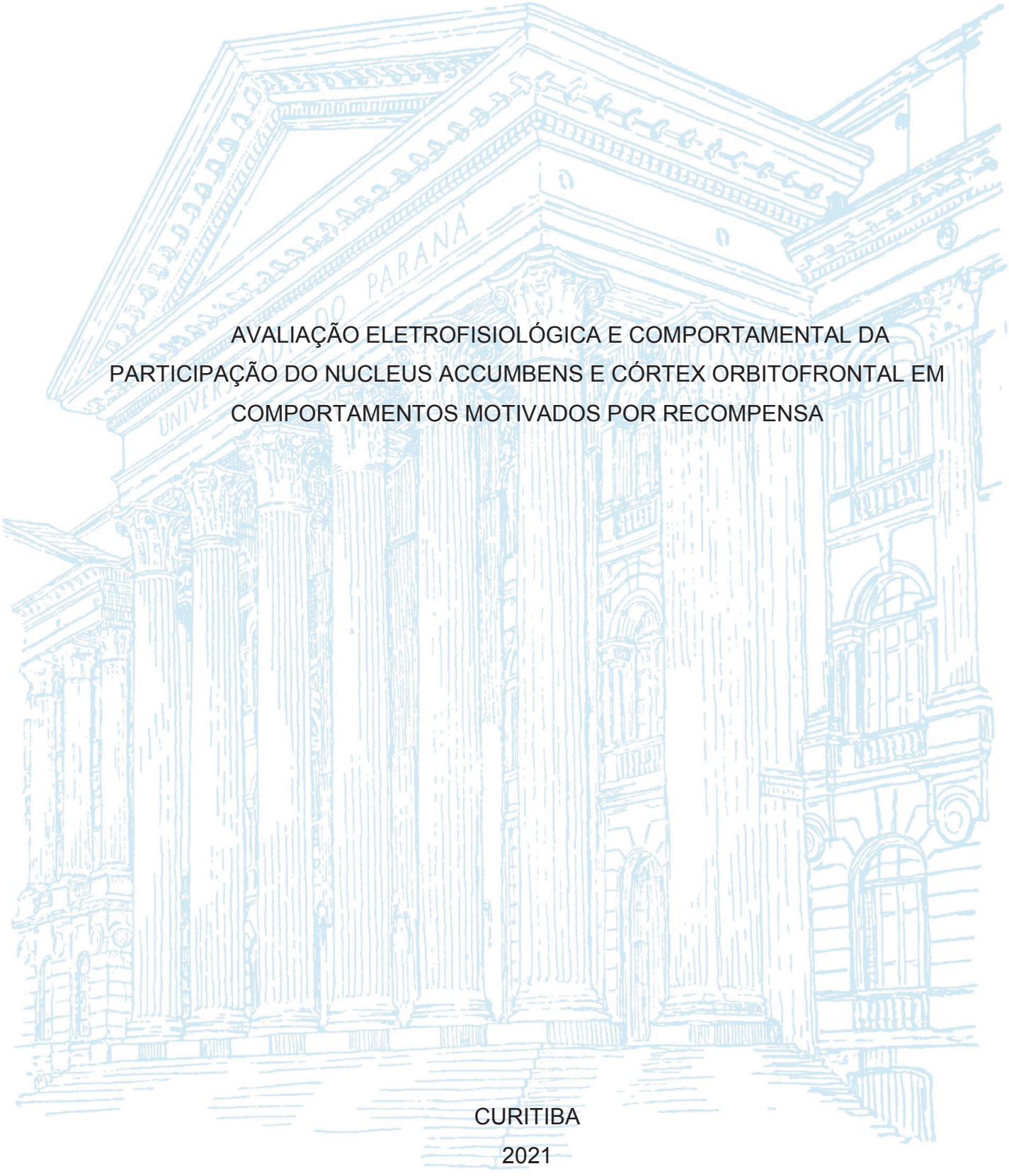

AVALIAÇÃO ELETROFISIOLÓGICA E COMPORTAMENTAL DA PARTICIPAÇÃO DO NUCLEUS ACCUMBENS E CÓRTEX ORBITOFRONTAL EM COMPORTAMENTOS MOTIVADOS POR RECOMPENSA

CURITIBA

2021

JOSÉ AUGUSTO POCHAPSKI

AVALIAÇÃO ELETROFISIOLÓGICA E COMPORTAMENTAL DA PARTICIPAÇÃO DO NUCLEUS ACCUMBENS E CÓRTEX ORBITOFRONTAL EM COMPORTAMENTOS MOTIVADOS POR RECOMPENSA

Tese apresentada ao curso de Pós-Graduação em Farmacologia, Setor de Ciências Biológicas, Universidade Federal do Paraná, como requisito parcial à obtenção do título de Doutor em Farmacologia.

Orientador: Prof. Dr. Cláudio da Cunha

CURITIBA

2021

Universidade Federal do Paraná
Sistema de Bibliotecas
(Giana Mara Seniski Silva – CRB/9 1406)

Pochapski, José Augusto
Avaliação eletrofisiológica e comportamental da participação do nucleus accumbens e córtex orbitofrontal em comportamentos motivados por recompensa. / José Augusto Pochaski. – Curitiba, 2021.
132 p.: il.

Orientador: Cláudio da Cunha.

Tese (doutorado) - Universidade Federal do Paraná, Setor de Ciências Biológicas. Programa de Pós-Graduação em Farmacologia.

1. Transtornos relacionados ao uso de substâncias. 2. Motivação. 3. Recompensa. 4. Núcleo accumbens. 5. Jovens – Consumo de álcool. I. Título. II. Cunha, Cláudio da, 1962-. III. Universidade Federal do Paraná. Setor de Ciências Biológicas. Programa de Pós-Graduação em Farmacologia.

CDD (22. ed.) 616.86

TERMO DE APROVAÇÃO

Os membros da Banca Examinadora designada pelo Colegiado do Programa de Pós-Graduação em FARMACOLOGIA da Universidade Federal do Paraná foram convocados para realizar a arguição da tese de Doutorado de **JOSÉ AUGUSTO POCHAPSKI** intitulada: **Avaliação eletrofisiológica e comportamental da participação do nucleus accumbens e córtex orbitofrontal em comportamentos motivados por recompensa**, sob orientação do Prof. Dr. CLAUDIO DA CUNHA, que após terem inquirido o aluno e realizada a avaliação do trabalho, são de parecer pela sua APROVAÇÃO no rito de defesa.

A outorga do título de doutor está sujeita à homologação pelo colegiado, ao atendimento de todas as indicações e correções solicitadas pela banca e ao pleno atendimento das demandas regimentais do Programa de Pós-Graduação.

CURITIBA, 26 de Fevereiro de 2021.

Assinatura Eletrônica
02/03/2021 11:57:47.0
CLAUDIO DA CUNHA
Presidente da Banca Examinadora

Assinatura Eletrônica
04/03/2021 12:09:30.0
FABIO CARDOSO CRUZ
Avaliador Externo (UNIVERSIDADE FEDERAL DE SÃO PAULO)

Assinatura Eletrônica
02/03/2021 10:47:36.0
ROBERTO ANDREATINI
Avaliador Interno (UNIVERSIDADE FEDERAL DO PARANÁ)

Assinatura Eletrônica
02/03/2021 11:58:57.0
RAINER KARL WILLI SCHWARTING
Avaliador Externo (PHILIPPS-UNIVERSITAT MARBURG)

ATA Nº296

ATA DE SESSÃO PÚBLICA DE DEFESA DE DOUTORADO PARA A OBTENÇÃO DO GRAU DE DOUTOR EM FARMACOLOGIA

No dia vinte e seis de fevereiro de dois mil e vinte e um às 09:00 horas, na sala Online via Microsoft Teams, Online via Microsoft Teams, foram instaladas as atividades pertinentes ao rito de defesa de tese do doutorando **JOSÉ AUGUSTO POCHAPSKI**, intitulada**: Avaliação eletrofisiológica e comportamental da participação do nucleus accumbens e córtex orbitofrontal em comportamentos motivados por recompensa**, sob orientação do Prof. Dr. CLAUDIO DA CUNHA. A Banca Examinadora, designada pelo Colegiado do Programa de Pós-Graduação em FARMACOLOGIA da Universidade Federal do Paraná, foi constituída pelos seguintes Membros: CLAUDIO DA CUNHA (UNIVERSIDADE FEDERAL DO PARANÁ), FABIO CARDOSO CRUZ (UNIVERSIDADE FEDERAL DE SÃO PAULO), ROBERTO ANDREATINI (UNIVERSIDADE FEDERAL DO PARANÁ), RAINER KARL WILLI SCHWARTING (PHILIPPS-UNIVERSITAT MARBURG). A presidência iniciou os ritos definidos pelo Colegiado do Programa e, após exarados os pareceres dos membros do comitê examinador e da respectiva contra argumentação, ocorreu a leitura do parecer final da banca examinadora, que decidiu pela APROVAÇÃO. Este resultado deverá ser homologado pelo Colegiado do programa, mediante o atendimento de todas as indicações e correções solicitadas pela banca dentro dos prazos regimentais definidos pelo programa. A outorga de título de doutor está condicionada ao atendimento de todos os requisitos e prazos determinados no regimento do Programa de Pós-Graduação. Nada mais havendo a tratar a presidência deu por encerrada a sessão, da qual eu, CLAUDIO DA CUNHA, lavrei a presente ata, que vai assinada por mim e pelos demais membros da Comissão Examinadora.

CURITIBA, 26 de Fevereiro de 2021.

Assinatura Eletrônica
02/03/2021 11:57:47.0
CLAUDIO DA CUNHA
Presidente da Banca Examinadora

Assinatura Eletrônica
04/03/2021 12:09:30.0
FABIO CARDOSO CRUZ
Avaliador Externo (UNIVERSIDADE FEDERAL DE SÃO PAULO)

Assinatura Eletrônica
02/03/2021 10:47:36.0
ROBERTO ANDREATINI
Avaliador Interno (UNIVERSIDADE FEDERAL DO PARANÁ)

Assinatura Eletrônica
02/03/2021 11:58:57.0
RAINER KARL WILLI SCHWARTING
Avaliador Externo (PHILIPPS-UNIVERSITAT MARBURG)

I dedicate this thesis to my parents
Jose Pochapski and Lidia Michalichen Pochapski
for the dedicated support across this long journey.

Acknowledgment

I am grateful to God for all the blessings.

Graduate school is a long, exciting, and demanding journey. I can confidently say that it was less difficult thanks to the wonderful people that I interacted over all these years.

I would like to immensely acknowledge my family for all the support during all these years. To my parents Jose and Lidia, my brothers Gabriel and Daniel, my great appreciation for everything. Thank you for all the effort and sacrifice that you had to make it happen.

I would like to specially acknowledge my Ph.D. advisor, Professor Claudio da Cunha, for being a fantastic mentor. I really appreciate all the opportunities you gave to me during my Ph.D., all the knowledge shared, friendship, and for being an example for my career.

Also, I would to specially acknowledge Professor Donita L. Robinson for also mentoring me during these years. I appreciate the opportunity, all the support and effort, the knowledge shared, kindness and patience since the very first day that I step a foot in your laboratory, thank you!

I am also especially thankful to Dr. Alexander Gomez-Acosta. Alex was the first person that I work with in my very first day in Da Cunha's lab, and I had the luck to work with also in Robinson's lab. Thanks for all your support and friendship.

After all these years, I am very thankful to Adam Sugi, William Sanchez, and Gabriel Baltazar for all shared ideas, projects, a lot of troubleshooting during the experiments, help on short deadlines and bureaucratic work, etc. Also, for all the laughs, talks about science, football, politics, etc. I really appreciate your friendship.

I have the great opportunity to meet and work with several amazing people in 3 different “generations” of students in Da Cunha’s lab. I would like to thank to all the students from Da Cunha’s lab that I had the great opportunity to work and share moments, especially Dr. David Levcik, Dra. Laura Pulido, Dra. Ana Segantine, Lillian Lisner, Daniele Ramos, Julie Esaki, Mayra T. Lopes, Joao Lucas Cardoso, Jackeline Mujica.

Also, I would also like to thank several members of Robinson’s lab, especially to Dra. Sierra J. Stringfield for all the support and knowledge shared on single-unit electrophysiology recordings.

A special thanks to Dra. Bruna Soley, Thais Yokoyama, Joao Lucas Xavier, Meira Machado, and Nivaldo Satiro for the friendship during all these years.

I am grateful for all the day-to-day work, troubleshooting, and laughs with Silvia Cordazo and Fernando Zonzini in the department. Thank you both for all the help. The bureaucratic work and troubleshooting could not be done without your help, so thank you both!

I would like to thank all the professors in the Pharmacology department and working staff for all the support.

Also, I appreciate and thank the funding agencies, CAPES and CNPQ, for all the financial support.

RESUMO

A motivação é uma variável comportamental essencial para a seleção de ações durante a busca por recompensas, sejam estas naturais ou drogas de abuso. Diferentes estruturas corticais e límbicas do nosso sistema nervoso central regulam constantemente a execução destes processos de seleção de ações. Entre tais estruturas estão o córtex orbitofrontal (OFC) e o nucleus accumbens (NAc). O OFC e o NAc apresentam importante função na codificação da expectativa, no comportamento motivado e nas ações direcionadas por recompensas. Nestes âmbitos, prejuízos nas atividades do OFC e NAc são classicamente descritos após o consumo de drogas de abuso. Entretanto, inúmeros aspectos relacionados ao funcionamento normal do OFC e NAc, tal como as alterações promovidas por drogas de abuso, ainda permanecem pouco elucidados. Desta forma, objetivo desta tese é contribuir para uma melhor compreensão dos mecanismos neuronais envolvidos na expressão de comportamentos motivados por recompensa e alterações promovidas por drogas de abuso. Para este objetivo, três artigos científicos são apresentados. No primeiro artigo científico desta tese, avaliamos os efeitos a longo prazo na atividade neuronal promovidos pelo consumo crônico e intermitente de álcool (AIE) durante a adolescência de ratas fêmeas. Neste trabalho, a partir de registros eletrofisiológicos demonstramos que animais expostos ao AIE apresentaram aumento da atividade de excitatória de neurônios do OFC em resposta a estímulos condicionados. Demonstramos também que a exposição ao AIE promoveu uma redução na atividade excitatória de neurônios do NAc durante comportamentos direcionados a recompensas. Estes resultados demonstram prejuízos a longo prazo na atividade neuronal do OFC e NAc promovidos pelo consumo de álcool durante a adolescência. No segundo artigo científico apresentado, demonstramos evidências eletrofisiológicas de uma nova função do NAc durante comportamentos motivados por recompensa. Nestes experimentos, realizamos registros eletrofisiológicos de neurônios do NAc durante a execução de uma tarefa de busca espontânea por recompensas. Os resultados obtidos assinalam que o vigor (velocidade e aceleração) e o comportamento de aproximação de locais previamente recompensados, podem ser preditos a partir da atividade de neurônios do NAc. A atividade do NAc é classicamente descrita como uma interface entre sistemas límbicos e motores, e os resultados deste estudo representam uma possível forma de como tais informações são codificadas pelos neurônios do NAc. Por fim, o terceiro trabalho que constitui esta tese avaliou a importância de receptores dopaminérgicos D2 para a expressão de comportamento motivado. A partir da utilização de inibição farmacológica de receptores dopaminérgicos D2, observamos prejuízos à motivação e eficiência de performace durante a execução de uma tarefa probabilística de busca por recompensa. Estes resultados evidenciam que, além do já descrito papel dos receptores D1 durante comportamento motivado, os receptores D2 também são necessários para a codificação de expectativa e

motivação por recompensa. Em suma, os resultados descritos nesta tese apresentam evidências para novos mecanismos relacionados com a codificação de comportamentos motivados em condições normais, bem como alterações a longo prazo no funcionamento de circuitos corticais e límbicos após o consumo de álcool na adolescência.

ABSTRACT

Motivation is an essential component evaluated during action-selection based on the goal of getting a desired reward. Cortical and limbic structures are constantly encoding and modulating these processes. Among these structures, the orbitofrontal cortex (OFC) and nucleus accumbens (NAc) display an important role over the reward-seeking, reward expectation, and reward approach behaviors. Drugs of abuse can impair cortical and limbic processes required to drive behavioral responses related to natural rewards (social interaction, food, sex, etc). However, several aspects of the normal functioning and the changes induced by drugs of abuse remain poorly understood. In this thesis, the manuscripts of 3 scientific articles are presented aiming to contribute to a better comprehension of reward-motivated behavior and changes promoted by drugs of abuse. On the first scientific article are presented long-term changes over the OFC and NAc neuronal activity promoted by adolescent alcohol administration. The second scientific article shows electrophysiological evidence of a new function of the NAc during a reward-motivated behavior. The third scientific article demonstrates the importance of D2 dopaminergic receptors on motivation processing. On the first article we evaluated the long-term effects promoted by adolescent ethanol exposure (AIE) in female rats. In this study, after AIE exposure, rats were trained on the Pavlovian conditioned approach task and electrophysiological recording of the OFC and NAc activity were performed. After analysis on sign-tracking subjects, we found that AIE exposure caused a decrease in goal-tracking behavior in adulthood as well as an increase in OFC excitatory response to conditioned stimulus. Also, we demonstrated that AIE exposure resulted in a decrease in NAc excitatory activity during goal-tracking behaviors. These results demonstrate long-term changes by alcohol consumption during adolescence on behavioral responses and neuronal activity. In the second study, by recording the electrophysiological activity of NAc neurons during spontaneous reward approach behavior, we showed that the vigor and the progress of a reward approach behavior expressed in kinematic parameters can be predicted from the electrophysiological activity of NAc neurons. Finally, in the third study, using pharmacological inhibition of D2 dopaminergic receptors, we observed impairment on motivation and accuracy to perform a reward probabilistic task. These results evidentiated the role of D2 receptors in reward expectation and motivation. In summary, the results from these studies provide evidence for proposed neuronal mechanisms underlying motivated behavior in normal subjects and in subjects exposed to alcohol during the adolescence.

Figure list

Abbreviations list

AIE - Adolescent intermittent ethanol
AUD - Alcohol use disorder
CS – Conditioned stimulus
FSIN - Fast spike interneurons
GABA-A receptor – Gamma-aminobutyric acid receptor A
MSN - Medium spiny neuron
MSN-D1- Medium spiny neuron expressing D1 receptor
MSN-D2 - Medium spiny neuron expressing D1 receptor
NAc – Nucleus accumbens
NMDA - N-methyl-D-aspartate
OFC – Orbitofrontal cortex
PCA – Pavlovian conditioned approach
RPE - Reward prediction error
TANs - Tonically active neurons
US – Unconditioned stimulus
VTA - Ventral tegmental area

Summary

Preface

This thesis consists of a brief introduction topic and three scientific articles.

In the introduction topic is presented a brief literature review regarding nucleus accumbens (NAc) and orbitofrontal cortex (OFC) function, general characteristics of drug addiction and adolescent ethanol consumption, and electrophysiological evidences of neuronal function during reward-motivated behavior.

The first scientific article presents behavioral and electrophysiological data recorded on the OFC and NAc in female rats pre-exposed to ethanol during the adolescence period. The second scientific article presents behavioral and electrophysiological data recorded on NAc during the spontaneous reward approach. And the third scientific article presents a study where the role of D2 dopaminergic receptor on reward motivation and expectancy was evaluated during a probabilistic task.

The methods, results, and discussion are presented individually for each of the scientific articles.

1. Introduction

How is motivation encoded in our central nervous system? Which neuronal mechanisms control these processes? What changes drugs of abuse can induce on these neuronal circuitries? These are questions that have been asked since the early times of the modern neuroscience field. Even although considerable progress was accomplished in the past decades, several questions remain unanswered as long as new questions arise.

Motivation is an essential factor accounted during the actions selection process. However, in order to obtain the expected outcome, several other internal and external components must be considered before and during the execution of the selected action (Schoenbaum et al., 2016). Similar to our ancient ancestors, we modern humans must learn which environmental stimuli signal the imminent encounter with a reward our maybe a threat, what is the associated value of the outcome and which actions are more appropriated to obtain or even to maximize the desired outcome. The computation of internal and external information allows us to properly select actions and define how vigorously we should perform them. However, internal and external variables are in constant change. An environmental stimulus that previously predicted a particular reward can now result in a different outcome. Similarly, the value assigned to a particular reward can also rapidly change. For example, the assigned value to a specific snack 5 minutes before our lunch is different to the assigned value to the same snack 5 minutes after our lunch. For this reason, cortical and limbic structures are continuously required to encode these changes in internal and external information (Sommer et al., 2014; Nieoullon, 2002). This functionally interconnected activity constantly aims to optimize the execution of selected behavioral responses, resulting in improved precision, speed, and motor coordination. As consequence of these processes, the more appropriate action in a given situation is selected and, furthermore, optimally executed.

In the studies presented in this thesis, we focused on evaluating two important brain structures related to the encoding of reward associated stimulus, reward value, motivation, among other functions. These structures being the orbitofrontal cortex (OFC) and the nucleus accumbens (NAc) (Nicola, 2007; Schoenbaum et al., 2006). The NAc is considered as one of the major reward processing structure in the brain. NAc function is related to encode associative

learning, reward processing, and motivation (Da Cunha et al., 2012; Ikemoto, 2010). Several studies describe the NAc activity as being essential for encoding motivational properties associated with a conditioned stimulus, action selection, approach to previous rewarded locations, and how vigorously this approach will be performed (Mcginty et al., 2013; Da Cunha et al., 2009; Day et al., 2007). OFC is also described as being an important structure related to codification of motivational properties attributed to a conditioned stimulus, reward value, reward expectancy, and goal-directed behavior (Goldstein and Volkow, 2011; Schoenbaum and Shaham, 2008). Both structures are required for processing information related to natural rewards. The NAc particularly is described as a "limbic-motor interface", a function that results in important control over approach behavior by the NAc neurons (Mcginty et al., 2013; Mogenson et al., 1980). However, it is importantly described in the literature the ability of drugs of abuse to alter the functional activity in cortical and limbic structures (Nestler, 2005). Drugs of abuse can promote anatomic, molecular, and functional changes on NAc and OFC (Goldstein and Volkow, 2011; Volkow and Fowler, 2000). Interestingly, besides some common effects promoted by the majority of the drugs of abuse, as the enhancement of dopamine release on NAc, several studies report important sex and age-dependent effects of drugs of abuse (Towner and Varlinskaya, 2020; Calipari et al., 2017; Madayag et al., 2017; Varlinskaya and Spear, 2015). Among sex differences related to addiction, it is described that female subjects present higher levels conditioned place preference promoted by drugs of abuse (Calipari et al., 2017) and also present higher expression of sign-tracking behavior (Madayag et al., 2017). Regarding age-dependent difference, adolescence is described as being a critical neurodevelopmental period, where exposure to drugs of abuse can induce more pronounced effects compared to adult pairs, resulting in long-lasting behavioral and neuronal changes (Spear, 2000).

Moreover, even though a high research interest was present in the past decades in studying fronto-limbic modulation of reward-related behaviors and the changes promoted by drugs of abuse, several important questions remain poorly understood. Based on it, the studies presented in this thesis present three primary focus:

1- Evaluate long-term effects of adolescent alcohol exposure on behavioral and OFC and NAc neuronal activity in female rats.

2- Evaluate the role of the activity of NAC individual neurons during spontaneous reward-approach behavior.

3- Evaluate the role of D2 dopaminergic receptors on reward motivation and expectancy.

Besides classical studies describing the important role of OFC and NAc on the codification of reward associated stimulus, reward processing, and changes promoted by drugs on abuse on these structures, recent studies demonstrated new mechanisms elucidating how these processes could be encoded (Fobbs et al., 2020; Mohebi et al., 2019; Coddington and Dudman, 2018; Dobbs et al., 2016; Broadwater et al., 2017; Engelhard et al., 2016). The following topics are presented intending to provide a brief literature review regarding NAc and OFC function, behavioral and neuronal changes promoted by drug of abuse, and insights regarding electrophysiological evidences of codification of motivation and approach behavior.

1.1 Nucleus Accumbens

The NAc is a subcortical structure, with its function related to associative learning, reward processing, and motivation (Kravitz et al., 2012; Day et al., 2007; Nicola, 2007). NAc is also referred to as ventral striatum and is a component of a conjunct of brain structures defined as the basal ganglia. The basal ganglia is also composed by the dorsal striatum (caudate and putamen nuclei), globus pallidum internal, globus pallidum external, subthalamic nuclei, substantia nigra pars compacta and substantia nigra pars reticulata. The basal ganglia activity is directly related to motor control, action selection, and motivational encoding (Da Cunha et al., 2009; Ikemoto, 2007; Obeso et al., 2000).

A classical definition by Mogenson et al. (1980) proposed that NAc acts as a limbic-motor interface, allowing the selection of the proper response after the presentation of a reward-associated stimulus. Support to this definition is provided by broad anatomic and functional connectivity existent on NAc. The NAc receives important inputs from limbic structures such as ventral tegmental

area (VTA), amygdala, hippocampus, prefrontal cortex (PFC), and the main neuronal output of NAc projection is the ventral pallidum (Cox and Witten, 2019; Ikemoto, 2007). This particular anatomic-functional connectivity allows the NAc, for example, to receive information about predictive cues and guide behavioral responses accordingly (Nicola et al., 2004; Mizumori et al., 1999; Mogenson et al., 1980).

An important source of modulation of the NAc activity is provided by the neurotransmitter dopamine. Dopaminergic neurons located in the VTA form the mesolimbic pathway, and one of the principal neuronal outputs for dopamine release is the NAc (Ikemoto, 2010; Sesack and Grace, 2010). Classical studies led by Wolfram Schultz demonstrate that midbrain dopaminergic neurons encode the reward prediction error (RPE) (Schultz, 1998). RPEs are represented by an increase in dopaminergic neuronal firing after the subject encounters a reward higher than expected. Furthermore, in these studies was also demonstrated that after repeated presentation of a conditioned stimulus (CS) paired with a subsequent presentation of the unconditioned stimulus (US), dopaminergic neurons changed their firing response pattern, no longer presenting phasic activity to the US but instead, phasically firing right after the CS presentation. This observation elegantly demonstrated the important role of the dopaminergic neurons activity for associative learning processes (Schultz, 2007, 1998).

As previously mentioned, one of the most important dopaminergic outputs is the NAc. Phasic dopamine release on the NAc is described to signalize novelty and motivational relevant events (Nicola, 2007). After release, dopamine can promote its modulatory effects by binding into two different families of dopaminergic receptors. Dopaminergic receptors are G-protein coupled receptors and can be divided into D1-like and D2-like families. Dopaminergic D1-like receptors are constituted by the D1 and D5 receptors. Conversely, dopaminergic D2-like receptors are subdivided into D2, D3, and D4 receptors (Flores-Barrera et al., 2011). D1-like receptors present around 10 to 100-fold lower affinity to dopamine than D2-like receptors (Beaulieu and Gainetdinov, 2011). Moreover, activation of D1-like receptors requires higher amounts of dopamine release, as usually provided by dopaminergic neurons phasic activity (high frequency of firing resulting in elevated levels of dopamine release). Dopaminergic neurons also present a tonic pattern of activity (low frequency of firing, resulting in constant low

levels of dopamine release), usually associated with D2-like receptors activity (Yapo et al., 2017; Schultz, 2007). NAc also presents a heterogeneous neuronal population, being composed of medium spiny neurons (MSN), fast spike interneurons (FSIN), and tonically active neurons (TAN) (Ikemoto, 2007). MSNs and FSIN are GABAergic cells, and TANs are cholinergic cells. The vast majority of these neurons (around 90%) are MSNs (Scudder et al, 2018) composed by the MSN-D1 and MSN-D2 based on the respective D1 or D2 dopaminergic receptor expression. Both populations of MSN-D1 or D2 are similarly expressed on NAc (Scudder et al., 2018). Previous studies described that the activation of MSN-D1 could contribute to action selection, and the activation of MSN-D2 results in the inactivation of non-optimal actions. The substantial coordinated activity of both MSN-D1 and D2 populations allows efficient selection and execution of intended actions, such as the approach to a previously rewarded location (Nicola, 2010; Ikemoto and Wise, 2004). However, it is important to mention that a small percentage of NAc MSNs co-express both D1 and D2 receptors. However, the activity of this population is not clearly described (Scudder et al., 2018).

Nevertheless, phasic dopamine release on NAc is described to invigorate reward-seeking behavior and facilitate reinforcement learning (Berke, 2018). Also, NAc neurons activity has been implicated in reward value encoding, this function resulting in the selection of actions that will maximize the final reward outcome (Saddoris et al., 2013). Recent studies demonstrated that optogenetic stimulation of VTA-NAc specific projection might elicit reward-seeking, approach behavior, and associative learning (Saunders et al., 2018). Also, inactivation of NAc activity may result in decreased CS evoked responses, decreased reward-seeking, and decreased approach behavior (Nicola, 2010; Ambroggi et al., 2008). As a consequence of the important modulatory effect of dopamine on NAc and other structures on the basal ganglia, changes in dopaminergic neurotransmission are associated with several pathologies, such as Parkinson's disease, schizophrenia, bipolar disorder and drug addiction (Da Cunha et al., 2012; Ikemoto, 2010; Kalivas and Volkow, 2005).

1.2 Orbitofrontal cortex

Every day we make decisions about what to seek and what to avoid, and important components that influence these decisions rely on the activity of the orbitofrontal cortex (OFC) (Rudebeck and Rich, 2018).

OFC is a brain region located in the prefrontal cortex and is implicated in executive functions (Schoenbaum et al., 2016). OFC presents important connections with the sensory cortex and subcortical regions such as amygdala and NAc. In virtue of these connections, OFC is uniquely positioned to encode the association between sensory stimuli and internal states (motivation, expectancy), using these information to guide behavioral decisions (Rudebeck and Rich, 2018). Previous studies described that the neuronal representation of expected value of outcomes is present or even generated in the OFC (Schoenbaum et al., 2016). According to this description, OFC would integrate previous information of stimulus-reward association resulting in a representation of the outcome expectancy (Schoenbaum and Shaham, 2008). Additionally, in the absence of an expected outcome, OFC function would be required to update reward predictions based on the new outcome, allowing us to appropriately update behavioral responses (Burke et al., 2009). As the contingency between stimulus and outcome can change momentarily, it is proposed that OFC is continuously encoding possible changes on contingency (Rolls, 2004; Schoenbaum et al., 2006). Interestingly, Riceberg et al. (2017), by recording neuronal activity from OFC demonstrated that when reward contingency was stable across the session, the OFC neuronal activity could predict the reward choice in each performed trial. However, changes in the reward contingency completely blunted this prediction in the following trials. Nevertheless, after repeated performance of trials with the new contingency, the authors observed that the neuronal activity of the OFC neuronal ensembles gradually started to predict the new response. These results demonstrated that the OFC activity evaluates the stimulus-reward association on a trial by trial basis, and after changes on contingency, the OFC neurons integrate information regarding reward history and also the new contingency over the trials to result in learning of a new association. These data emphasize the important role of OFC for encoding responses based on internal representations of expected outcomes and the association with environmental stimuli (Schoenbaum and Shaham, 2008). However, even though OFC neuronal activity could predict reward choices, the

OFC activity is described as being necessary for decision-making processes instead of directly selecting or initiating reward-related actions (Nogueira et al., 2017).

Previous studies proposed that OFC activity would promote adaptive behavior based on encoding specific stimulus-outcome association (Riceberg and Shapiro, 2017; Volkow and Fowler, 2000). This view of OFC activity is supported by studies that evaluated the OFC activity during reversal learning tasks (Ghahremani et al., 2010; Remijnse et al., 2005). Usually during reversal learning tasks, two different stimuli are presented, however, only one of them being paired with a reinforce outcome. After several trials with this stable contingency a reversal is performed. On this reversal, the previous paired stimulus no longer indicates the expected outcome. Instead, the previous neutral stimulus now indicates the expected outcome. Neuroimaging studies demonstrated that the OFC activity is highly increased during this reversal, possibly encoding this new association (Ghahremani et al, 2010). This role of OFC on promoting adaptive behavior is evidenciated by studies where the inactivation of OFC resulted in significant impairment on reversal learning task. (Burke et al. 2009).

OFC function is also associated with controlling over impulsive behaviors (Zeeb et al., 2010). Because the OFC processing of sensorial and motivational information, OFC activity could be implied in the encoding of the consequences of specific actions, and if this action is not appropriated, OFC could exert inhibitory control over this action (Rudebeck and Rich 2018). Hardung et al., (2017) demonstrated that optogenetic inhibition of OFC resulted in impairment in inhibitory control. Moreover, inactivation or lesions on OFC may result in impulsive behavior expression (Zeeb et al. 2010). Another important function of OFC is related to behavioral flexibility (Gremel et al., 2016; Bradfield et al., 2015; Saddoris et al., 2005). Changes in the OFC activity can result in engagement in maladaptive behaviors, where the behavioral responses are not guided by cognitive representations of the outcome (Pascoli et al., 2018).

Encoding of reward value, associative learning processes, and outcome expectancy are importantly derived from the connectivity between several limbic structures (Broadwater et al., 2017; Schoenbaum et al., 2016; Nicola, 2010). OFC present important connectivity with VTA and NAc. An important OFC function in this regard could be contributing to RPE codification by VTA

dopaminergic neurons. Takahashi et al., (2011) demonstrated by single-unit recordings of OFC neuronal activity that in the presence of highly predicted reward the OFC neurons presented high firing activity, oppositely to the low firing activity recorded on VTA neurons. Using a functional disconnectivity protocol on VTA and OFC, the authors observed impairments in the learning driven by RPE. However, OFC presents sparse direct projections to VTA. A possible candidate of indirectly mediate OFC-VTA signalization is the NAc because it receives strong inputs from OFC and presents direct projections to VTA (Schoenbaum et al., 2016). OFC and NAc also present interesting similar functions as mediators of goal-directed behavior and associative learning. This functional connectivity between OFC and NAc is expected based on the strong bi-directional projections between these two structures (Reynolds and Zahm, 2005).

1.3 Drug addiction

Motivated behaviors elicited by natural rewards such as food, water, and social interaction are essential responses modulated by the mesocorticolimbic system. However, drugs of abuse demonstrated the ability to overtake neurobiological mechanisms that control motivated behavior (Nestler, 2005). Drug addiction is described as a chronic relapsing disorder, where addicted subjects present compulsive drug-seeking, loss of control over drug intake, and present negative affect upon drug withdrawal (Koob and Volkow, 2016; Goldstein and Volkow, 2011; Volkow et al., 2006). In vulnerable subjects, repeated drug consumption leads to maladaptive associative learning, consequently, the presentation of drug-associated cues elicits craving and drug-seeking behavior (Koob and Volkow, 2016). Another classical characteristic of addiction is a pathological inflexible behavior, where drug seeking and consumption are observed at expense of negative consequences (Volkow et al., 2006). A commonly shared mechanism among most drugs of abuse is promoting a direct or indirect increase in dopamine release on NAc (Nestler, 2005). However, drugs of abuse can induce a complex spectrum of anatomic, functional, and molecular changes over the brain (for reviews see Crews et al., 2007; Kalivas, 2008; Kalivas and Hu, 2006; Koob and Volkow, 2009; Nestler and Luscher, 2019)

Alcohol is one of the many chemical substances that can promote addiction. Alcohol is a licit substance, and by consequence, is extensively consumed around the world (Koob and Volkow, 2016; Koob, 2003). A common pattern of alcohol consumption is binge-drinking, which is characterized as five or more drinks in a session for men and 4 or more drinks for women (Chung et al., 2015). Binge-drinking episodes are often associated with several adverse effects, including increased risk-taking, physiological damage, injury, or death (Molina and Nelson, 2018). Alcohol use disorder (AUD) is a chronic relapsing disorder, where the patient presents repeated cycles of intoxication, withdrawal, and relapse. Classically the GABAergic neurotransmission is directly related to the effects of alcohol (Coleman et al., 2014). More specifically, GABA-A receptors (gamma-aminobutyric acid A receptors) are allosterically modulated by alcohol. Acutely alcohol can promote sedative symptoms, anxiolytic effect, and impairment in motor control. These effects result from the increase in GABAergic activity. However, chronic use of alcohol results in neuroadaptative processes. Changes in the GABA-A receptors composition and decrease in its expression are observed after chronic alcohol consumption (Coleman et al., 2014; Coleman et al., 2011; Nestler, 2005). These effects result in neuronal hyperexcitability upon abstinence and increase in anxiety levels (Lovinger and Roberto, 2013). Nevertheless, alcohol consumption can also promote changes in glutamatergic signalization (mostly via inhibition on NMDA receptors) (McKim et al., 2016), decrease of hippocampal neurogenesis (Liu and Crews, 2015), increases on spine density of the MSNs in the dorsal striatum (Vetreno and Crews, 2018) and other anatomic and functional changes on OFC, NAc, amygdala, hippocampus, and many other brain structures (Crews et al., 2016; Coleman et al., 2014; Koob, 2003).

Moreover, studies described age-dependent effects of alcohol. Compared to adults, adolescents are more sensitive to alcohol-induced stimulation, social facilitation, and behavioral disinhibition and less sensitive to sedative, hypnotic, and motor impairments. These characteristics can promote a risk factor for high levels of alcohol consumption by adolescents (Ornelas et al., 2014; Risher et al., 2013). Also, sex differences in the alcohol effects are described. Preclinical studies demonstrate that compared to male rats, female subjects presented higher levels of alcohol consumption. However, male rats presented higher levels

of anxiety after alcohol exposure (Varlinskaya and Spear, 2015). Besides the advances accomplished in the past decades on elucidating molecular, anatomic, and functional mechanisms by which alcohol and other drugs of abuse are promoting its novice effects, no efficient treatment for drug addiction is currently available (Koob and Volkow, 2016). A possible reason is because of the complex and broad spectrum of changes promoted by drugs of abuse, briefly addressed in this introduction chapter. Besides, not all subjects that eventually consume a particular drug of abuse will further develop the addiction syndrome, a fact that reinforce that particular variables can strongly contribute to the vulnerability to addiction. Among them, biological and social components can influence the individual variability over addiction (Spear, 2018).

In this regard, Berridge (2004) proposed that the presentation of a drug-associated stimulus could acquire motivational salience, and the further presentation of this stimulus can strongly exert control over behavioral responses on these subjects. A preclinical model to study the effects of CS attributed salience is by the Pavlovian conditioned approach task (PCA). During a PCA session, the repeated CS presentation is associated with the US presentation, eliciting the performance of conditioned behaviors. However, in PCA the CS is usually presented as a composed stimulus (cue light + lever), and after the repeated presentation of the CS and US the animals usually develop two distinct phenotypes: sign-tracking and goal-tracking. Characteristically, after the CS onset, sign-tracking animals approach and interact with the CS, and goal-tracking animals approach the site of reward, as illustrated in figure 1.

Figure 1. Sign-tracking and goal-tracking behavior illustrative representation. **A.** Representation of a receptacle entry, common a goal-tracking behavior. **B.**

Representation of the usual CS+lever interaction presented by sign-trackers. Source: Robinson D. L. lab.

In sign-tracking animals, the CS presentation can acquire incentive salience (Flagel et al., 2007; Robinson and Kent, 1993). Sign-trackers present higher levels of impulsivity (Flagel et al., 2009; Saunders et al., 2013), increased phasic dopamine release on NAc (Spoelder et al., 2015), and increased levels of drug self-administration (Saunders and Robinson, 2011; Tomie et al., 2008), and by consequence, sign-tracking behavior is proposed as an indicator of impulsive behaviors and addiction vulnerability (Flagel et al., 2009; Robinson and Kent, 1993). Being an indicator of addiction vulnerability, the development of a sign-tracking phenotype can be stimulated by exposure to drugs of abuse during brain developmental phases. Studies described that alcohol administration during the adolescent period resulted and increased sign-tracking behavior expression in adulthood (Madayag et al., 2017), and this observation coherent with the description that alcohol consumption during adolescence can lead to alcohol use disorders (AUD) in adulthood (Landin et al., 2020).

1.4. Adolescent alcohol consumption

Adolescence is a complex and gradual transition phase, usually referred to as the transition from childhood to adulthood and typically marked by social and physiological changes, representing a critical period for executive function development in the brain (Hiller-sturmhöfel and Spear, 2018). This period is marked by the presence of high social interaction and engagement in risk-taking behavior, novelty-seeking, and impulsivity (Luna et al., 2015; Varlinskaya and Spear, 2015; Doremus-Fitzwater et al., 2012; Yurgelun-todd, 2007). These behavioral changes occur in the context of important neurodevelopmental processes that are influenced by external environmental and internal factors (Jaworska and Macqueen, 2015).

Adolescent subjects present limitations in “top-down control” promoted by the different developmental characteristics of cortical and limbic brain regions (Bava and Tapert, 2010; Caballero et al., 2016). The connectivity between cortical and limbic structures undergoes important structural and functional changes during adolescence (Broadwater et al. 2017). For example, subcortical limbic regions, such as NAc and VTA are reported to present early development,

contrasting with the later development of the prefrontal cortex (Caballero et al., 2016; Casey et al., 2011; Bava and Tapert, 2010). This higher activity of limbic regions, directly related to motivation and reward-seeking, along with lack of cortical control can facilitate the engagement in risk-taking behavior and impulsivity, characteristics that can render the adolescent brain particular vulnerability to alcohol's effects (Crews et al., 2000).

Previous studies demonstrated that adolescent intermittent ethanol (AIE) exposure can promote structural and functional changes in OFC and NAc (Renteria et al., 2018; Vetreno and Crews, 2018; Broadwater et al., 2017; Coleman et al., 2014). Renteria et al. (2018) demonstrated that AIE exposure promoted a decrease in the OFC neuronal excitability, particularly on the neuronal projection to dorsal medial striatum, and this effect was associated with a decrease in behavioral flexibility. Whole-cell patch-clamp recordings also demonstrated that AIE resulted in increased intrinsic excitability in NAc MSNs (Shan et al., 2019). Changes in dopamine release in NAc promoted by AIE are also previously reported (Shnitko et al., 2016). Interestingly, Broadwater et al. (2017) demonstrated that AIE exposure promoted significant changes in functional connectivity, as presented in figure 2. Particularly, a significant AIE-induced decrease in the OFC and NAC resting-state connectivity was observed. Moreover, these AIE-induced changes in fronto-limbic activity can result in impairment in reward processing, decision making, increasing the addiction vulnerability (Spear, 2018; Spoelder et al., 2015; Alaux-cantin et al., 2013).

Also, it is further described that AIE exposure can results in memory impairments (Galaj et al., 2020; Swartzwelder et al., 2015), deficits in cognitive flexibility and reversal learning (Sey et al., 2019; Coleman et al., 2011), increased alcohol self-administration (Amodeo et al., 2017; Pascual et al., 2009) deficits on attention (Fernandez and Savage, 2017; Sanchez-Roige et al., 2014), decrease in social interaction (Varlinskaya et al., 2017), increasing anxiety levels (Towner and Varlinskaya, 2020), risk-taking preference (Qin et al., 2013), impulsivity (White et al., 2011) and induce sign-tracking behavior (Madayag et al. 2017). Sex differences on the AIE-promoted effects are also described (Dannenhoffer et al., 2019; Madayag et al., 2017; Varlinskaya et al., 2017).

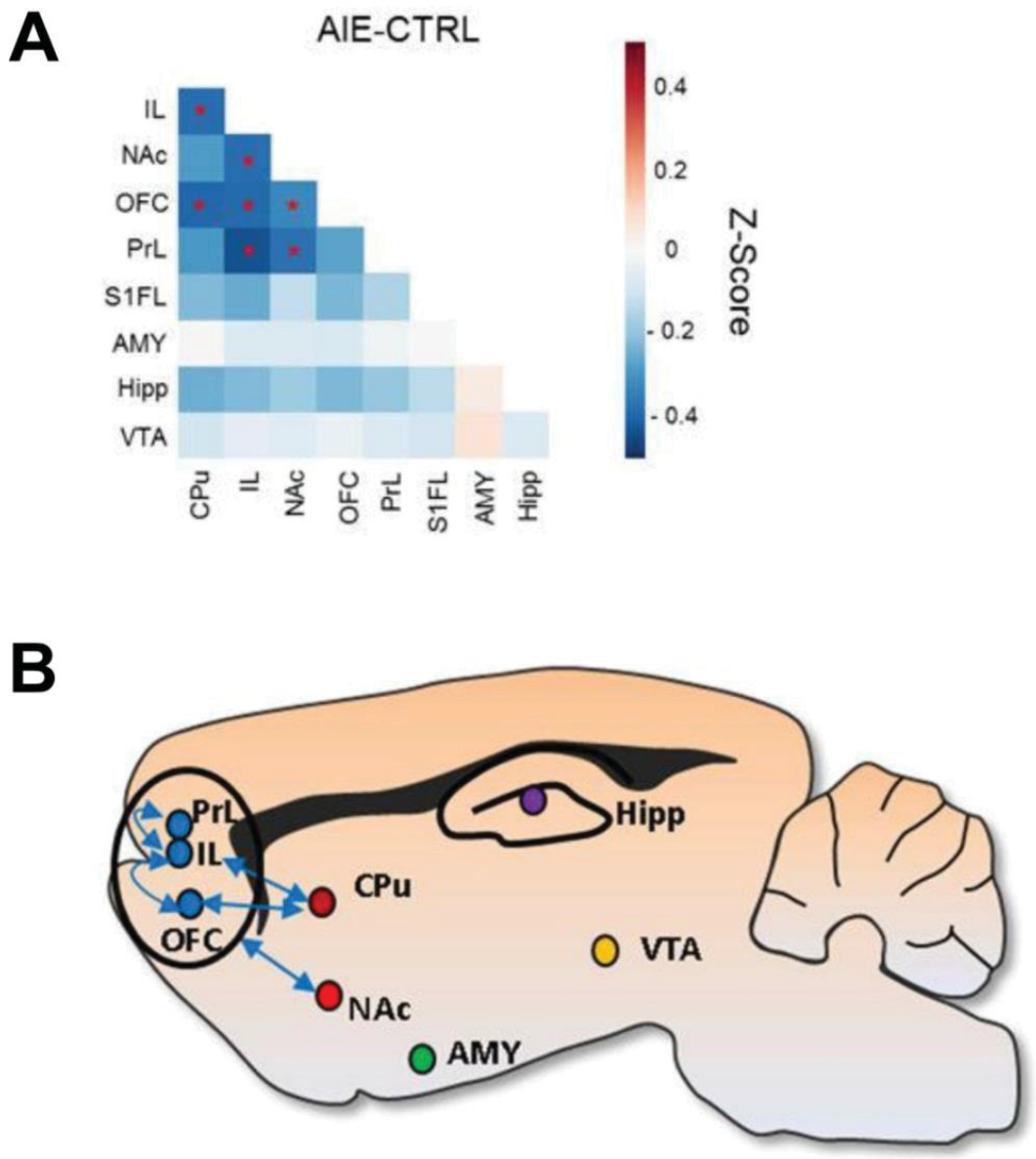

Figure 2 – Adolescent alcohol exposure effects on neuronal connectivity **A.** Functional connectivity among cortical and limbic structures. Data represented by z-score normalized data. Increased connectivity represented in red scale. Decreased connectivity represented in the blue scale. Red dots represent significant reduction in the functional connectivity between the two compared structures promoted by AIE exposure. **B.** Illustrative representation brain functional connectivity affected by AIE. Blue arrows represent the AIE affected brain structures functional connectivity. Adapted from Broadwater et al., 2018.

Nevertheless, AIE exposure can result in long-lasting effect and persist into adulthood, making AIE exposure a potential risk factor to development of alcohol use disorder in adulthood. However, the specific mechanisms by which AIE promotes these effects are still unknown (Crews et al., 2016; Spoelder et al., 2015; Füllgrabe et al., 2007).

1.5 Electrophysiological evidences of neuronal mechanisms underlying motivated behavior.

Understanding the neuronal substrates underlying the behavioral encoding and control has been the focus of several studies in the past years (Engelhard et al., 2019; Mohebi et al., 2019; Coddington and Dudman, 2018; Saunders et al., 2018; Panigrahi et al., 2015; Mcginty et al., 2013; Jin and Costa, 2010).

As previously discussed in this introductory chapter, cortico-limbic regions are directly required for reward processing and motivated behavior control (Nicola 2004, 2007). Single-unit electrophysiological recordings provided important information about individual and population neuronal activity during reward-motivated behaviors (Morrison et al., 2017; Mcginty et al., 2013; Roitman et al., 2005). A series of studies from Carelli's lab for example, provided an important contribution for the understanding of the NAc neuronal activity during classical Pavlovian or operant conditioning (Robinson and Carelli, 2008; Day et al., 2007, 2006; Wheeler et al., 2008; Roitman et al., 2005; Carelli et al., 2000; Carelli and Deadwyler, 1994). In these studies it was described the distinct firing activity of NAc in response to CS and US and during conditioned responses. Also, it was demonstrated that NAc neurons can present selective activity for different US (water x ethanol, water x cocaine, or even cocaine x heroin), as illustrated in figure 3.

Further studies demonstrated that NAc neuronal activity could predict the vigor of the reward approach (McGinti et al. 2013). After the CS presentation, the greater the firing activity the faster the animal initiated the approach response (McGinty et al. 2013). A similar activity pattern was recorded in neurons on the dorsal striatum (Rueda-orozco et al. 2015; Pahigrahi et al. 2015). Carbonell et al. (2018), recording neuronal activity in the dorsal striatum, observed certain neurons presented activity only before or after locomotion towards rewarded locations, which were described as start/stop neurons. Other studies also reported control of locomotion kinetics by dorsal striatum neurons (Ytri and Dudman 2016; Jin and Costa 2010). Information of when motor actions should be initiated and when they should be finished, associated with the codification of reward location and locomotion speed during the approach, are examples of important variables that are modulated during approach behavior.

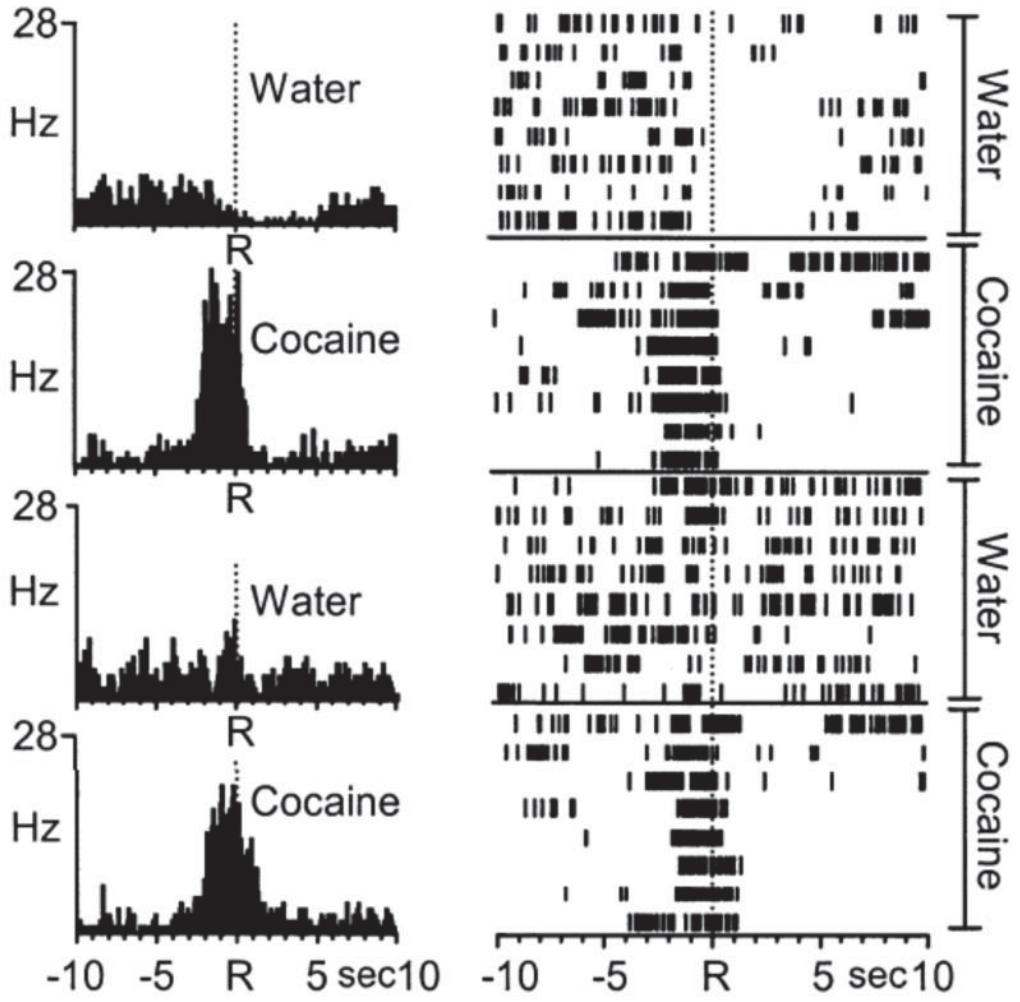

Figure 3 – Single-unit electrophysiological recordings of nucleus accumbens response to delivery of water versus cocaine. Carrelli et al., 2002.

The encoding of these variables is performed by complex and multi-structural processes. For example, studies from John O'keeffe, May-Brit and Edward Moser, which granted them the 2014 Nobel Prize in Physiology and Medicine, describe that spatial location is encoded by place cells in hippocampus and by grid cells in the entorhinal cortex neuronal (Rowland et al., 2016; O'Keefe, 1976). Hippocampus presents a direct connection with NAc, and information about the spatial location of rewards could be encoded by place and grid cells and further sent to NAc via subiculum projections (Witter et al., 1990). Hippocampus is also described to encode speed information (Gois and Tort, 2018), and neurons named speed cells were discovered in the hippocampus and in the entorhinal cortex (Kropff et al., 2015). Kinematics-related information (speed and acceleration), spatial position, and accuracy of the response were also extracted from neurons recorded in VTA (Engelhard et al., 2019), which is

one of the principal neuronal inputs to the NAc (Ikemoto 2007). Considering the anatomic connectivity presented NAc, and the role of NAc on approach behavior, these reports are consistent with the view of the NAc as an interface between motor and limbic systems (Mogeson 1980), which activity could result in control over the approach to previously rewarded locations (Da Cunha et al. 2012).

2. Thesis goals

2.1 Main goal

Evaluate the NAc and OFC neural mechanisms underlying reward motivated behavior and ethanol pre-exposure effects on neuronal and behavioral responses.

2.2 Specific goals

Evaluate long-term effects of adolescent ethanol exposure of female rats on behavioral responses and neuronal activity of the OFC and NAc during a Pavlovian conditioning approach task.

Evaluate the activity of NAc neurons during spontaneous reward-approach behavior.

Evaluate the role of D2 dopaminergic receptors on motivation and reward expectancy.

3.1 Adolescent ethanol exposure persistently alters neuronal firing in orbitofrontal cortex and nucleus accumbens during Pavlovian conditioned approach

Jose A. Pochapski[1], Alexander Gomez-A[2], Sierra J. Stringfield[5], Hannah D. Jaggers[2], Claudio Da Cunha[1], Charlotte A. Boettiger[2,3,4], Donita L. Robinson[2,3*]

[1] Laboratório de Fisiologia e Farmacologia do Sistema Nervoso Central, Department of Pharmacology, Universidade Federal do Paraná, Curitiba, PR, Brazil.

[2] Bowles Center for Alcohol Studies, University of North Carolina at Chapel Hill, Chapel Hill, NC.

[3] Department of Psychiatry, University of North Carolina at Chapel Hill, Chapel Hill, NC.

[4] Department of Psychology & Neuroscience, University of North Carolina at Chapel Hill, Chapel Hill, NC.

[5] Department of Psychiatry, University of Pittsburgh, Pittsburgh, PA.

* Corresponding author.

Abstract

Exposure to drugs of abuse, including alcohol, during the adolescent period can lead to impairments in cortical and limbic brain regions that are still undergoing development processes. Long term effects on behavior and neuronal activity have been described after adolescent intermittent ethanol (AIE) exposure. However, these effects are less described in female rodent models. In this study we test the hypothesis that AIE exposure increases sign tracking behavior expression and promotes long-lasting changes in orbitofrontal cortex (OFC) and nucleus accumbens (NAc) activity during reward-motivated behavior in female rats. Using the Pavlovian conditioned approach (PCA), we evaluated behavioral and neuronal effects of AIE in Sprague-Dawley female rats that were pre-exposed to AIE (5g/kg I.G., 2-day-on/2-days-off) or water control (CON) throughout adolescence. Our results demonstrated that both AIE and CON groups presented a high expression of the sign-tracking phenotype. Behavioral analysis conducted specifically on these sign-tracking animals demonstrated that AIE exposure promoted a decrease in goal-tracking behavior expression. Analysis of neuronal activity recorded during PCA baseline and reward omission sessions demonstrated that OFC neurons recorded in AIE-exposed animals presented higher excitatory activity in response to conditioned stimulus presentation compared to CON-exposed animals. This effect was consistent across the recording session and was still observed in the absence of the unconditioned stimulus. Also, AIE exposure resulted in significantly lower NAc excitatory activity during goal-tracking behavior. In summary, our findings suggest that AIE exposure promoted persistent changes in fronto-limbic processing of conditioned cues and approach behavior, resulting in lasting effects on the neurocircuitry of reward-motivated behavior in female rats.

Acknowledgements

Funding: This research was funded by the National Institutes of Health (P60AA011605 and U24AA020024) and CAPES/CNPQ.

The authors acknowledge Dr. Aric Madayag, Madeline Watson, Nancy Sey, and Kyle S. Czarnecki for the important assistance during the experiment data collection and Adam Sugi for programming support.

1. Introduction

Adolescence is a period of gradual transition from childhood to adulthood, marked by social and physiological changes, representing a critical period for executive function development in the brain. This period commonly includes high engagement in risk-taking behavior, novelty-seeking, and impulsivity, relative to other developmental periods (Doremus-Fitzwater et al., 2012; Luna et al., 2015; Varlinskaya and Spear, 2015; Yurgelun-todd, 2007). The occurrence of these behaviors is linked to limitations in "top-down control" promoted by the developmental characteristics of cortical and limbic brain regions during adolescence (Bava and Tapert, 2010; Caballero et al., 2016). Subcortical limbic regions that are important for reward processing and motivation, such as the nucleus accumbens (NAc) and ventral tegmental area, mature earlier than the prefrontal cortex, which is essential for executive functions such as inhibitory control (Bava and Tapert, 2010; Caballero et al., 2016; Casey et al., 2011). Activation of limbic regions along with a lack of cortical control can facilitate the use of alcohol and other drugs in adolescents (Spear, 2018a).

Compared to adults, adolescents are more sensitive to alcohol-induced stimulation, social facilitation, and behavioral disinhibition, and less sensitive to sedative and motor impairments – characteristics that can promote alcohol consumption (Spear, 2014, 2013). In 2018, about 4.3 million 12 to 20-year-olds in the United States reported having consumed alcohol; importantly, 29.8% of early adolescents (15 years old or younger) had reported alcohol consumption at least once (SAMHSA, 2018). A common pattern of drinking presented by adolescents is binge-drinking, which is characterized as five or more drinks in a session for men and 4 or more drinks for women (Chung et al., 2015). Binge-drinking episodes are often associated with several adverse effects, including increased risk-taking that can make adolescents more susceptible to physiological damage, injury, or death (Molina and Nelson, 2018).

Animal studies demonstrate that adolescent intermittent ethanol (AIE) exposure results in memory impairments (Galaj et al., 2019; Swartzwelder et al., 2015), deficits in cognitive flexibility (Coleman et al., 2014; Sey et al., 2019), and increased alcohol self-administration (Amodeo et al., 2017; Pascual et al., 2009). Interestingly, Broadwater et al. (2017) showed that ethanol exposure during adolescence reduces resting-state functional connectivity between the orbitofrontal cortex (OFC) and the NAc, important regions for reward-related

information processing. On this regard, neuronal activity in the OFC is necessary for encoding the contingency between a stimulus and outcome and the motivational value of expected outcomes (Riceberg and Shapiro, 2017), resulting in important modulation over reward-seeking behaviors (Moorman and Aston-Jones, 2014; Saddoris et al., 2005). Moreover, NAc function is implicated in associative learning and reward-motivated behavior (Day et al., 2007; Saddoris et al., 2013). NAc activation can invigorate reward-seeking and induce reward-approach behavior (Ambroggi et al., 2011; Mcginty et al., 2013). Also, OFC and NAc activity are implicated in Pavlovian conditioned approach (PCA) (Gillis and Morrison, 2019; Stringfield et al., 2017). Studies have described AIE-induced changes in OFC and NAc that can lead to impairment in reward processing and decision making (Coleman et al., 2014; Shan et al., 2019; Spear, 2018b; Spoelder et al., 2015). Importantly, AIE effects are long-lasting and persist into adulthood, making AIE exposure a potential risk factor in the development of alcohol use disorder in adulthood (Crews et al., 2016; Füllgrabe et al., 2007; Spoelder et al., 2015).

In this study, we used Pavlovian conditioned approach (PCA) to evaluate long-term changes in reward-motivated behavior promoted by AIE exposure. In this task, the repeated association of a cue light (conditioned stimulus, CS) and reward delivery (unconditioned stimulus, US) results in the performance of conditioned behaviors. After the CS onset, animals can present two distinct phenotypes: sign-tracking and goal-tracking behaviors. Characteristically, after the CS onset, sign-tracking animals will approach and interact with the CS, while goal-tracking animals will approach the site of reward delivery. In sign-tracking animals, the CS can acquire incentive salience (Flagel et al., 2007; Robinson and Kent, 1993). Sign-tracking behavior is thought to associate with impulsive behaviors and addiction vulnerability, and studies show that alcohol exposure during adolescence can increase the expression of sign-tracking behavior (McClory and Spear, 2014; Spoelder et al., 2015). Moreover, Madayag et al (2017) found that while AIE exposure increased sign tracking and reduced goal tracking in both males and females compared to controls, and female rats presented higher levels of sign-tracking behavior than male rats.

The present study aimed to evaluate behavioral and neuronal effects of AIE exposure on reward-motivated behavior in female rats. We hypothesized that AIE-induced sign-tracking behavior is associated with changes in the neuronal firing patterns during CS presentation and behavioral approach. We tested this hypothesis by performing single-unit electrophysiological recordings during PCA in brain regions involved in reward prediction in rats with and without AIE exposure. We tested this hypothesis by performing single-unit electrophysiological recordings during PCA in brain regions involved in reward prediction in rats with and without AIE exposure. We focused on the OFC and NAc due to their important roles in reward-motivated behavior and Pavlovian-approach (Flagel et al., 2007; Ogawa et al., 2013; Stringfield et al., 2017). During PCA, different neuronal substrates can modulate the expression of

behavioral responses. Subcortical structures are described to play an important role in mediating the expression of sign-tracking behavior, in opposite to a more cortical circuitry dependence of goal-tracking behavior (Flagel and Robinson 2017). Previous studies report that NAc presents different activity profiles during PCA (Flagel et al., 2007; Gillis and Morrison, 2019), and sign and goal-tracking behavioral expression may result in part from different learning mechanisms encoded by the NAc (Flagel et al., 2011). The OFC role on Pavlovian-approach was also previously demonstrated (Ostlund and Balleine, 2007; Flagel et al., 2011; Stringfield et al., 2017). Electrophysiological recordings during PCA demonstrate robust OFC neuronal activity to predictive CS and conditioned-approach (Stringfield et al., 2017). Previous studies demonstrate that sing-trackers present increased OFC c-fos mRNA expression (Flagel et al., 2011), and pharmacologic inactivation of OFC decreases sign-tracking behavior (Stringfield et al., 2017). However, AIE effects on OFC and NAc activity are less described in female rats. The important roles of OFC and NAc activity during PCA and the AIE effects on these structures denotes the importance of a better comprehension of these effects on female rats.

2. Methods

2.1. Animals

Female Sprague-Dawley rats (n=40) bred in-house were pair-housed during the alcohol exposure and initial training period. Animals received food and water ad libitum and were housed in a temperature - and humidity-controlled vivarium with a 12:12 hour light:dark cycle (lights on at 07:00). All experiments occurred during the light cycle. Experimental procedures were performed in accordance with the NIH Guide for Care and Use of Laboratory Animals and approved by the Institutional Animal Care and Use Committee of the University of North Carolina at Chapel Hill.

2.2. Adolescent Alcohol Exposure

Alcohol exposure and behavioral training procedures were performed as previously described (Madayag et al., 2017). Starting at postnatal day (P) 25, adolescent intermittent ethanol (AIE) or control exposure began. Rats received 5 g/kg of intragastric ethanol (25% v/v in water) or the equivalent volume of water (CON). The administration was performed once per day on a 2-days-on, 2-days-off regimen through P54, completing a total of 16 doses. We previously reported that this regimen did not affect developmental weight gain in females and produced blood ethanol concentrations of approximately 230 mg/dl at 60 min post-administration (Madayag et al., 2017).

2.3. Pavlovian Conditioning

Between P68 and P70, rats started PCA training. One hour prior to the beginning of the first session, a bottle of 20% sucrose (w/v in water) was placed in the rats' home cages, allowing them to familiarize themselves with the US solution. Next, the animals were placed in standard behavior chambers (MedAssociates, St. Albans, VT). Each of the behavior chambers contained a receptacle for dispensing liquid rewards (with photobeam detector to record receptacle entries), a cue light, and a retractable lever positioned below the cue light. White noise and a house light were active throughout the session. During the first training session, rats became familiar with non-contingent US delivery at the receptacle. In this session, 15 US deliveries (0.1 ml of 20% sucrose) were made on a variable inter-trial interval of 60-300 seconds (s), and no CS was presented in this session. Subsequent PCA sessions occurred daily on a Monday – Saturday schedule. Animals were placed in the behavioral chambers 5-minutes prior to the start of the session. During each PCA session, 15 CS-US trials occurred with a variable inter-trial interval of 60 to 300 s. Each trial consisted of a 30 s presentation of the CS (cue light illumination concurrent with the lever extension). The CS offset (cue light off and lever retraction) was immediately followed by the delivery of the US at the receptacle. After 15 training sessions, animals were separated into individual housing cages and 5 additional sessions were performed. Next, rats underwent 5 PCA sessions in larger, custom-built Plexiglas chambers (MedAssociates, ST. Albans, VT) that were similar to the training chamber, but optimized for electrophysiology recording, with angled walls to prevent the electrophysiological headstage from hitting the walls of the chamber.

2.4. Surgery

After the habituation to the custom-build chambers, stereotaxic surgery was performed for electrode array implantation. Rats were anesthetized with isoflurane (5% induction, 2-3% maintenance). During the surgery, two microwire electrode arrays were implanted; each array contained 8 stainless-steel Teflon-coated wires, 50-μm in diameter, and spaced 0.5 mm apart with a 2 x 4 configuration (NB Labs, Denison, TX). One array was placed in the OFC (3.7 mm anterior, 2.6 mm lateral from bregma, 5.0 mm ventral from the adjacent skull surface) and the second array was placed in the contralateral NAc (1.7 mm anterior, 1.5 mm lateral from bregma and 7.4 mm ventral from the adjacent skull surface), with side counterbalanced across animals. After the surgery, animals were monitored and received 50 mg/kg meloxicam s.c. daily for 3 days.

2.5. Behavioral and electrophysiology experiments

After at least 7 days of recovery from surgery, PCA sessions resumed in the customized behavior chambers. The animals first underwent 1-2 PCA sessions to reinstate the conditioned behavior. During the next 4 sessions, the

animals were gradually habituated to a flexible tether that connected electrode arrays to the headstage assembly. Thereafter, rats were tethered in all sessions.

Electrophysiological data was recorded during two sessions: a PCA baseline (typical) session followed by a reward omission session. The omission session was performed in order to evaluate behavioral flexibility due to changes in US availability (Stringfield et al., 2018). During the omission session, no US was delivered after any of the 15 CS presentations.

During the PCA baseline and omission sessions, neuronal activity was recorded as previously described (Fanelli et al., 2013; Robinson and Carelli, 2008; Stringfield et al., 2017) using a multichannel acquisition processor (MAP system with SortClient software; Plexon Inc., Dallas, TX, USA). For the recording sessions, the animals were tethered and placed in the behavioral chamber 15 minutes before the start of the PCA session; during this time the threshold setting for the electrode channels was set, and one of the channels in each array was manually selected as a differential reference channel for all channels in that array. During PCA sessions, MedAssociates software provided timestamps of the behavioral events (CS onset, lever presses, US delivery, and receptacle entry) that were temporally aligned by the MAP system with the electrophysiological recordings.

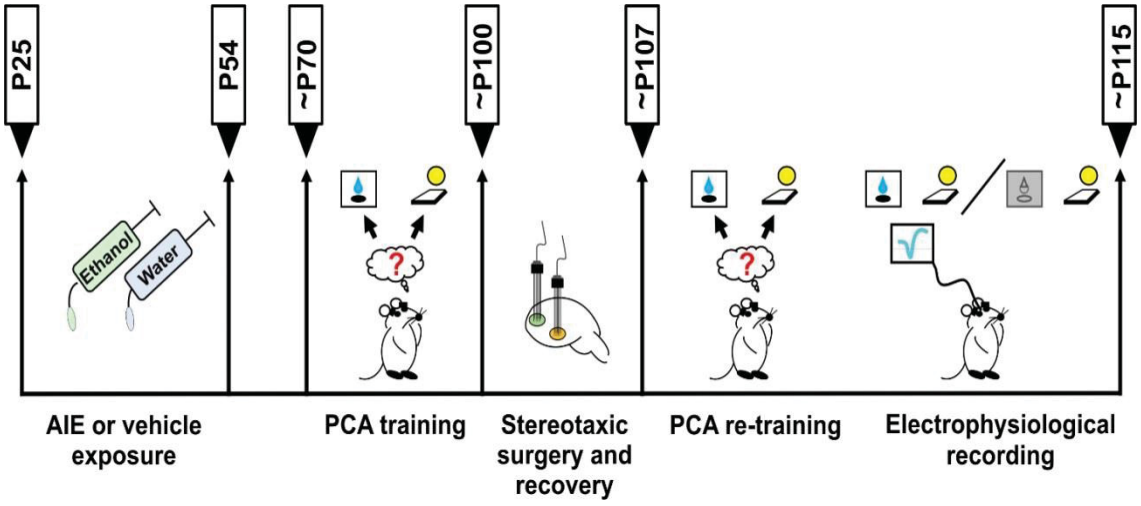

Fig. 1: Experiment timeline illustrative representation. Female Sprague-Dawley rats received ethanol administration across the adolescent period, through postnatal day (P) 25 to P 54 in a 2 days in 2 days off schedule. Starting around P 70, a total of 20 Pavlovian condition approach (PCA) training sessions were performed. Each PCA session consisted of 15 trials where a 30 seconds (s) CS (cue light/lever) was presented, followed by the US presentation (0.1 ml of a 20% sucrose solution) right after the CS offset. After the training phase, a stereotaxic surgery procedure was performed for electrodes array implantation on OFC and NAc, followed by 7 days of recovery. At least 5 additional PCA sessions were performed after the surgery recovery in order to habituate the animals with the electrophysiological recording procedure. Next, to evaluate possible AIE promoted effects on the neuronal activity, single-unit recordings in OFC and NAc were performed during a regular PCA baseline session followed by a reward omission session. During the reward omission session, all 15 trials were performed similarly to the PCA baseline session, with one important exception, after the 30 s CS period, no reward solution was delivered on the reward receptacle. For more details see methods.

2.6. Histology

Animals were anesthetized using 1.5 g/kg urethane i.p. (50% w/w in saline). A 10-μA current was applied for approximately 5 s to each stainless-steel wire to produce an iron deposit at the electrode tip, allowing determination of the recording site. Next, rats were perfused with a formaldehyde solution and the brains were removed. Histological confirmation of electrode placement was performed as previously described (Stringfield et al., 2017). Briefly, 40-μm brain slices were taken on a cryostat. The slices were stained with potassium ferracyanide and thionin to determine the electrode placements, and compared to a rat brain atlas (Paxinos and Watson 1998) to map the OFC and NAc electrode placements. Only data from microwires confirmed to reside in the target regions were included in the analysis.

2.7. Data analyses

2.7.1. Behavior data analyses

Behavioral data were digitally collected by MedAssociates software during all PCA sessions. The following behavioral metrics were analyzed: receptacle entries, receptacle elevation score, lever presses, latencies to approach the receptacle and to press the lever after CS onset to approach the receptacle and to press the lever, and probabilities of receptacle entry and lever press. The receptacle elevation score was calculated as the number of receptacle entries during the CS presentation minus the number of entries during the 30 s prior to the CS presentation; this metric reveals the conditioned response promoted by CS (Palmatier et al., 2014). Probabilities were calculated based on the number of trials when the animal performed the specific behavior (lever press or receptacle entry) at least once divided by 15 (total number of trials). To describe the relative performance of sign-tracking and goal-tracking conditioned responses, we adapted a ST-GT formula previously described by Madayag et al (2017) that included number of lever presses, elevation score, response latencies, and response probabilities, as presented in the following formula:

$$\frac{\left(\frac{\text{lev. press.} - \text{elev. score}}{\text{lev. press} + \text{abs. value of elev. score}}\right) + \left(\frac{recept.latency - lev.latency}{30}\right) + \left(\frac{Lev.prob. - Recept.prob.}{Lev.prob. + Recept.prob.}\right)}{3}$$

The resulting score could range from -1 to +1, and an animal was classified as “sign-tracking” with a score between +0.3 to +1, “intermediate” with a score from +0.29 to -0.29, and “goal-tracking” with a score between -0.3 to -1.

2.7.2. Neuronal firing analyses

Neuronal activity recorded from individual neurons during baseline and US-omission sessions was sorted using Plexon Offline Sorter software. Units were identified using automated cluster sorting based on principal component analysis and template sorting, informed by signal-to-noise ratios collected during the recording session. We considered a signal-to-noise ratio ≥2 and the existence of specific clusters after the principal component analysis for the sorting process criteria of inclusion. Timestamped data were imported into NeuroExplorer software (NEX Technologies, Madison AL), for the generation of perievent histograms of firing rates. Custom-written MATLAB programs (Mathworks, Natick, MA) were used to analyze the firing patterns of neurons surrounding experimental events, as previously described (Fanelli et al., 2013; Stringfield et al., 2017). Firing rates surrounding behavioral or experimental events were normalized by dividing the firing rate by the mean of the whole session firing rate. For population activity analysis in the NAc and OFC, the normalized neuronal activity was aligned to the events of interest and smoothed with a moving average of 250 ms in 50 ms steps. Neuronal population activity analysis was performed by calculating the mean firing rate of all neurons during selected events. To capture the neuronal firing pattern in response to an external event (CS onset, CS offset), the analysis window was 1 s immediately after the events. To capture the neuronal firing pattern surrounding a conditioned response (lever press, receptacle entry), the analysis window was 500 ms before and 500 ms after the event. To compare neuronal firing between groups or across sessions, we calculated the mean firing rate during the above analysis windows.

For individual neuronal analysis, a z-score calculation was performed to identify phasic changes in firing rate surrounding a particular event. The z-score calculation considerded the mean firing rate during the target window minus the mean firing rate during the baseline window, divided by the standard deviation of firing during the baseline window (2 s prior to the target window). Neurons with z-score >2 or <2 were classified as “excitatory” or “inhibitory” phasic neurons, respectively, and other neurons (z-score between -2 and 2) were classified as “non-phasic” neurons. Firing rate amplitude of excitatory phasic neurons was further analyzed by selection of the peak firing rate during the target window.

2.7.3. Statistical analysis

Behavioral parameters were measured using the D’Agostino & Person normality test, behavioral parameters that did not present a normal distribution were analyzed using nonparametric tests. Behavioral data from the last 5 days of the PCA training phase were analyzed using Mann-Whitney U (MWU) or t-test, depending on the normality distribution. Group comparison on the ST-GT score was also performed using MWU test. Behavioral data from the PCA baseline and reward omission session were analyzed using a generalized linear

regression (GLM) model with a Poisson distribution, a link log function, and Wald chi-square. However, for the variables that presented a normal distribution (elevation score, receptacle entries 30 s before CS onset, and receptacle entries during the CS period), a repeated-measures 2-way ANOVA was performed.

For the electrophysiological data analysis, comparisons of neuronal population activity and the peak firing rate of excitatory phasic neurons for each group were performed using the MWU test. Comparisons of the percentage of phasic neuronal activity between groups were analyzed using the chi-squared test. Because of the low numbers of inhibitory phasic neurons in both groups, we did not statistically compare them between groups. The GLM model was applied on behavioral and electrophysiological data analysis across the recording sessions.

To evaluate the hypothesis that OFC and NAc neuronal firing associates with subsequent behavioral responses, neuronal activity and behavioral data were correlated in each of the 15 trials in both recording sessions. For each OFC and NAc neuron, mean firing rate during the 1-s analysis window after CS onset was correlated with the total number of lever presses and receptacle entries (after the CS onset) and the latency to perform each of these responses. Fisher's correlation test was conducted to evaluate the possible existence of correlations between firing rate and behavioral parameters. Neurons that presented significant correlation (positive or negative correlation) were selected. Then, using a chi-squared test, we compared the percentage of neurons significantly correlated. Group and session comparisons were performed separately.

Analysis using the GLM model were performed using SPSS Statistics (IBM, Armonk, New York). The remaining analysis were performed using GraphPad Prism software (San Diego, CA). Statistical differences were considered when $P \leq 0.05$. Marginal differences were reported when $P > 0.05$ and < 0.1.

3. Results

3.1. PCA training phase

To evaluate potential effects of AIE exposure on conditioned approach, animals began Pavlovian conditioning at P68-P70, at least 15 days after the final ethanol administration (Fig. 1). The rats progressively acquired conditioned approach to the CS and reward receptacle across the initial 20 training sessions (Supplemental Fig. S1 A). Data from the last 5 sessions were averaged for analysis. While AIE-exposed rats exhibited slightly stronger sign-tracking behavior (lever presses, latency to press, probability of lever press) as a group compared to control-exposed rats, no statistical differences emerged (Mann Whitney test, P's>0.05; Supplemental Fig. S1 B and Supplemental Table 1).

Similarly, goal-tracking behavior (elevation score, latency to enter receptacle, probability of receptacle entry) did not differ between exposure groups (Mann Whitney test, P's>0.05; Supplemental Fig. S1 B and Supplemental Table 1).

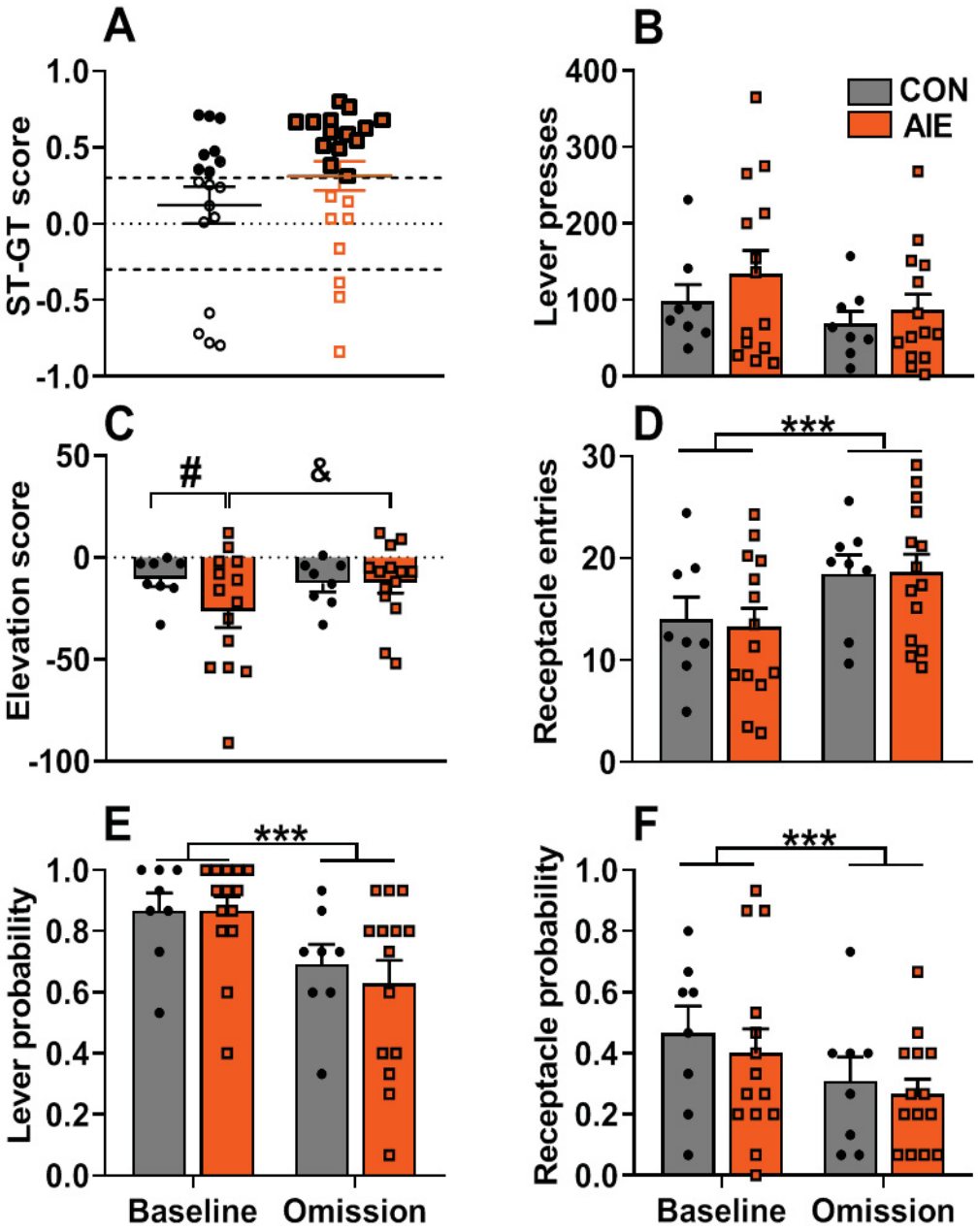

Fig. 2: AIE exposure promoted decrease in the reward receptacle interaction. Behavioral data acquired during the baseline session was used for the sign-tracking/goal-tracking score calculation. After classification, data analysis was performed only in sign-tracking animals. **A.** Sign-tracking/goal-tracking score calculation: animals were categorized as goal-trackers if the score was between -1 and -0.3 (CON n= 4, AIE n= 3), sign-trackers if presented a score between 1 and 0.3 (CON n= 8, AIE n=14), and as intermediate if the score was between -0.29 and 0.29 (CON n= 6, AIE n= 5). No significant group difference was observed on score calculation (P= 0.21). **B.** Total number of lever presses: no significant AIE effect was observed (P's>0.05). **C.** Receptacle elevation score: data analysis demonstrated significant main effects of exposure (P=0.01), and session (P=0.03), and also a significant interaction between exposure versus session (P=0.02). Sidak's post-hoc comparisons demonstrated a more

negative elevation score presented by AIE group during the baseline session compared to CON group (P=0.03). Also, the elevation score presented by AIE group on baseline session was significantly lower when compared to omission session (P=0.01). **D.** Total number of receptacle entries during the 30s CS period: a significant main effect of session was observed (P<0.001). However, no significant main effect of exposure or interaction between the factors was observed (P's>0.05). **E.** Lever press probability: a marginal exposure effect was observed (P=0.08) and also a significant main effect of session (P<0.001). However, no interaction between the factors was observed (P=0.19). **F.** Receptacle entry probability: a marginal exposure effect was observed (P=0.08) and a significant main effect of session (P<0.001). However, no interaction between the factors was observed (P=0.88). Data are expressed as mean ± SEM. In figure **A**, sign-tracking animals are specifically represented by the filled symbols, black circles for CON, and orange squares for AIE. **B-F** The symbols in black for CON (n=8) and orange on AIE (n=14) represent individual subjects data. *** main effect of session (P<0.001). # group difference in baseline session (P≤0.05). & session difference in the AIE group (P≤0.05). For statistical details see Supplemental Table 2.

3.2- Behavioral data during PCA baseline and reward omission sessions

After the training phase, animals underwent stereotaxic surgery and recovery for implantation of electrodes arrays in the OFC and NAc. Electrophysiological recording occurred after rats were habituated to the tether in two sessions: a regular conditioning session (baseline) and a session in which the CS was presented, but the US reward was omitted (omission session).

As the animals can present distinct phenotypes during the conditioning sessions (sign-tracking, goal-tracking, or intermediate), we first classified rats by the phenotype exhibited in the baseline session. Using a composite score of the relative sign-tracking to goal-tracking behavior, each of these phenotypes was observed in both groups, but the majority of the animals presented the sign-tracking phenotype. Specifically, 14/22 (63.6%) AIE rats and 8/18 (44.4%) CON rats were classified as sign-trackers, a proportion that was not significantly different (P>0.05; Fig. 2 A and Supplemental Table 1). As both behavioral phenotype and AIE exposure could contribute to differences in neuronal firing patterns, and because we primarily aimed to evaluate the consequences of AIE on reward processing, the remaining analyses focused exclusively on sign-trackers. By equating the behavioral phenotype to the predominant group, we could more confidently attribute group differences in neuronal firing patterns to exposure.

We next assessed specific metrics of conditioned approach in the sign-tracking subset of rats, comparing the baseline to the omission session. As expected, sign-tracking behavior was similar between groups, with no significant main effect of exposure (P's>0.05; Fig. 2 B, E and Supplemental Fig S2 B, Supplemental Table 2). Moreover, while lever presses and lever latency did not significantly differ by day, the probability of pressing the lever during a trial was lower on the omission day than the baseline day in both groups (P<0.001; Fig 2 E, Supplemental Table 2).

A significant effect of exposure was observed when elevation scores were calculated to investigate interaction with the location of reward delivery during CS presentation, a measure of goal-tracking (P=0.01; Fig 2 C). The AIE group presented a more negative elevation score on the baseline day (P=0.02), and post-hoc comparisons revealed a difference in elevation score between baseline and omission sessions only for animals in the AIE group (P=0.01). These changes in elevation score demonstrate that AIE exposure promoted a decrease in interactions with the reward receptacle that were driven by CS presentation. Next, we analyzed the total number of receptacle entries performed during the CS period (Fig 3 D) or during the 30 s before CS onset (Supplemental Fig S2 A). We found significant differences between the baseline and omission sessions where a significant increase emerged for entries during CS presentation (P<0.001), while a significant decrease emerged for receptacle entries that occurred in the 30 s prior to CS onset (P<0.001). AIE exposure did not result in a significant difference in either behavior. A decrease in the probability of entering the receptacle was observed between the baseline and omission sessions, but there was no effect of AIE exposure on the latency to enter or probability of entering the receptacle (P<0.001; Fig. 3 F and Supplemental Fig S2 C; Supplemental Table 2).

To evaluate possible behavioral changes during the baseline and omission sessions, we averaged the data from the first 5 trials (trials 1 to 5) and last 5 trials (trials 11 to 15) of each session. As expected, sign-tracking behavior was consistently performed throughout the baseline session and no significant effect of AIE was observed (P's>0.05; Supplemental Fig. S3 A, C, and E, Supplemental Table 3). During the omission session, both groups significantly decreased sign-tracking behavior (P's<0.01; Supplemental Fig. S3 G, I, K. Supplemental Table 3). A significant interaction was observed for lever presses during the omission session (P=0.02), but post-hoc comparisons did not yield significant differences. For measures of goal-tracking behavior, we observed a marginal effect of time on elevation scores during the baseline session (P=0.06) and a significant group × time interaction (P=0.03). However, post-hoc comparisons demonstrated no significant differences (P>0.05; Supplemental Fig. S3 B. Supplemental Table 3). Elevation scores increased significantly across the omission session (P=0.002), where both groups altered the proportion of receptacle entries that occurred before or during CS presentation at the end of the session compared to the beginning. However, there was no effect of AIE (P>0.05; Supplemental Fig. S3 H). No change was observed for the latency and probability to perform a receptacle entry across both sessions (P's>0.05; Supplemental Fig. S3 D, F, J, and L. Also see Supplemental Table 3).

3.3 – Single-unit recording during PCA baseline and reward-omission sessions

To evaluate whether AIE exposure altered neuronal activity in the OFC and NAC of these sign-tracking animals, single-unit recordings were conducted during the baseline and reward-omission sessions. We performed histological analysis to confirm the anatomical placement of electrodes. In CON rats, 57 electrodes were located in the OFC and 55 in the NAc, with 11.6 ± 2.1 neurons recorded from each rat (range 18 – 5 neurons). In AIE rats, 93 electrodes were located in the OFC and 89 in the NAc, with 8.15 ± 2.7 neurons recorded from each rat (range 13 – 2 neurons). CON and AIE groups presented similarly distributed electrodes location in the medial and lateral OFC, and the majority of the placements were located in the core of the NAc for both groups (Supplemental Fig. S4).

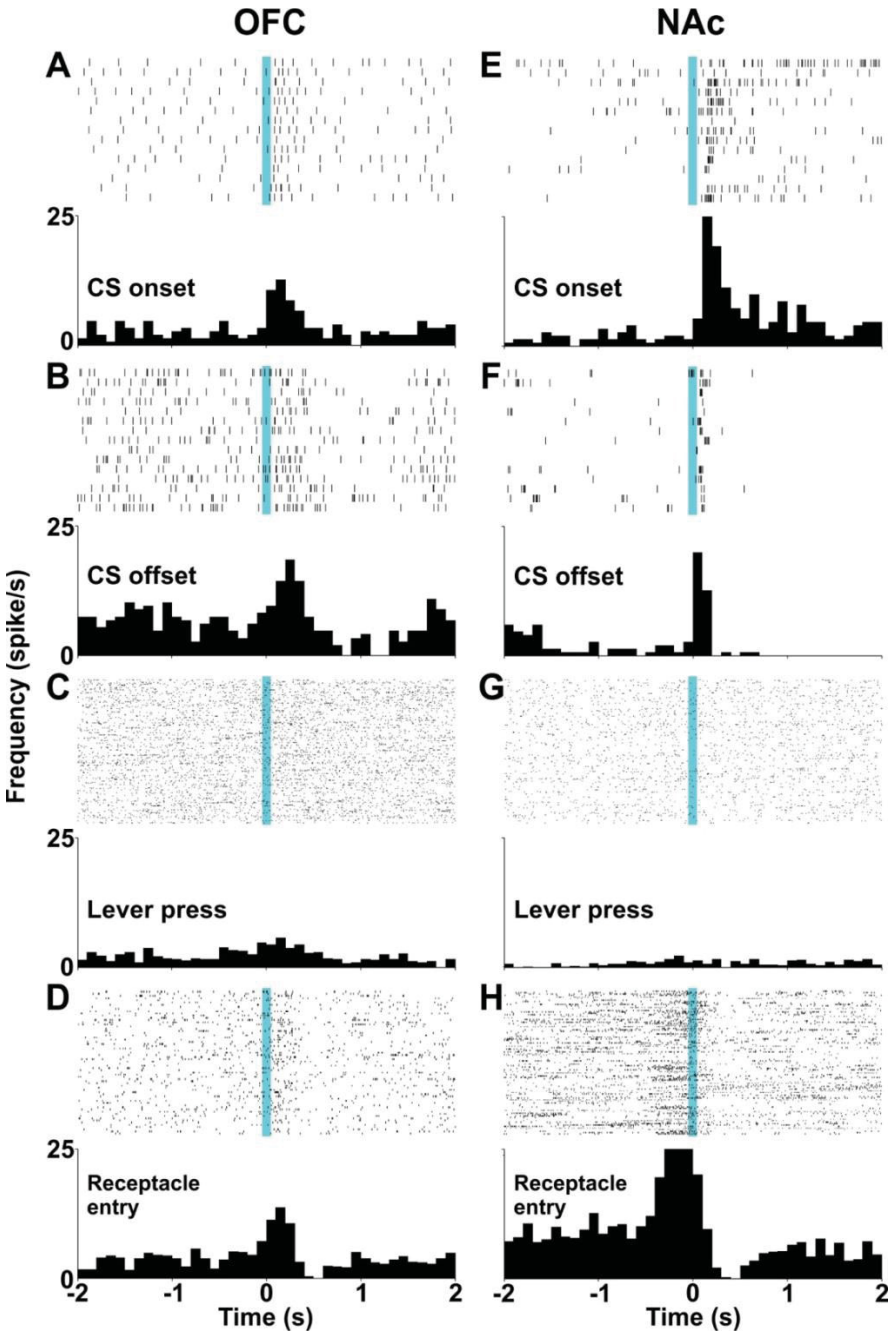

Fig 3. Examples of individual neuron activity. A – H Neuronal activity during events of interest (blue bar) is presented in rasters and perievent histograms for individual neurons. A 2-second (s) window before and after the events of interest was used for neuronal activity representation.

To determine whether AIE exposure altered the basal firing rate of OFC or NAc neurons, we compared firing rate during the 60 s before the start of the PCA sessions. Neurons recorded from AIE-exposed rats presented a marginal difference in the OFC basal firing rate during the baseline session (P=0.08), but no difference was observed during the omission session (P=0.76) (Baseline - CON: 3.03 ± 0.41 Hz, AIE: 4.02 ± 0.54 Hz. Omission - CON: 4.06 ± 0.58 Hz, AIE: 4.24 ± 0.46). No differences in NAC basal firing rate were observed during baseline (P=0.47) and omission sessions (P=0.33) (Baseline - CON: 3.15 ± 0.54 Hz, AIE: 2.81 ± 0.45 Hz. Omission - CON: 3.54 ± 0.63 Hz, AIE: 4.19 ± 0.54). A marginal difference in firing rate over the whole session was observed in the OFC during the PCA baseline session (CON: 3.19 ± 0.36 Hz, AIE: 4.05 ± 0.41 Hz), where the AIE group presented a higher whole session firing rate (P=0.09). However, no difference was observed during the omission session (CON: 4.03 ± 0.43 Hz, AIE: 3.60± 0.35 Hz) (P=0.67). No difference was observed in the NAc for the whole session firing rate during baseline (P=0.82) or omission sessions (P=0.34) (Baseline - CON: 3.26 ± 0.41 Hz, AIE: 3.43 ± 0.44 Hz. Omission - CON: 3.40 ± 0.47 Hz, AIE: 3.99 ± 0.41).

3.3.1 – OFC and NAc neuronal activity during the PCA baseline session.

To evaluate the effect of AIE exposure on neuronal activity associated with conditioned cues and behavior, we assessed changes in firing rate of OFC and NAc neurons time-locked to the CS, lever presses, and receptacle entries, signal-averaged across the 15 trials of the baseline session (Fig 3).

We analyzed OFC neuronal population activity by creating peri-stimulus time histograms centered at CS onset, the predictive cue that stimulated conditioned responding, and cue offset, the cue that predicted imminent reward delivery. We observed higher mean firing rates in AIE rats than CON rats (Fig. 4 A and C, Supplemental Table 4) in response to both CS onset (P=0.05) and CS offset (P=0.02). Next, we determined whether individual neurons displayed phasic excitation, phasic inhibition, or neither based on their firing pattern at CS onset and offset (Fig. 4 B and D). In AIE rats, 25% of OFC neurons exhibited phasic excitation to the CS onset and 31% to the offset, while in CON rats, the proportions were 15% and 18%, respectively. No significant differences were found for peak firing rates of phasically excited neurons compared between groups (inset, P's > 0.05; Supplemental Table 4). Fewer than 10% of OFC neurons exhibited phasic inhibition to either stimulus in either group. Thus, the greater proportion of neurons exhibiting phasic excitation in AIE rats compared to CON rats, rather than the magnitude of excitation, appeared to underlie the population difference.

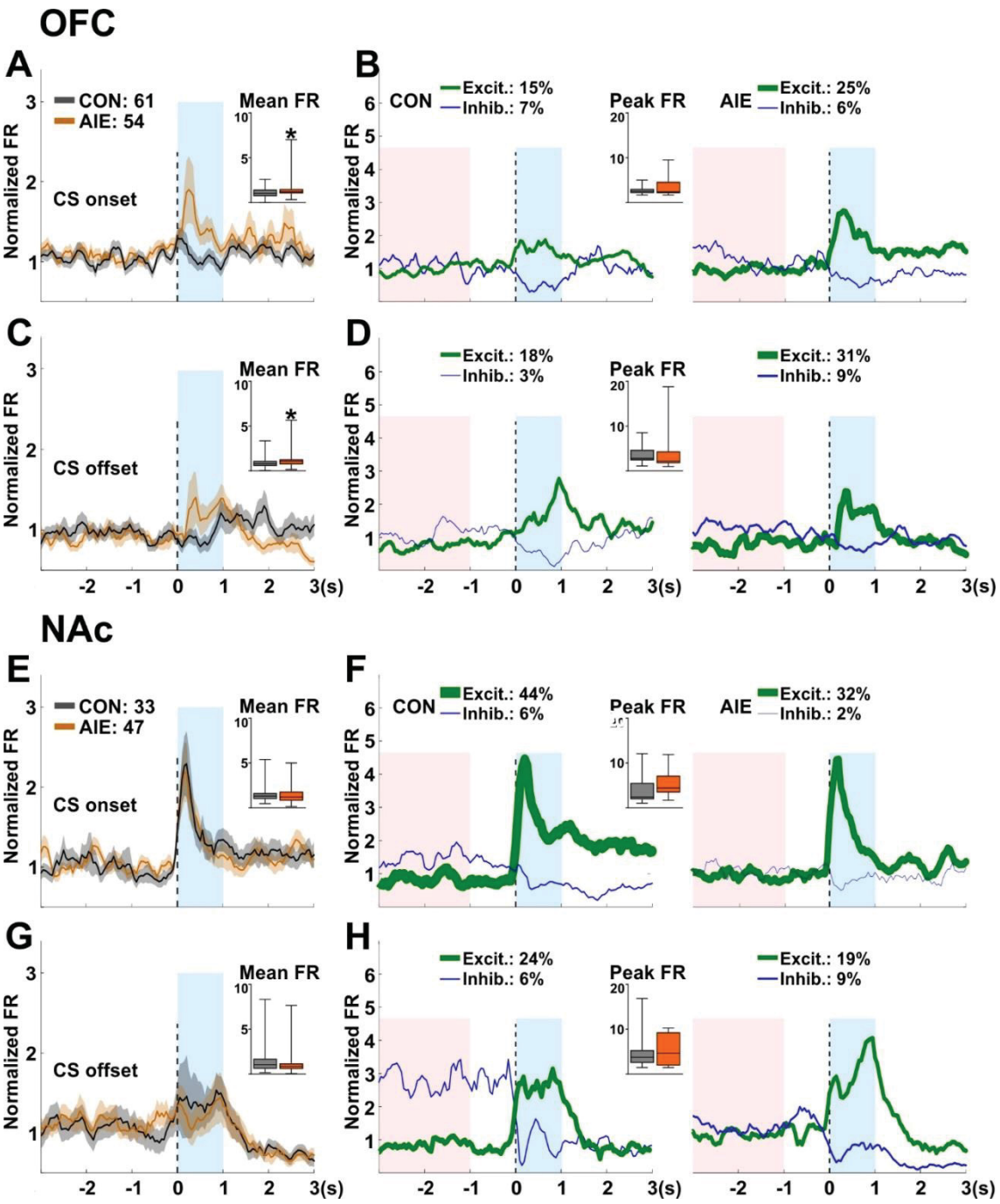

Fig. 4: AIE exposure increased neuronal excitatory activity in OFC but not NAc at CS onset and CS offset. Single-unit activity of OFC and NAc neurons were recorded during the PCA baseline session in sign-tracking rats. Neuronal population activity data (**A, C, E, G**) are normalized to the whole session firing rate and presented as mean firing rate (line) ± SEM (shading) for CON (gray) and AIE (orange) groups. Number of recorded cells: OFC= 61 cells on CON and 54 cells on AIE, NAc= 33 cells on CON and 47 cells on AIE. Inset: box plots show the mean firing rate in the target window (blue box). Phasic firing patterns (**B, D, F, H**) for neurons that showed significant changes (excitations: green, inhibitions: blue) in firing rate are shown for CON (left graphs) and AIE (right graphs) groups, with line thickness reflecting the proportion of neurons exhibiting that phasic activity (non-phasic cells are not shown). Inset: box plots show the amplitude of excitation during the target window (blue box) compared to the baseline period (red box) for each phasic excitatory cell**. A.** OFC population activity during CS onset: neurons from AIE-exposed rats showed significant higher excitatory activity after CS onset (P=0.05). **B.** OFC phasic activity during CS onset: peak amplitude and percentage of phasic excitatory activity were not affected by AIE. **C.** OFC population activity during CS offset:

neurons from AIE-exposed rats displayed significant higher excitatory activity compared to CON group (P=0.02). **D.** OFC phasic activity during CS offset: the percentage of phasic excitatory activity was marginally affected by AIE (P=0.09). No AIE effect on peak amplitude. Figures **E** to **H** represent NAc neuronal population and phasic activity during CS onset and CS offset events. No statistical difference was observed in the NAc neuronal population activity or in the neuronal phasic activity after CS onset and CS offset events (P's>0.05). *significant group difference on mean firing rate on neuronal population activity (P<0.05). For statistical details see Supplemental Table 4.

Similar analyses were carried out on NAc neuronal firing patterns. Robust excitation to the CS onset was observed in NAc neurons in AIE and CON rats, and a lesser excitation to the CS offset, with no differences between groups (P's > 0.05; Fig. 4 E and G, Supplemental Table 4). When individual NAc neurons were classified by firing pattern, 32% of neurons in AIE rats and 44% in CON rats exhibited phasic excitation to the CS onset, and 19% of neurons in AIE rats and 24% in CON rats exhibited excitation to the CS offset. No group difference was found in the peak firing rate of these phasically excited neurons (P's > 0.05; Fig. 4 F and H, Supplemental Table 4). As in the OFC, fewer than 10% of NAc neurons in either group displayed phasic inhibition to either stimulus. In summary, while cue-evoked excitation was generally greater in the NAc than the OFC, AIE exposure only enhanced cue-evoked excitation in the OFC but not the NAc.

To evaluate AIE effects on neuronal activity during conditioned behavioral responses, we analyzed neuronal firing around the first lever press and first receptacle entry performed after the CS onset. In the OFC, little change in firing rate to conditioned responses was observed at the population level, and no differences were observed between AIE and CON groups (Fig. 5 A and C, Supplemental Table 4). Individual neurons analysis demonstrated a similar pater of phasic excitation in both conditioned responses for AIE and CON groups (25% and 13% for the first lever press and 20% and 21% for first receptacle entry in respective groups). Also, no difference was observed after comparing the peak firing rate (P's>0.05; Fig. 5 B and D, Supplemental Table 4). Similarly, in the NAc we observed little change in population firing rate at lever presses (P>0.05; Fig. 5 E), and there was no statistical difference between AIE and CON groups in the firing rates of phasically excited neurons (P>0.05; Fig. 5 F). However, a significant group difference was observed in the population firing rate during the first receptacle entry after CS onset, in that CON rats exhibited greater excitation than AIE rats (P = 0.002; Fig. 5 G and Supplemental Table 4). Underlying this population effect, phasic activity analysis demonstrated that a significantly larger proportion of NAc neurons displayed phasic excitation in CON rats compared to AIE rats (56% versus 6% of the neurons, respectively. P<0.001; Fig. 5 H and Supplemental Table 4), even though the amplitude of excitation was similar (P> 0.05).

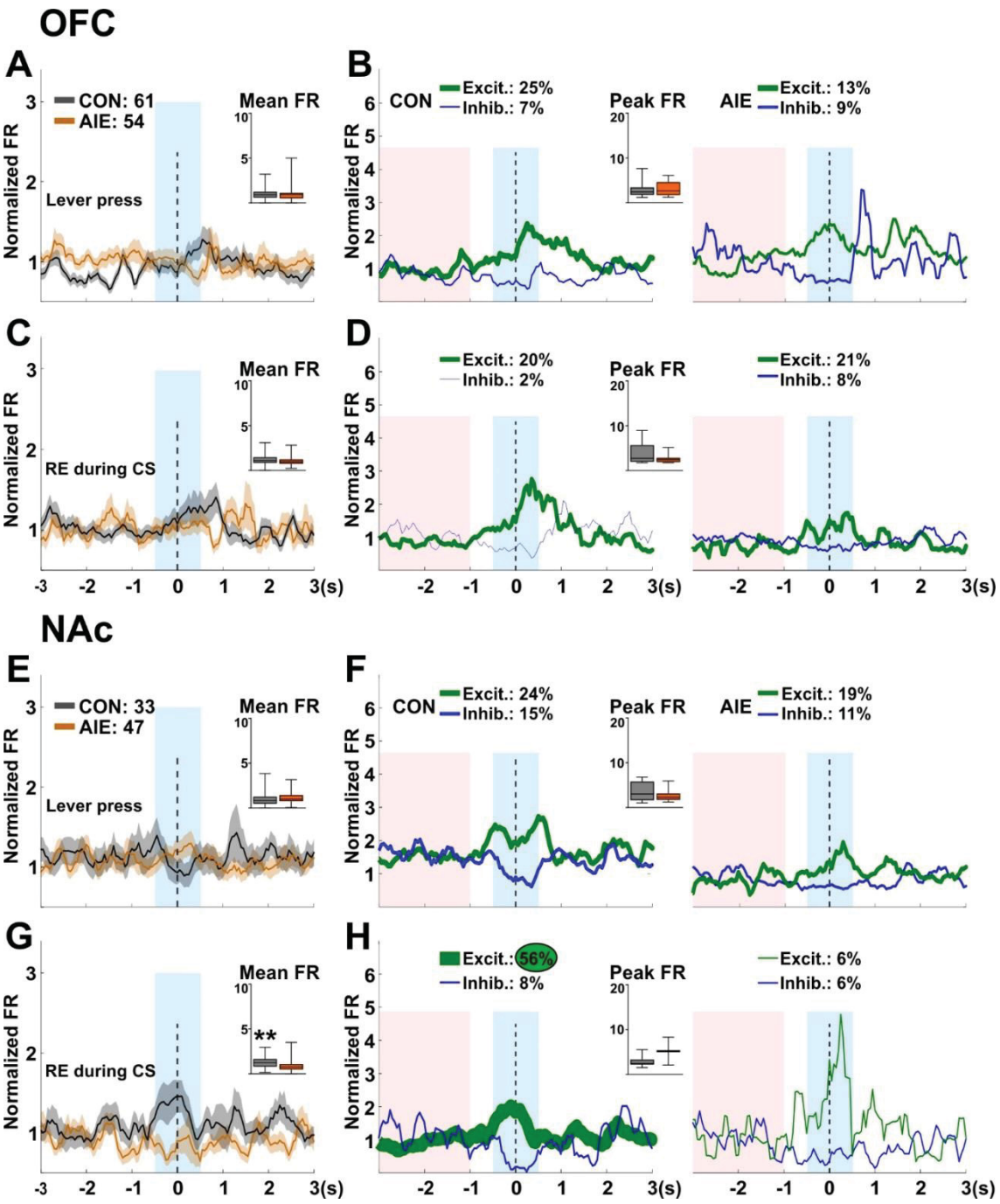

Fig. 5: AIE exposure promoted a decrease in NAc activity during the first receptacle entry on the CS period, but no effect on the lever press. Single unit activity for the first LP and first RE during the CS onset events were analyzed on OFC and NAc during the PCA baseline session. **A.** OFC neuronal population activity on the first LP. **B.** OFC neuronal population activity on the first RE during the CS onset. No statistical difference was observed in OFC population activity in response to the first LP (P=0.65) and first RE during the CS onset (P=0.35). **C**. NAc population activity in response to the first LP. **D.** NAc population activity in response to first RE during the CS onset. A significant group difference was observed in response to the first RE during the CS onset (MWU=223, P=0.002), but no statistical difference was found for NAc activity for the first LP (P=0.14). **E.** Neuronal phasic activity in OFC in response to the first LP demonstrated no statistical difference in both percentage and peak of FR of phasic excited neurons (P=0.33 and P=0.11, respectively). **F.** Also, no differences were observed on OFC on the analysis of the percentage and peak of FR of phasic excited neurons for the first RE during the CS onset (P=0.58 and P=0.44, respectively). **G.** On NAc phasic activity in response to the first LP no statistical difference was observed (Percentage of phasic

excitation: P=0.58; Peak of FR on phasic excited neurons: P=0.67). **H.** However, a group difference was observed on the comparison of percentage (X^2=17.65, df=1, P<0.001) but no difference in the peak of FR for the phasic excited neurons (P=0.81). For statistical details see supplementary table 4. Neuronal population activity data are presented as mean firing rate (FR) ± SEM (shaded color) and normalized by the whole session FR for CON (gray) and AIE (orange) **(A-D)**. On neuronal phasic activity graphs neurons that presented a phasic excitation are represented in the green histograms, and neurons that presented a phasic inhibition are represented in the blue histograms. The histograms line thickness demonstrates the proportion of the neurons that presented these patterns of activity **(E-H)**. Blue boxes represent the analysis window for the neuronal activity (-0.5 to 0.5 s). Red boxes represent the baseline window for z-score calculation (2 s). The inside box plots data are presented in median, interquartile range, and minimum and maximum data values. MWU test was used for group comparisons on mean FR (on neuronal population analysis), and for analysis of the peak FR (on phasic excited neurons). Chi-square test was used for group comparisons on the percentage of phasic excited neurons. ** significant group difference on mean FR (P<0.01).

While lever presses only occurred during CS presentation, receptacle entries could occur either during the CS or apart from the CS. Thus, to further explore the relationship between conditioning and the behavior of receptacle entry, we assessed neuronal activity surrounding receptacle entries in the 30 s before CS onset and after CS offset when the rat retrieved the reward (Supplemental Fig. S5). In both OFC and NAc, receptacle entries prior to the CS were not associated with changes in population firing rates (P's> 0.05; Supplemental Fig. 3 A and E). At the individual neuronal level, approximately 30% of neurons in the OFC and over 20% of neurons in the NAc exhibited phasic excitation, with no differences in the proportion or amplitude of excitation between groups (P's> 0.05; Supplemental Fig. 3 B and F). In contrast, we observed higher population firing rates in both OFC and NAc to receptacle entries after CS offset, when rats approached to retrieve the reward. This was supported at the individual neuronal level by a larger proportion of neurons exhibiting phasic excitation (28-50%) and by larger amplitudes of excitation, although these were not different by group. These results demonstrate that the higher NAc activity observed in CON rats during conditioned receptacle entries was specifically related to conditioned approach and not the behavior per se.

3.3.2 – OFC and NAc neuronal activity during reward omission session.

To evaluate whether AIE exposure could alter neuronal activity in response to changes in the CS-US contingency, we recorded from the OFC and NAc in the same rats during the reward omission session. Our initial analysis focused on trials 6-15, after the rats learned that the reward would not be delivered. Consistent with the result from the baseline session, we observed a group difference on OFC population activity in response to the CS onset (Fig. 6 A) where the mean firing rate to CS onset was significantly higher in the AIE group (P=0.04, Supplemental Table 4). This result demonstrates a consistent change in OFC activity in response to the CS onset promoted by AIE, an effect that was observed even in the absence of the US. However, in contrast to the

baseline session, no group difference was observed on OFC in response to the CS offset (P>0.05; Fig. C and Supplemental Table 4).

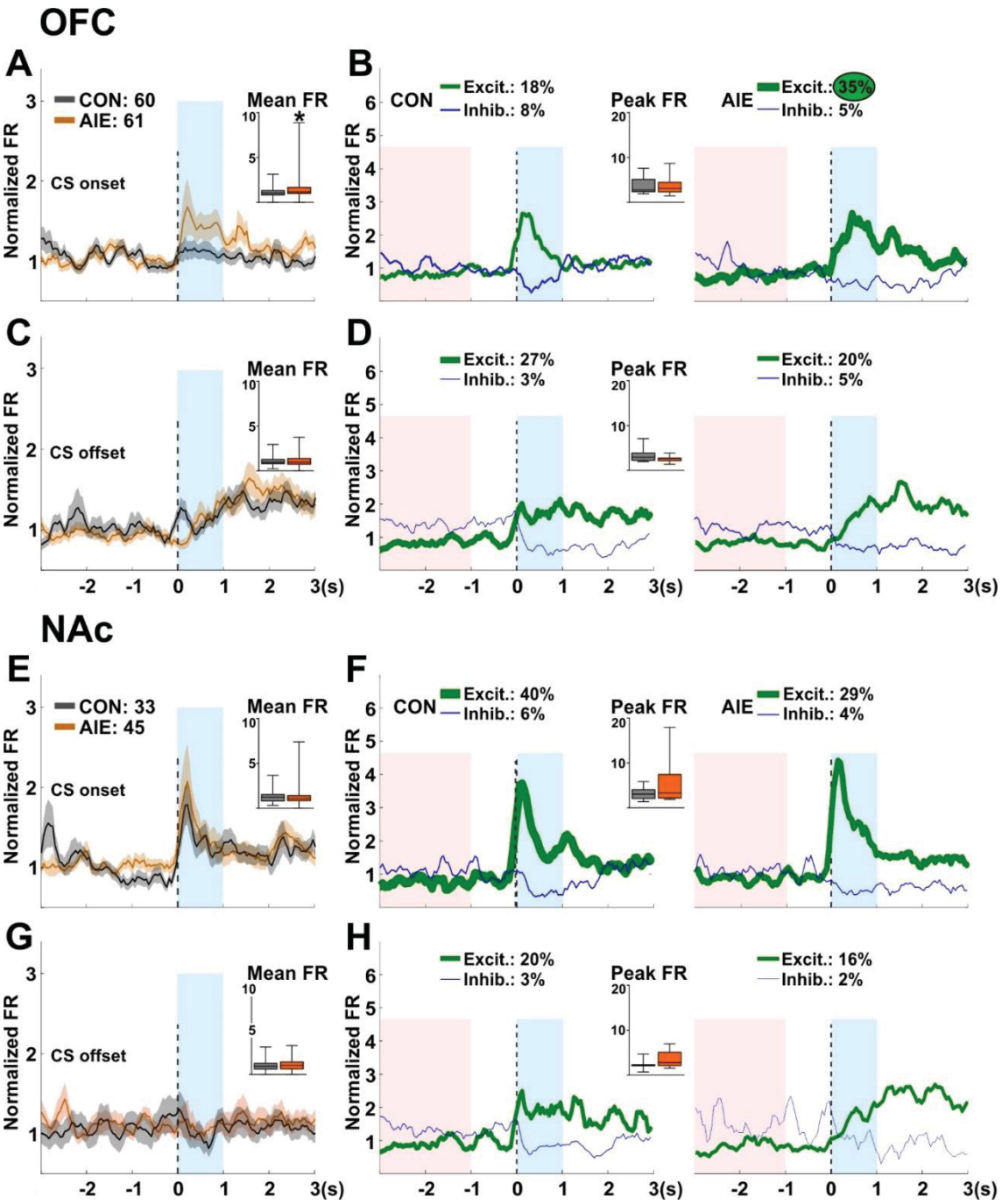

Fig. 6: On OFC, the higher excitatory activity after CS onset promoted by AIE exposure was observed even after changes in CS-US contingency. Single-unit activity of OFC and NAc neurons were recorded during the reward omission session in sign-tracking rats. Neuronal population activity data (A, C, E, G) are normalized to the whole session firing rate and presented as mean firing rate (line) ± SEM (shading) for CON (gray) and AIE (orange) groups. Number of recorded cells: OFC= 60 cells on CON and 61 cells on AIE, NAc= 33 cells on CON and 45 cells on AIE. Inset: box plots show the mean firing rate in the target window (blue box). Phasic firing patterns (B, D, F, H) for neurons that showed significant changes (excitations: green, inhibitions: blue) in firing rate are shown for CON (left graphs) and AIE (right graphs) groups, with line thickness reflecting the proportion of neurons exhibiting that phasic activity (non-phasic cells are not shown). Inset: box plots show the amplitude of excitation during the

target window (blue box) compared to the baseline period (red box) for each phasic excitatory cell. A. OFC population activity during CS onset: a significant higher excitatory activity after CS onset was observed in OFC cells recorded on AIE-exposed animals (P=0.04). B. OFC phasic activity during CS onset: AIE exposed animals displayed a significantly higher percentage of phasic excited cells compared to CON group (P=0.04). However, no significant group difference was observed in the amplitude of the phasic excitation (P=0.78). C. OFC population activity during CS offset: no significant AIE effect was observed (P=0.56). D. OFC phasic activity during CS offset: no group difference was observed on the percentage of cells that displayed phasic excitation (P=0.60), neither on the amplitude of the excitatory activity (P=0.28). Figures E to H represent NAc neuronal population and phasic activity during CS onset and CS offset events. No statistical difference was observed in the NAc neuronal population activity or in the neuronal phasic activity after CS onset and CS offset events (P's>0.05). *significant group difference on mean firing rate on neuronal population activity (P<0.05). The green circle represents a significant group difference in the percentage of neurons that displayed phasic excitatory activity. For statistical details see Supplemental Table 4.

A significant larger proportion of individual neurons from the AIE group presented phasic excitation after CS onset (18% versus 35% of neurons on CON and AIE groups, respectively. P=0.04; Fig 6 B, Supplemental Table 4). However, the amplitude of the excitatory activity to CS onset did not differ between groups (P>0.05). At CS offset, a comparable proportion and amplitude of excitatory activity was observed from CON and AIE groups (27% and 20% of neurons, respectively). Similarly to the results from the baseline session, no group difference in population activity to CS onset or CS offset was observed (P's>0.05; Fig. 6 E and G, Supplemental Table 4). Consistent with the baseline session, strong phasic excitatory activity was observed from NAc neurons after CS onset where 40% of CON and 29% of AIE neurons presented this phasic excitatory activity. However, CON and AIE groups did not differ on the proportion or in the amplitude of this activity (P>0.05; Fig. 6 F, Supplemental Table 4). No group difference was observed in the proportion of phasic excitation after CS offset (20% and 16% of neurons from CON and AIE groups, respectively. P>0.05; Fig. 6 H, Supplemental Table 4), or in the amplitude of the excitatory response.

As expected from previous studies (Holland, 1979; Stringfield et al., 2018) during the omission session most of the animals did not perform receptacle entries during the 30 s CS presentation (Supplemental Fig. 2), preventing analysis of neuronal activity surrounding this behavior. No statistical difference in neuronal population activity in the OFC or NAc was observed for receptacle entries before CS onset, lever presses, and receptacle entries after CS offset (P's>0.05; Supplemental Fig. S6 A, C, E and G, Table 4). Although no group differences were observed in the percentage of phasically excited OFC or NAc neurons during behavioral responses, (P's>0.05, Table 4), a significant difference was demonstrated in the NAc activity in the response for the first receptacle entry that occurred before the CS onset where phasically excited neurons recorded from the CON group presented a significantly higher peak firing rate (P=0.02; Supplemental Fig. S6 H). No other difference in the peak firing rate was found for the other behavioral responses in both brain structures (P's > 0.05. For more detailed statistical information see Supplemental Table 4).

3.3.3 – Behavioral data and single-unit recording across trials

Next, we evaluated if the elevated neuronal response to CS presentation in the AIE group was consistent across different stages of the recording sessions. Neuronal population data after CS onset and CS offset was averaged across trials 1 to 5 and trials 11 to 15. Consistent with results presented previously, a significant effect of exposure was observed in both baseline ($P=0.01$) and omission sessions ($P=0.04$). AIE enhanced excitatory activity in the OFC after CS onset and this effect was consistent at the beginning and end of both sessions (Fig. 8 B and F. Also see Supplemental Table 5). When we compared excitatory activity to CS offset, we observed a marginal main effect of AIE exposure during the baseline session ($P=0.06$; Fig. 8 D) and no group differences during the omission session ($P>0.05$; Fig. 8 H; Supplemental Table 5). No AIE effect or changes across the different stages of the session were observed in the NAc after CS onset and CS offset ($P's>0.05$, Supplementary Fig. 6 A to H. Also see Table 5).

3.4 – Neuronal activity to CS onset and subsequent conditioned approach

We hypothesized that the firing pattern to the CS onset in a subset of neurons would predict subsequent conditioned behavior. To test this, w computed the mean firing rate in the 1 s after CS onset for each neuron and each trial, then performed Spearman correlation analysis to correlate neuronal activity with behavioral measures in each trial: the number of lever presses, the number of receptacle entries, and the latency to perform a lever press or receptacle entry. We found that the CS-associated firing rate in a subset of neurons in both the OFC and NAc significantly correlated with some aspect of subsequent behavior (Fig. 9). Next, we used separate chi-squared tests to determine the effects of exposure and session on the proportion of predictive neurons. The proportion of OFC-correlated neurons in CON rats was similar between baseline and omission sessions, while there were significantly fewer correlated neurons in AIE rats during the omission session compared to the baseline session ($X^2=3.589$, $df=1$, $P=0.04$) and compared to the proportion of correlated neurons in CON rats during the omission session ($X^2=4.334$, $df=1$, $P=0.03$). In the NAc, the proportion of correlated neurons did not differ by session in either CON or AIE rats, but AIE rats exhibited more correlated neurons during the baseline session than CON rats ($X^2=8.681$, $df=1$, $P=0.002$). Thus, AIE exposure altered the association between neuronal response to the CS and subsequent conditioned approach, although the nature of the alteration was different depending on the brain region.

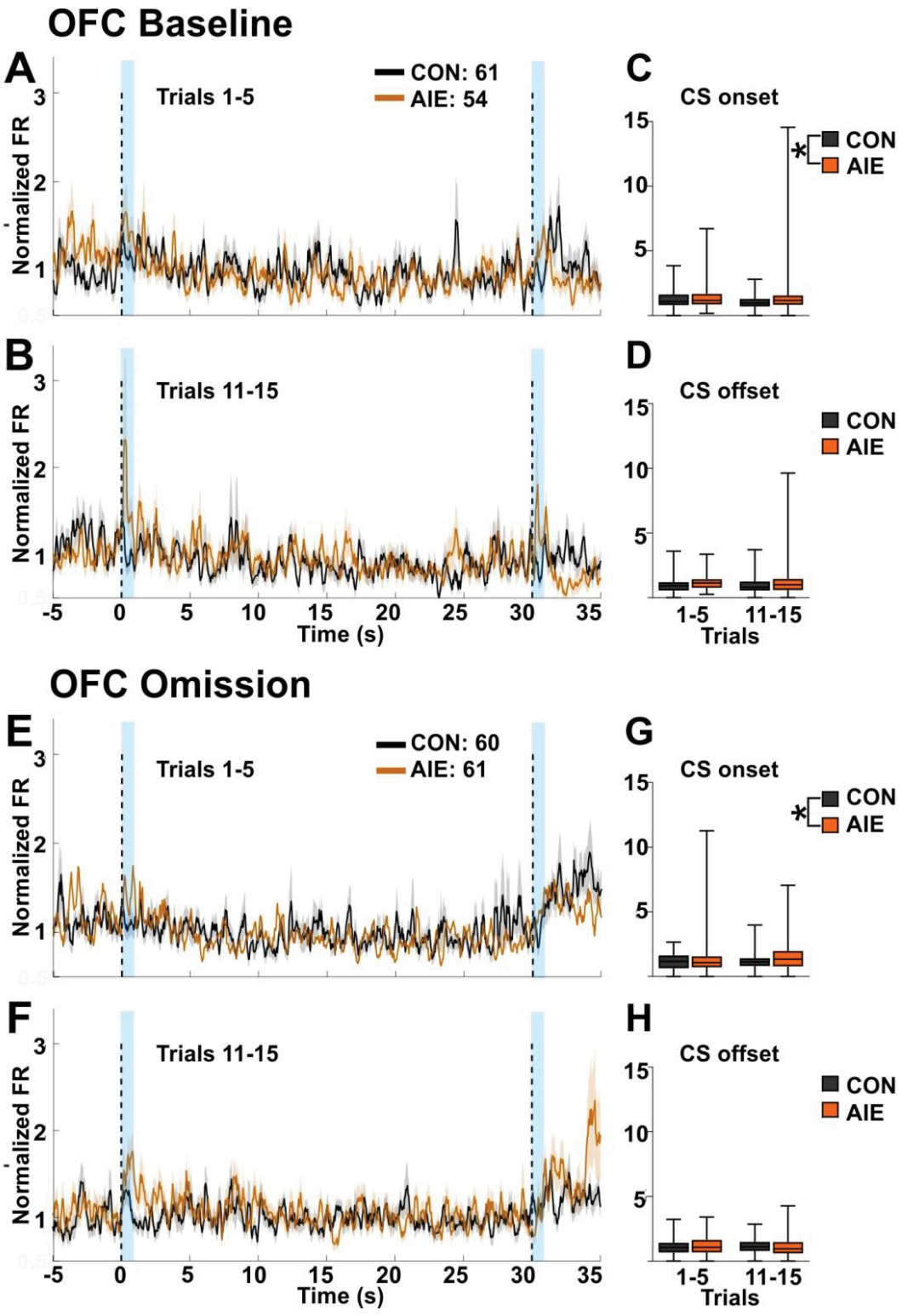

Fig. 8: The AIE promoted effect on OFC population activity after CS onset was consistently observed across baseline and omission session. Single-unit activity on OFC in response to CS onset and CS offset (dashed lines) was acquired during trials 1 to 5 and trials 11 to 15 in both baseline and omission session. Figures **A**, **B, E,** and **F** represent OFC neuronal population activity around the 30 second CS period on trials 1-5 and 11-15 during the baseline session and omission session. Neuronal activity was normalized to the whole session firing rate and presented as mean firing rate (line) ± SEM (shading) for CON (gray) and AIE (orange) groups. Figures **C, D, G**, and **H** represent the mean firing rate in the target window (blue box) during first and late trials. **C**. OFC activity after CS onset on baseline session: after comparison

of the mean firing rate activity, a significant main effect of exposure was observed (P=0.01). No main effect of time or interaction between factors were observed (P's>0.05). **D**. OFC activity after CS offset on baseline session: a marginal main effect of exposure (P=0.08) was observed. However, no main effect of time or interaction between factors was observed (P's>0.05). **G.** OFC activity after CS onset on omission session: a significant main effect of exposure was observed (P=0.04). However, no main effect of time or interaction between the factors was observed (P>0.05). **H**. OFC activity after CS offset on omission session. No significant main effects or interaction was observed (P>0.05). * significant mean effect of exposure (P≤0.05). For statistical details see Supplemental Table 5.

4. Discussion

The present study examined AIE effects on Pavlovian conditioned approach and concurrent neuronal firing patterns in female rats. Focusing on sign-tracking rats, AIE exposure decreased expression of goal-tracking behavior and promoted increased phasic firing in OFC neurons in response to CS presentation, even in the absence of the US. Moreover, NAc neurons in AIE-exposed rats exhibited less excitation during conditioned receptacle entries, demonstrating AIE effects on neural correlates of goal-tracking behavior. Adolescence is a critical period for brain development in which cortical and limbic structures undergo structural and synaptic maturation processes, and disruptions in these processes can promote long-lasting impacts on behavior and cognitive functions (Riceberg and Shapiro, 2017; Spear, 2000). Indeed, persistent AIE effects are well documented in animal models, including impairments in memory (Contreras et al., 2019; Galaj et al., 2019), reversal learning (Garland et al., 2014; Sey et al., 2019) and attention (Fernandez and Savage, 2017; Sanchez-Roige et al., 2014). Additional AIE-induced effects are decreased social interaction (Varlinskaya et al., 2017) and increased anxiety-like behavior (Pandey et al., 2015; Towner and Varlinskaya, 2020), risk-taking preference(Qin et al., 2013), and impulsivity (Gilpin et al., 2012). Together, these changes are hypothesized to increase the risk of developing AUD in adulthood (Spear, 2018a; Varlinskaya and Spear, 2015).

In our study, the majority of female rats in both experimental groups developed a sign-tracking phenotype. This result was expected, as we have previously shown that female rats exhibited higher expression of sign-tracking behavior compared to males (Madayag et al., 2017). Interestingly, in our study we observed an increase of OFC activity in the AIE-exposed group after CS presentation. In sign-tracking individuals, the repeated presentation of reward-predictive cues results in the attribution of incentive salience towards the CS (Berridge, 2007; Flagel et al., 2010). OFC activity is described to be important for the expression of Pavlovian approach (Stringfield et al., 2017), motivated behavior (Goldstein and Volkow, 2011) and representing the value associated to expected outcomes (Bradfield et al., 2015; Ogawa et al., 2013). Our results may represent an enhancement on OFC encoding of motivational salience towards CS promoted by AIE exposure. Stringfield et al. (2017) demonstrated that in naïve animals, OFC activity increased in response to CS presentation

and was necessary for the expression of Pavlovian approach responses. Additionally, exposure to nicotine resulted in changes in OFC firing activity in response to the CS, which may induce behavioral changes during conditioned approach (Stringfield et al., 2017).

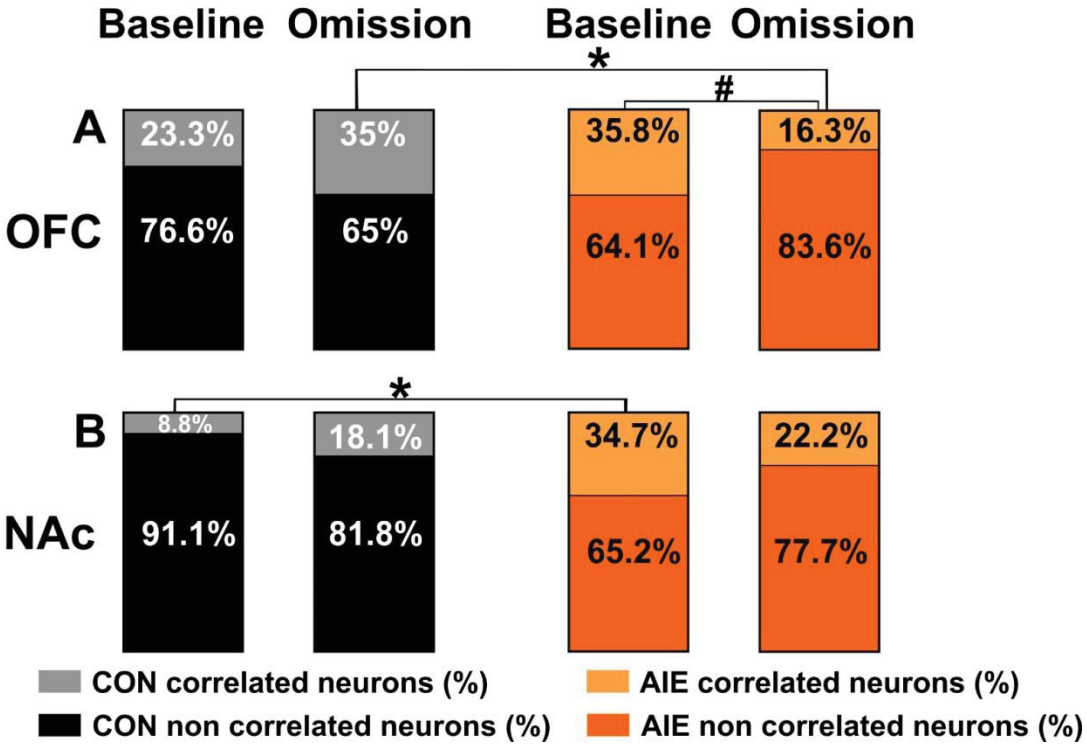

Fig. 9: A subset of OFC and NAc neurons presented a significant correlation between firing activity and subsequent behavioral response, and AIE exposure altered this association. Correlation analysis between the mean firing rate after CS onset and behavioral responses were performed in both OFC and NAC during baseline and omission session. **A. Left panels.** Percentage of OFC correlated neurons on CON group: no statistical difference was observed comparing baseline versus omission session (P=0.15). **Right panels.** Percentage of OFC correlated neurons on AIE group: chi-square analysis demonstrated a significant decrease in the percentage of correlated neurons comparing the baseline versus omission session (P=0.04). Also, group comparisons specifically on baseline or omission sessions were performed. No difference was observed after group comparison on baseline session (P=0.87). However, on omission session CON group presented a significantly higher percentage of correlated neurons (P=0.03). **B. Left panels.** Percentage of NAc correlated neurons on CON group: no statistical difference was observed on the sessions comparison (P=0.26). **Right panels.** Percentage of NAc correlated neurons on AIE group: no statistical difference was observed on the sessions comparison (P=0.50). Group comparison demonstrated that AIE group presented a significantly higher percentage of correlated neurons during baseline session (P=0.002). However, no difference was observed in the omission session (P=0.81). Bars represent the percentage of neurons with significant or non-significant correlation. Significantly correlated neurons are presented in the gray bars for CON and in light orange for AIE. Non significantly correlated neurons are presented in the black for CON and in dark orange for AIE. * significant group difference (P≤0.05). # significant session difference (P≤0.05).

Previous imaging studies in human subjects demonstrated higher OFC activity after the presentation of a drug-associated stimulus (Stapleton et al., 1995; Volkow and Fowler, 2000). Even though that in our study the CS was associated with a non-drug reward, the repeated CS presentation can result in

the attribution of incentive salience towards the CS (Berridge, 2004; Robinson et al., 2014). However, higher motivational salience could result in a more vigorous interaction with the compound stimulus (cue/lever), an effect that we do not directly observed in our study. A possible reason for this is that sign-tracking animals can present a broader spectrum of behavioral responses evoked by the CS presentation, compared to the parameters that were measured in this study. We evaluated interaction with the compound stimulus based on the total number of lever presses, latency, and probability to press. However, others have shown that after CS presentation, sign-tracking animals approach the CS location and exhibit behaviors other than pressing the lever such as sniffing, biting, and gnawing directed towards the lever (Gillis and Morrison, 2019b) that do not result in a lever press. In this regard, our analysis was focused on sign-tracking animals in both experimental groups, and the high levels of lever presses presented by these animals. In our study, the expression of other behavioral forms of sign-tracking behavior could have masked a possible increase in sign-tracking associated with the higher OFC activity in AIE-exposed animals. Future studies should address the possible relationship between OFC activation in response to salient stimuli and the expression of sign-tracking behavior. This relationship would be particularly interesting, based on findings that demonstrated a reduction of sign-tracking behavior after pharmacologic inactivation of the OFC (Stringfield et al., 2017).

AIE effects on the OFC have been characterized previously (Coleman et al., 2014; McMurray et al., 2016). Coleman et al. (2014) demonstrated that AIE exposure resulted in changes in OFC volume and structural components of the neuronal extracellular matrix, where AIE exposure was associated with a high expression of molecular components typically associated with the juvenile form of the extracellular matrix. Importantly, changes in cortical maturation may result in impairments in decision making processes and enhancement of impulsive behaviors (Spear, 2018a). This evidence demonstrated that AIE promoted impairments in the OFC neuronal maturation process, resulting in anatomical and behavioral changes in adulthood. Broadwater et al. (2017) demonstrated that AIE also resulted in changes in the functional connectivity of fronto-limbic structures, in which the connectivity between OFC and NAc was significantly affected. In our study, a possible increase in encoding of motivational salience by OFC neurons in AIE-exposed animals, associated with a decrease in NAc excitation during goal-tracking also promoted by AIE, could reflect impairments in brain development and maturation promoted by AIE exposure. AIE may promote changes in maturation processes (Galaj et al., 2020), decreases in synaptic plasticity (Carzoli et al., 2019; Peñasco et al., 2019) and other anatomic and molecular changes (Cozzoli et al., 2016; Trantham-Davidson and Chandler, 2015; Vetreno and Crews, 2018). The outcome of this maladaptive development could result in the changes on behavior and neuronal activity observed in our analysis.

Interestingly, in our study we observed that AIE exposure resulted in decreased NAc excitatory activity during goal-tracking behavior. Previous studies demonstrate that NAc neurons exhibit a substantial excitatory activity during cue-evoked reward-receptacle approach (Nicola et al., 2004). We observed a similar pattern in NAc neurons from the CON-exposed group, but a significant lower NAc excitation was observed in the AIE-exposed group. Consistent with previous reports (Madayag et al., 2017), we observed that AIE promoted a decrease in goal-tracking behavior. Our results demonstrating a decrease in the NAc excitatory activity during goal-tracking behavior could reflect the decrease in goal-tracking behavior presented by AIE-exposed animals. These effects could result from changes in important NAc functions, such as encoding motivation and reward seeking behavior (Ambroggi et al., 2011; Nicola et al., 2004). However, more studies are needed to provide a better understanding of AIE effects on NAc activity during reward motivated behaviors. Moreover, drugs of abuse, such as alcohol, can induce changes in fronto-limbic circuitry, which can result in a decrease in behavioral responses to natural rewards and enhancements on responses towards reward-associated stimuli (Broadwater et al., 2017; Kalivas and Hu, 2006). Madayag et al. (2017) described that AIE could produce a shift toward the sign-tracking phenotype, possibly by a significant inverse correlation between cue and goal interactions. In our study, even although we did not observe a direct increase in sign-tracking behavior promoted by AIE, we observed a decrease in goal-tracking behavior after AIE exposure, and also a decrease in excitatory NAc neuronal activity in response to goal-tracking behaviors. These results are in agreement with the description of changes promoted by drugs of abuse during Pavlovian approach (Berridge, 2004; Madayag et al., 2017; McClory and Spear, 2014; Palmatier et al., 2013; Saunders et al., 2013; Stringfield et al., 2018).

In our study we evaluate the possibility that a subset of NAc and OFC neurons exhibit correlated neuronal firing activity with the subsequent behavioral responses. Interestingly, AIE-exposed animals presented different patterns of correlation compared to CON-exposed animals. In the subset of correlated neurons in the OFC, neurons recorded from the AIE presented an opposite correlation pattern compared to the CON group when the US was omitted. The CON group presented an enhancement in the percentage of correlated neurons compared to baseline, a result that was not observed in the AIE group. This finding could be associated with the well-described requirement of OFC activity for encoding reward value (Schoenbaum and Roesch, 2005). After the omission of the US, OFC activity could be required to recognize and respond to the changes in the expected outcome (Schoenbaum et al., 2003). Moreover, OFC activity is also thought to integrate associative information to predict and then signal the value of future events (Schoenbaum et al., 2006). The OFC appears to generate and represent outcome expectancies, information that is critical not only to the guidance of behavior according to expectations about the future, but also to the ability to learn from violations of

those expectations (Schoenbaum et al., 2006). We also observed a subset of correlated neurons in the NAc, where a larger subset of correlated neurons was observed in AIE-exposed animals compared to CON-exposed during the baseline session. As our analysis focused only on sign-tracking animals, we could initially expect that most OFC and NAc neurons that presented correlation were indeed correlated with the sign instead goal-tracking behaviors. However, we did not observe this more pronounced correlation of neuronal activity with sign-tracking behavior. A possible explanation could be that these neurons presented more positive correlation with sign-tracking behavior and a more negative correlation with goal-tracking behavior. We tested this hypothesis, however, and did not observed differences on the correlation patterns (positive or negative correlation). This result may indicate that OFC and NAc neurons could be correlated with both sign and also goal-tracking behavioral expression.

Interestingly, Morrison et al. (2019) demonstrated that subsets of neurons in the NAc were correlated with the vigor of behavioral responses. Also, McGuinty et al. (2014) described that the neuronal activity in response to CS presentation was directly correlated to the latency of locomotion initiation towards rewarded location. These evidences demonstrating that the activity of a subset of NAc neurons could be modulating reward-approach behavior. NAc activity is related to engagement of reward associated approach (du Hoffmann and Nicola, 2014), goal-directed behavior (Mcginty et al., 2013), and locomotor vigor (Levcik et al., 2021; Sjulson et al., 2018). AIE exposure also may induce changes on NAc medium spiny neurons intrinsic excitability, neurotransmitters release, neuronal activation and connectivity (Broadwater et al., 2017; Liu and Crews, 2015; Pascual et al., 2009; Shan et al., 2019; Shnitko et al., 2016). These AIE effects may result in changes in the NAc codification of behavioral responses, as observed in our study. However, we acknowledge limitations to this analysis that should be accounted for, as the small sample of neurons recorded and used on the correlation between firing activity and behavioral responses. Future studies should address more closely the AIE effects on the relationship between neuronal activity and subsequent behavior expression.

In summary, evaluating the long-term effects of AIE-exposure, we observed a decrease in goal-tracking behavior expression promoted by AIE. This behavioral effect could be reflecting the AIE-promoted changes in fronto-limbic codification of motivated behavior. AIE exposure promoted a consistent increase in OFC excitatory activity after CS. While a decrease in NAc excitatory activity was observed during goal-tracking behaviors. These results demonstrate long-lasting behavioral and OFC and NAc neuronal activity promoted by AIE exposure in female rats. The findings of our study contribute to the description of the adolescence period as an important window for harmful effects promoted by ethanol.

References

Ambroggi, F., Ghazizadeh, A., Nicola, S.M., Fields, H.L., 2011. Roles of Nucleus Accumbens Core and Shell in Incentive-Cue Responding and Behavioral Inhibition. J. Neurosci. 31, 6820–6830.

Amodeo, L.R., Kneiber, D., Wills, D.N., Ehlers, C.L., Neuroscience, C., Jolla, L., 2017. Alcohol drinking during adolescence increases consumptive responses to alcohol in adulthood in Wistar rats. Alcohol 43–51.

Badanich, K.A., Fakih, M.E., Gurina, T.S., Roy, E.K., Hoffman, J.L., Uruena-Agnes, A.R., Kirstein, C.L., 2016. Reversal learning and experimenter-administered chronic intermittent ethanol exposure in male rats. Psychopharmacology (Berl). 233, 3615–3626.

Bava, S., Tapert, S.F., 2010. Adolescent Brain Development and the Risk for Alcohol and Other Drug Problems. Neuropsychol Rev 398–413. https://doi.org/10.1007/s11065-010-9146-6

Berridge, K.C., 2007. The debate over dopamine's role in reward: The case for incentive salience. Psychopharmacology (Berl). 191, 391–431.

Berridge, K.C., 2004. Motivation concepts in behavioral neuroscience. Physiol. Behav. 81, 179–209.

Bradfield, L.A., Dezfouli, A., Holstein, M. Van, Chieng, B., Balleine, B.W., 2015. Medial Orbitofrontal Cortex Mediates Outcome Retrieval in Partially Observable Task Situations Article Medial Orbitofrontal Cortex Mediates Outcome Retrieval in Partially Observable Task Situations. Neuron 88, 1268–1280.

Broadwater, M.A., Lee, S., Yu, Y., Zhu, H., Crews, F.T., Robinson, D.L., Shih, Y.I., 2017. Adolescent alcohol exposure decreases frontostriatal resting-state functional connectivity in adulthood. Addict. Biol.

Brown, E.E., Fibiger, H.C., 1992. Evidence for Conditional Neuronal Activation following Exposure to a Environment : Role of Forebrain Limbic Structures 2.

Caballero, A., Granberg, R., Tseng, K.Y., Chicago, N., 2016. Mechanisms contributing to Prefrontal Cortex Maturation during Adolescence. Neurosci Biobehav Rev. 70, 4–12.

Carzoli, K.L., Sharfman, N.M., Lerner, M.R., Miller, M.C., Holmgren, E.B., Wills, T.A., Kash, T.L., 2019. Regulation of NMDA Receptor Plasticity in the BNST Following Adolescent Alcohol Exposure 13, 1–15.

Casey, B., Jones, R.M., Somerville, L.H., 2011. Braking and Accelerating of the Adolescent Brain. J Res Adolesc 21, 21–33.

Chung, T., Creswell, K.G., Bachrach, R., Clark, D.B., Martin, C.S., 2015. Adolescent Binge Drinking. Alcohol Res. Current Reviews 39, 5–15.

Coleman, L.G., He, J., Lee, J., Styner, M., Crews, F.T., 2011. Adolescent binge drinking alters adult brain neurotransmitter gene expression, behavior, brain regional volumes, and neurochemistry in mice. Alcohol Clin Exp Res 35, 671–688.

Coleman, L.G., Liu, W., Oguz, I., Styner, M., Crews, F.T., 2014. Adolescent binge ethanol treatment alters adult brain regional volumes, cortical extracellular matrix protein and behavioral flexibility. Pharmacol Biochem Behav 142–151.

Contreras, A., Polın, E., Miguens, M., Perez-Garcıa, C., Perez, V., Ruiz-Gayo, M., Morales, L., Olmo, N. Del, 2019. Intermittent-Excessive and Chronic-Moderate Ethanol Intake during Adolescence Impair Spatial Learning , Memory and Cognitive Flexibility in the Adulthood. Neuroscience 418, 205–217.

Cozzoli, D.K., Kaufman, M.N., Nipper, M.A., Hashimoto, J.G., Wiren, K.M., Finn, D.A., 2016. Functional Regulation of PI3K-Associated Signaling in the Accumbens by Binge Alcohol Drinking in Male but not Female Mice. Physiol. Behav. 176, 139–148.

Crews, F.T., Vetreno, R.P., Broadwater, M.A., Robinson, D.L., 2016. Adolescent Alcohol Exposure Persistently Impacts Adult Neurobiology and Behavior 1074–1109.

Day, J.J., Roitman, M.F., Wightman, R.M., Carelli, R.M., 2007. Associative learning mediates dynamic shifts in dopamine signaling in the nucleus accumbens. Nat. Neurosci. 10, 1020–1028.

Doremus-Fitzwater, T.L., Barreto, M., Spear, L.P., 2012. Age-related differences in impulsivity among adolescent and adult Sprague-Dawley rats. Behav Neurosci. 126, 735–741.

du Hoffmann, J., Nicola, S.M., 2014. Dopamine invigorates reward seeking by promoting cue-evoked excitation in the nucleus accumbens. J. Neurosci. 34, 14349–14364.

Fanelli, R.R., Klein, J.T., Reese, R.M., Robinson, D.L., 2013. Dorsomedial and dorsolateral striatum exhibit distinct phasic neuronal activity during alcohol self-administration in rats. Eur J Neurosci. 38, 2637–2648.

Fernandez, G.M., Savage, L.M., 2017. Adolescent binge ethanol exposure alters specific forebrain cholinergic cell populations and leads to selective functional deficits in the prefrontal cortex. Neuroscience 361, 129–143.
Flagel, S.B., Akil, H., Robinson, T.E., 2010. SALIENCE TO REWARD-RELATED CUES : IMPLICATIONS FOR ADDICTION 56, 139–148.
Flagel, S.B., Clark, J.J., Robinson, T.E., Mayo, L., Czuj, A., Willuhn, I., Akers, C.A., Clinton, S.M., Phillips, P.E.M., Akil, H., 2011. ARTICLE A selective role for dopamine in stimulus – reward learning. Nature 3–9.
Flagel, S.B., Watson, S.J., Robinson, T.E., Akil, H., 2007. Individual differences in the propensity to approach signals vs goals promote different adaptations in the dopamine system of rats. Psychopharmacology (Berl). 191, 599–607.
Füllgrabe, M.W., Vengeliene, V., Spanagel, R., 2007. Influence of age at drinking onset on the alcohol deprivation effect and stress-induced drinking in female rats. Pharmacol. Biochem. Behav. 86, 320–326.
Galaj, E., Guo, C., Huang, D., Ranaldi, R., Ma, Y., 2020. Contrasting effects of adolescent and early-adult ethanol exposure on prelimbic cortical pyramidal neurons 216.
Galaj, E., Kipp, B.T., Floresco, S.B., Savage, L.M., Columbia, B., 2019. Persistent alterations of accumbal cholinergic interneurons and cognitive dysfunction after adolescent intermittent ethanol exposure. Neuroscience.
Garland, L., Jr, C., Liu, W., Oguz, I., Styner, M., Crews, F.T., 2014. Pharmacology , Biochemistry and Behavior Adolescent binge ethanol treatment alters adult brain regional volumes , cortical extracellular matrix protein and behavioral fl exibility. Pharmacol. Biochem. Behav. 116, 142–151.
Gillis, Z.S., Morrison, S.E., 2019b. Sign Tracking and Goal Tracking Are Characterized by Distinct Patterns of Nucleus Accumbens Activity. eNeuro 6, 1–15.
Gilpin, N.W., Karanikas, C.A., Richardson, H.N., 2012. Adolescent binge drinking leads to changes in alcohol drinking, anxiety, and amygdalar corticotropin releasing factor cells in adulthood in male rats. PLoS One 7.
Goldstein, R.Z., Volkow, N.D., 2011. Dysfunction of the prefrontal cortex in addiction : neuroimaging findings and clinical implications 12.
Holland, P.C., 1979. Differential effects of omission contingencies on various components of Pavlovian appetitive conditioned responding in rats. J. Exp. Psychol. Anim. Behav. Process. 5, 178–193.
Kalivas, P.W., Hu, X., 2006. Exciting inhibition in psychostimulant addiction. Reviews in Neurosc. 3, 190-04.
Levcik, D., Sugi, A.H., Pochapski], J.A., Baltazar, G., Pulido, L.N., Villas-Boas, C., Aguilar-Rivera, M., Fuentes-Flores, R., Nicola, S.M., Cunha, C. Da, 2021. Nucleus accumbens neurons ecode initiation and vigor of reward approach behavior. BiorxV 2, 31-30.
Liu, W., Crews, F.T., 2015. ADOLESCENT INTERMITTENT ETHANOL EXPOSURE ENHANCES ETHANOL ACTIVATION OF THE NUCLEUS 92–108.
London, E.D., Ernst, M., Grant, S., 2000. Orbitofrontal Cortex and Human Drug Abuse : Functional Imaging 334–342.
Luna, B., Marek, S., Larsen, B., Tervo-clemmens, B., 2015. An Integrative Model of the Maturation of Cognitive Control. Annu Rev Neurosci. 08, 151–170.
Madayag, A.C., Stringfield, S.J., Reissner, K.J., Boettiger, C.A., Robinson, D.L., 2017. Sex and Adolescent Ethanol Exposure Influence Pavlovian Conditioned Approach. Alcohol Clin Exp Res. 41, 846–856.
McClory, A.J., Spear, L., 2014. EFFECTS OF ETHANOL EXPOSURE DURING ADOLESCENCE IN SPRAGUE-DAWLEY RATS. Alcohol 48, 755–763.
Mcginty, V.B., Lardeux, S., Taha, S.A., Kim, J.J., Nicola, S.M., 2013. Article Invigoration of Reward Seeking by Cue and Proximity Encoding in the Nucleus Accumbens. Neuron 78, 910–922.
McMurray, M.S., Amodeo, L.R., Roitman, J.D., 2016. Consequences of Adolescent Ethanol Consumption on Risk Preference and Orbitofrontal Cortex Encoding of Reward. Neuropsychopharmacology 41, 1366–1375.
Molina, P.E., Nelson, S., 2018. Binge Drinking ' s Effects on the Body. ALCOHOL Res. Curr. Rev. 39, 99–109.
Moorman, D.E., Aston-Jones, G., 2014. Orbitofrontal cortical neurons encode expectation-driven initiation of reward-seeking. J. Neurosci. 34, 10234–10246.

Nicola, S.M., 2007. The nucleus accumbens as part of a basal ganglia action selection circuit 521–550.
Nicola, S.M., Yun, I.A., Wakabayashi, K.T., Fields, H.L., 2004. Cue-Evoked Firing of Nucleus Accumbens Neurons Encodes Motivational Significance during a Discriminative Stimulus Task. J. Neurophysiol. 91, 1840–1865.
O'Doherty, J., Rolls, E.T., Francis, S., Bowtell, R., McGlone, F., Kobal, G., Renner, B., Ahne, G., 2000. Sensory-specific satiety-related olfactory activation of the human orbitofrontal cortex. Neuroreport 11, 399–403.
Ogawa, M., Meer, M.A.A. van der, Esber, G.R., Cerri, D.H., Stalnaker, Thomas A. Schoenbaum, G., 2013. Risk-responsive orbitofrontal neurons track acquired salience. Neuron 23, 1–7
Palmatier, M.I., Kellicut, M.R., Sheppard, A.B., Brown, R.W., Robinson, D.L., 2014. The incentive amplifying effects of nicotine are reduced by selective and non-selective dopamine antagonists in rats. Pharmacol Biochem Behav 126, 50–62.
Palmatier, M.I., Marks, K.R., Jones, S.A., Freeman, K.S., Wissman, K.M., Sheppard, A.B., 2013. The effect of nicotine on sign-tracking and goal-tracking in a Pavlovian conditioned approach paradigm in rats. Psychopharmacology (Berl). 247–259.
Pandey, S.C., Sakharkar, A.J., Tang, L., Zhang, H., Biology, C., 2015. Potential role of adolescent alcohol exposure-induced amygdaloid histone modifications in anxiety and alcohol intake during adulthood. Neurobiol Dis. 607–619.
Pascual, M., Boix, J., Felipo, Vi., Guerri, C., 2009. Repeated alcohol administration during adolescence causes changes in the mesolimbic dopaminergic and glutamatergic systems and promotes alcohol intake in the adult rat. J. Neurochem. 108, 920–931.
Peñasco, S., Rico-barrio, I., Puente, N., Fontaine, C.J., Ramos, A., Reguero, L., Gerrikagoitia, I., Fonseca, F.R. De, Suarez, J., Barrondo, S., Aretxabala, X., García, G., Sallés, J., Elezgarai, I., Nahirney, P.C., Christie, B.R., Grandes, P., 2019. Intermittent ethanol exposure during adolescence impairs cannabinoid type 1 receptor-dependent long-term depression and recognition memory in adult mice. Neuropsychopharmacology.
Qin, L., Liu, Y., Hong, J.-S., Crews, F.T., 2013. NADPH oxidase and aging drive microglial activation, oxidative stress and dopaminergic neurodegeneration following systemic LPS administration. Glia 23, 1–7.
Renteria, R., Baltz, E.T., Gremel, C.M., 2018. Chronic alcohol exposure disrupts top-down control over basal ganglia action selection to produce habits. Nat. Commun. 9, 1–11.
Riceberg, J.S., Shapiro, M.L., 2017. Orbitofrontal cortex signals expected outcomes with predictive codes when stable contingencies promote the integration of reward history. J. Neurosci. 37, 2010–2021.
Robinson, D.L., Carelli, R.M., 2008. Distinct subsets of nucleus accumbens neurons encode operant responding for ethanol versus water. Eur J Neurosci 28, 1887–1894.
Robinson, T.E., Kent, C., 1993. The neural basis of drug craving: an incetive-sensitization theory of addiction. Brain Res. Rev. 8, 247–291.
Robinson, T.E., Yager, L.M., Cogan, E.S., Saunders, B.T., 2014. On the Motivational Properties of Reward Cues: Individual Differences 76, 1–22.
Saddoris, M.P., Gallagher, M., Schoenbaum, G., 2005. Rapid associative encoding in basolateral amygdala depends on connections with orbitofrontal cortex. Neuron 46, 321–331.
Saddoris, M.P., Sugam, J.A., Cacciapaglia, F., Carelli, R.M., 2013. Rapid dopamine dynamics in the accumbens core and shell: Learning and action. Front. Biosci. - Elit. 5 E, 273–288.
Sanchez-Roige, S., Peña-Oliver, Y., Ripley, T.L., Stephens, D.N., 2014. Repeated Ethanol Exposure During Early and Late Adolescence: Double Dissociation of Effects on Waiting and Choice Impulsivity. Alcohol. Clin. Exp. Res. 38, 2579–2589.
Saunders, B.T., Robinson, T.E., 2011. Individual Variation in the Motivational Properties of Cocaine. Neuropsychopharmacology 1668–1676.
Saunders, B.T., Yager, L.M., Robinson, T.E., 2013. Preclinical Studies Shed Light on Individual Variation in Addiction Vulnerability Fractionating the Impulsivity Construct in Adolescence. Neuropsychopharmacology.
Schoenbaum, G., Roesch, M., 2005. Orbitofrontal Cortex, Associative Learning, and Expectancies Neural Activity in OFC and OFC-Dependent Behavior Reflect Outcome Expectancies NIH Public Access. Neuron 47, 633–636.
Schoenbaum, G., Roesch, M.R., Stalnaker, T.A., 2006. Orbitofrontal cortex, NIH Public Access 29, 116–124

Schoenbaum, G., Setlow, B., Nugent, S.L., Saddoris, M.P., Gallagher, M., 2003. Lesions of orbitofrontal cortex and basolateral amygdala complex disrupt acquisition of odor-guided discriminations and reversals. Learn. Mem. 10, 129–
Sey, N.Y.A., Gómez-a, A., Madayag, A.C., Boettiger, C.A., 2019. Adolescent intermittent ethanol impairs behavioral fl exibility in a rat foraging task in adulthood. Behav. Brain Res. 373, 112085.
Shan, L., Galaj, E., Ma, Y.Y., 2019. Nucleus accumbens shell small conductance potassium channels underlie adolescent ethanol exposure-induced anxiety. Neuropsychopharmacology 44, 1886–1895.
Shnitko, T.A., Spear, L.P., Robinson, D.L., 2016. Adolescent binge-like alcohol alters sensitivity to acute alcohol effects on dopamine release in the nucleus accumbens of adult rats 361–371. https://doi.org/10.1007/s00213-015-4106-8
Sjulson, L., Peyrache, A., Cumpelik, A., Cassataro, D., Buzsáki, G., 2018. Cocaine Place Conditioning Strengthens Location-Specific Hippocampal Coupling to the Nucleus Accumbens. Neuron 98, 926-934.e5.
Spear, L.P., 2018. Effects of adolescent alcohol consumption on the brain and behaviour. Nat. Rev. Neurosci.
Spear, L.P., 2014. Adolescents and Alcohol: Acute Sensitivities, Enhanced Intake, and Later Consequences. Neurotoxicol Teratol. 51–59.
Spear, L.P., 2000. Neurobehavioral changes in adolescence. Curr. Dir. Psychol. Sci. 9, 111–114.
Spoelder, M., Tsutsui, K.T., Lesscher, H.M.B., Vanderschuren, L.J.M.J., Clark, J.J., 2015. Adolescent Alcohol Exposure Amplifies the Incentive Value of Reward-Predictive Cues Through Potentiation of Phasic Dopamine Signaling. Neuropsychopharmacology 40, 2873–2885.
Stalnaker, T.A., Cooch, N.K., Schoenbaum, G., 2015. What the orbitofrontal cortex does not do. Nat. Neurosci. 18, 620–627.
Stapleton, J.M., Morgan, M.J., Phillips, R.L., Wang, D.F., Yung, B.C., Shaya, E.K., Dannals, R.F., Liu, X., Grayson, R.L., London, E.D.1995. Cerebral Glucose Utilization Polysubstance Abuse .
Stringfield, S.J., Boettiger, C.A., Robinson, D.L., 2018. Nicotine-enhanced Pavlovian conditioned approach is resistant to omission of expected outcome. Behav Brain Res. 343, 16–20.
Stringfield, S.J., Palmatier, M.I., Boettiger, C.A., Robinson, D.L., 2017. Orbitofrontal participation in sign- and goal-tracking conditioned responses: Effects of nicotine. Neuropharmacology 116, 208–223.
Swartzwelder, H.S., Acheson, S.K., Miller, K.M., Sexton, G., Liu, W., Crews, F.T., Risher, M., 2015. Adolescent Intermittent Alcohol Exposure : Deficits in Object Recognition Memory and Forebrain Cholinergic Markers. PLoS One 1–13.
Tomie, A., Grimesa, K.L., Pohorecky, L.A., 2008. Behavioral Characteristics and Neurobiological Substrates Shared by Pavlovian Sign-Tracking and Drug Abuse. Brain Res Rev 58, 121–135.
Towner, T.T., Varlinskaya, E.I., 2020. Adolescent Ethanol Exposure: Anxiety-Like Behavioral Alterations, Ethanol Intake, and Sensitivity. Front. Behav. Neurosci.
Trantham-Davidson, H., Chandler, L.J., 2015. Alcohol-induced alterations in dopamine modulation of prefrontal activity. Alcohol 49, 773–779.
Varlinskaya, E.I., Kim, E.U., Spear, L.P., 2017. Chronic intermittent ethanol exposure during adolescence: effects on stress-induced social alterations and social drinking in adulthood. Brain Res. 1654, 145–156.
Varlinskaya, E.I., Spear, L.P., 2015. SOCIAL CONSEQUENCES OF ETHANOL: IMPACT OF AGE, STRESS AND PRIOR HISTORY OF ETHANOL EXPOSURE. Physiol Behav. 1, 145–150.
Vetreno, R.P., Crews, F.T., 2018. Adolescent binge ethanol-induced loss of basal forebrain cholinergic neurons and neuroimmune activation are prevented by exercise and indomethacin 1–22.
Volkow, D., Fowler, S., Wolf, P., Hoff, A., Ph, D., Ph, D., Burr, G., Carciello, R., Chnstman, D., Redvanly, C., Schlyer, D., Shea, C., 1991. Cocaine in Brain Glucose and Withdrawal.
Volkow, N.D., Chang, L., Wang, G., Fowler, J.S., Ph, D., Logan, J., Ph, D., Hitzemann, R., Ph, D., Gifford, A., Ph, D., Wong, C., Pappas, N., 2003. Low Level of Brain Dopamine D 2 Receptors in Methamphetamine Abusers : Association With Metabolism in the Orbitofrontal Cortex I, 150–157.

Volkow, N.D., Fowler, J.S., 2000. Addiction , a Disease of Compulsion and Drive : Involvement of the Orbitofrontal Cortex 318–325.
White, H.R., Marmorstein, N.R., Crews, F.T., Bates, M.E., Mun, E.-Y., Loeber, R., 2011. Associations between Heavy Drinking and Changes in Impulsive Behavior among Adolescent Males. Alcohol Clin Exp Res 23, 1–7.
Yurgelun-todd, D., 2007. Emotional and cognitive changes during adolescence. Curr. Opin. Neurobiol.

Supplemental figures

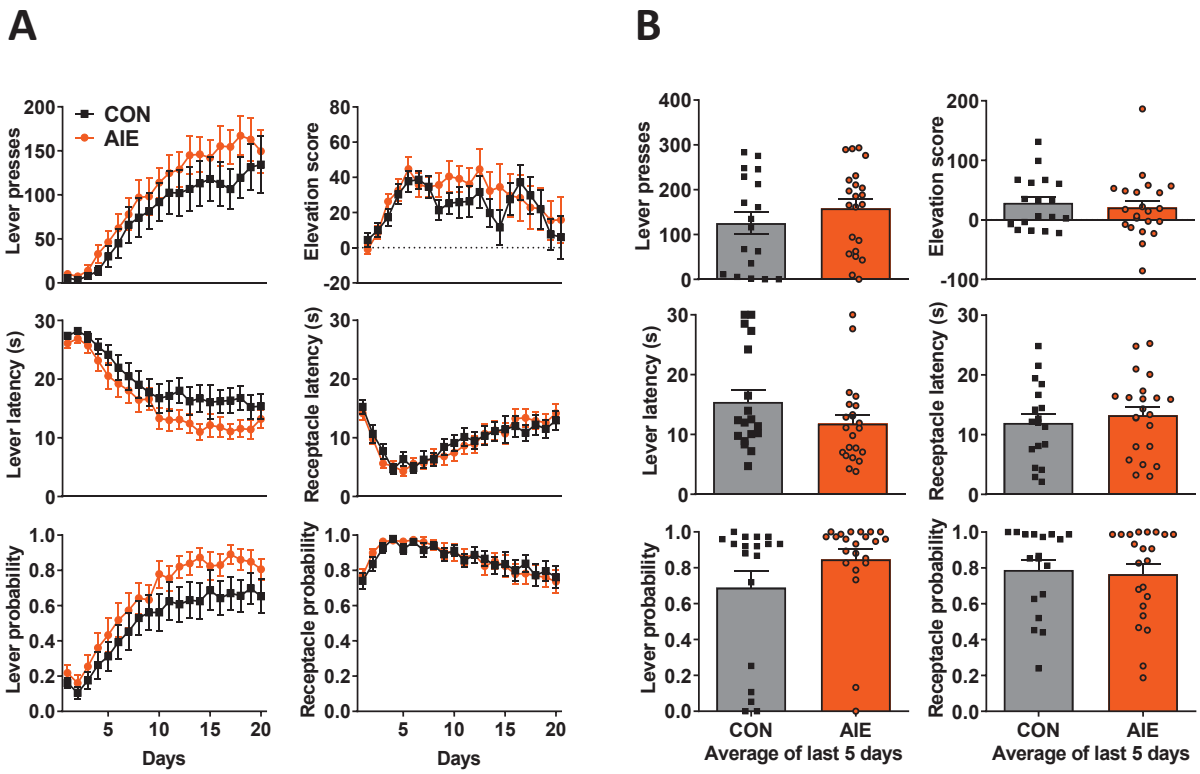

Supplemental Fig. S1. AIE exposure did not change **behavioral acquisition during PCA training phase. A.** Behavioral data across the PCA training sessions. **B.** Averaged behavioral data presented on last 5 PCA sessions. Mann-Whitney U or t-test was used to analyze the averaged behavioral data from last 5 PCA sessions. No significant group difference was observed for the total number of lever presses (P=0.29), elevation score (P=0.61), or for the latencies to perform a lever press (P=0.19) or a receptacle entry (P=0.61), neither on the probabilities to perform a lever press (P=0.13) or a receptacle entry (P=0.97). All data are expressed as mean ± SEM. The symbols on panel B represent individual animal data, in black for CON (n=18) and orange on AIE (n=22). For statistical analysis details see Supplemental Table 1.

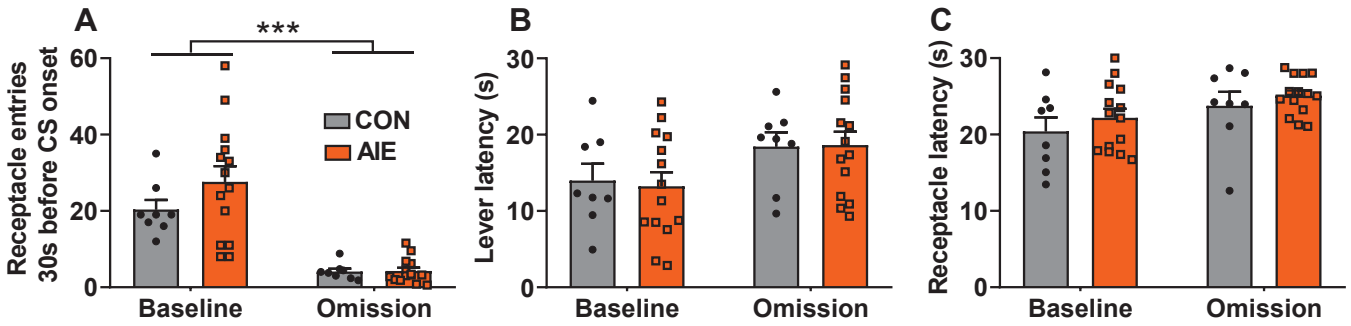

Supplemental Fig. S2: AIE exposure did not change the receptacle interaction before CS onset neither the latencies to perform conditioned responses. A. Receptacle entries performed 30 seconds (s) before the CS onset: Data analysis demonstrated a significant main effect of session ($P<0.001$). However, no significant main effect of exposure or interaction between factors was observed ($P's>0.05$). **B.** Lever press latency: no significant main effect of exposure or session was observed, neither an interaction between factors ($P's>0.05$). **C.** Receptacle entry latency: no significant main effects of exposure or session were observed, neither an interaction between factors ($P's>0.05$). Data are expressed as mean ± SEM. Individual animal data are presented by the symbols in black for CON (n=8) and orange for AIE (n=14). *** significant main effect of session ($P<0.001$). For statistical details see Supplemental Table 2.

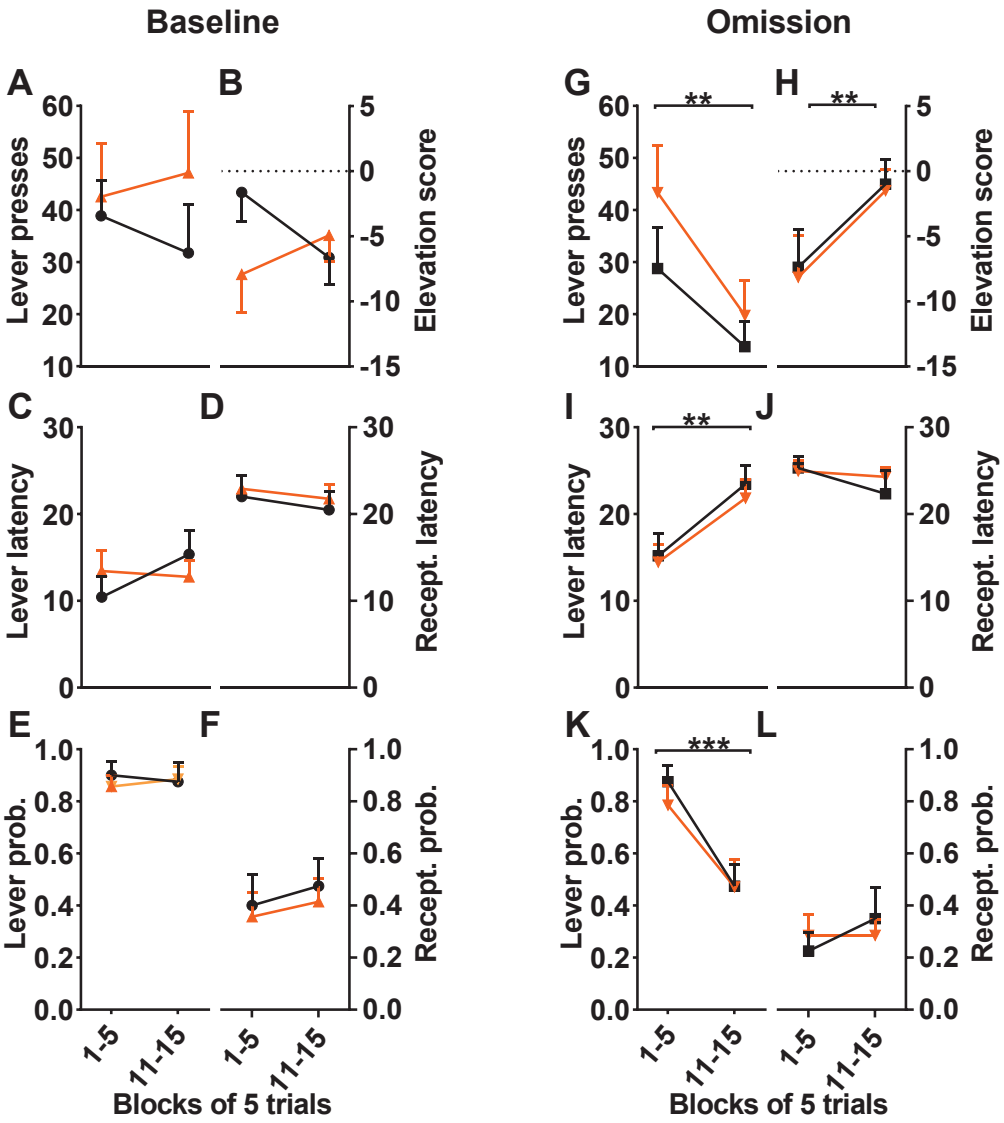

Supplemental Fig. 3: Behavioral data across PCA baseline and reward omission session. Averaged behavioral data performed during trials 1 to 5 and 11 to 15 were compared during baseline and omission session. Figures **A** to **F** represents baseline session data**.** No statistical difference was observed on sign-tracking behaviors across baseline session (P's>0.05; **A**, **C**, **E**). **B.** Receptacle elevation score: a marginal main effect of time was observed (P=0.06), and also a significant exposure versus time interaction was observed (P<0.001). However, Sidak's post-hoc comparisons did not demonstrate statistical differences (P>0.05). No exposure effect was observed. **D.** Receptacle entry latency: no significant difference was observed. **F.** Receptacle entry probability: no significant difference was observed. Figures **G** to **L** represent omission session data. A significant main effect of time was observed for the total number of lever presses (**G**), lever press latency (**I**), and lever probability (**K**) (P's<0.01). However, no main effect of exposure or interaction between factors was observed (P's>0.05). Also, a significant main effect of time was observed for the elevation score on omission session (**H**) (P=0.002). Nevertheless, no significant effect was observed for the latency (**J**), neither for probability (**L**)to perform a receptacle entry (P's>0.05). All data are expressed as mean ± SEM for CON (n=8, black) and AIE group (n=14, orange). ** P<0.01 and *** P<0.001. For statistical details see Supplemental Table 3.

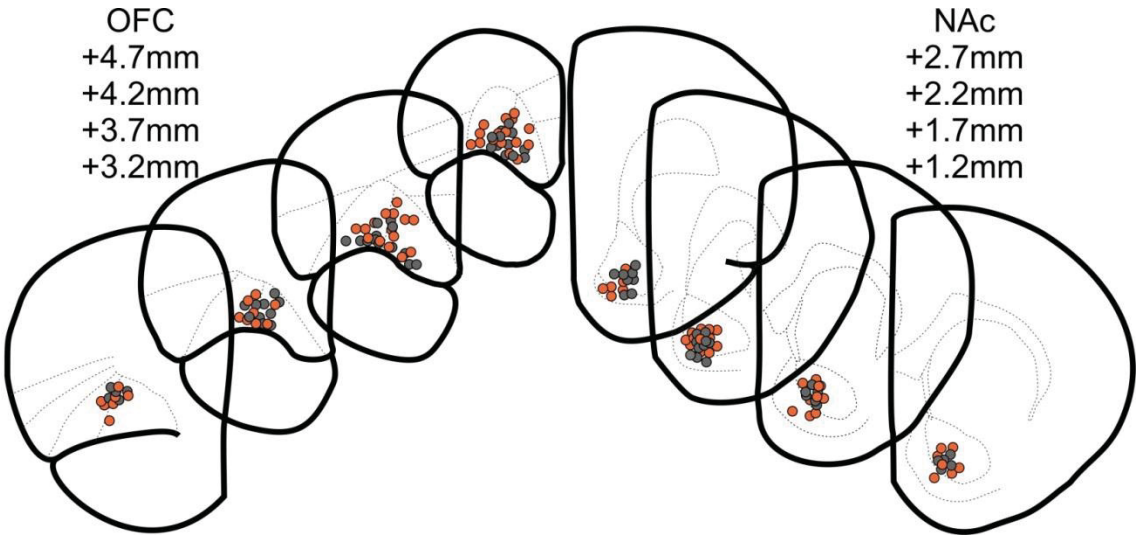

Supplemental Fig. S4. Representative illustration of the electrode placements on OFC or NAc. Electrode placements in CON (gray) and AIE group (orange) illustrate the approximated anatomical position of electrode wires in which successful electrophysiological recordings were performed. Anatomic coordinates were obtained from Paxinos and Watson (2007), demonstrating the antero-posterior coordinates of the electrode placements.

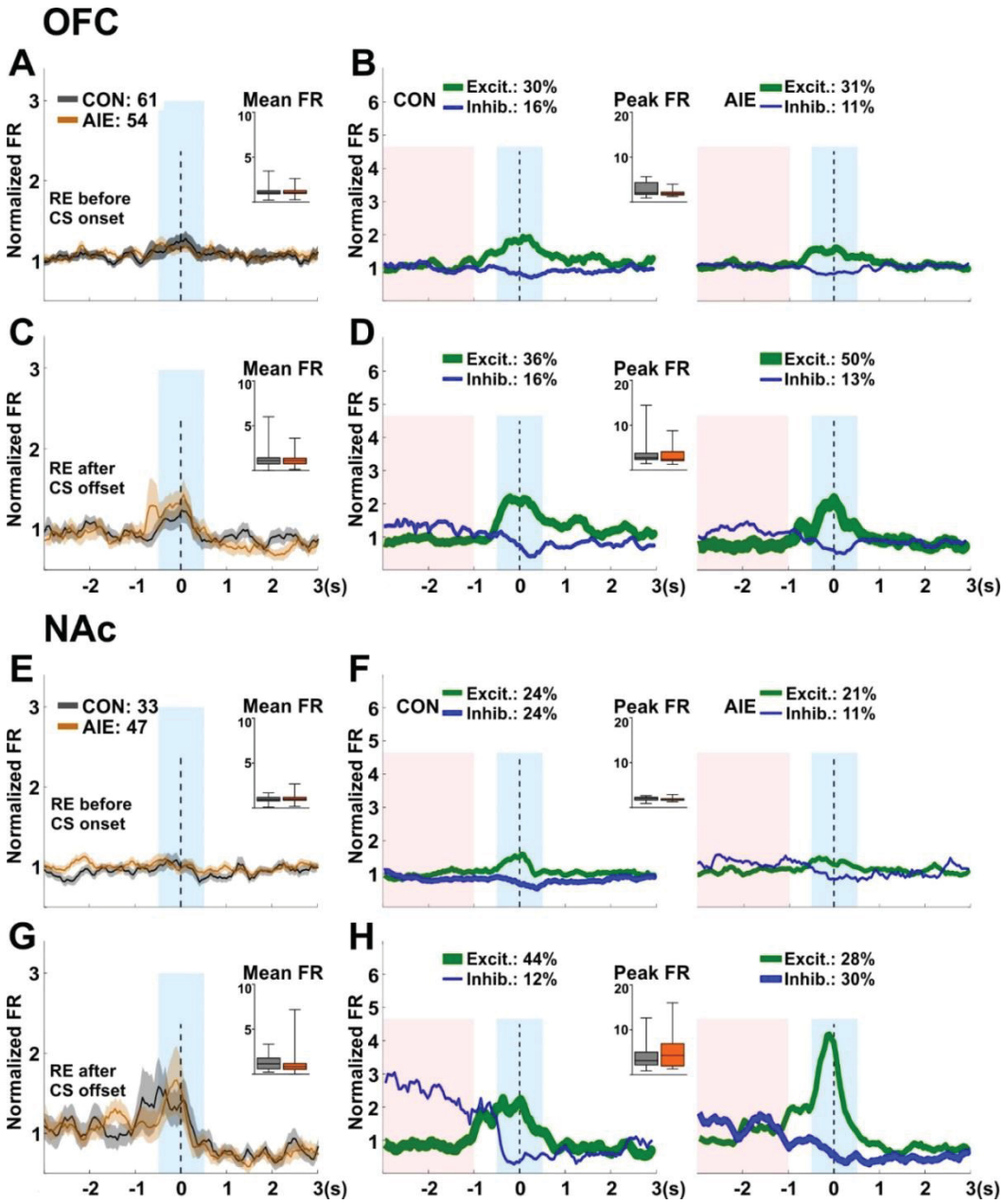

Supplemental Fig. S5: On receptacle entries that were not evoked by CS onset, no AIE effect was observed on OFC and NAC activity. Single-unit activity of OFC and NAc neurons were recorded during the PCA baseline session in sign-tracking rats. Neuronal population activity data (**A, C, E, G**) are normalized to the whole session firing rate and presented as mean firing rate (line) ± SEM (shading) for CON (gray) and AIE (orange) groups. Number of recorded cells: OFC= 61 cells on CON and 54 cells on AIE, NAc= 33 cells on CON and 47 cells on AIE. Inset: box plots show the mean firing rate in the target window (blue box). Phasic firing patterns (**B, D, F, H**) for neurons that showed significant changes (excitations: green, inhibitions: blue) in firing rate are shown for CON (left graphs) and AIE (right graphs) groups, with line thickness reflecting the proportion of neurons exhibiting that phasic activity (non-phasic cells are not shown). Inset: box plots show the amplitude of excitation during the target window (blue box) compared to the baseline period (red box) for each phasic excitatory cell. Figures **A** to **H** represents OFC and NAC neuronal population activity and phasic activity during the first receptacle entry performed 30 s before the CS onset and the first receptacle entry after CS offset. No AIE effect was observed on OFC or NAc neuronal activity (P's>0.05). For statistical details see Supplemental Table 4.

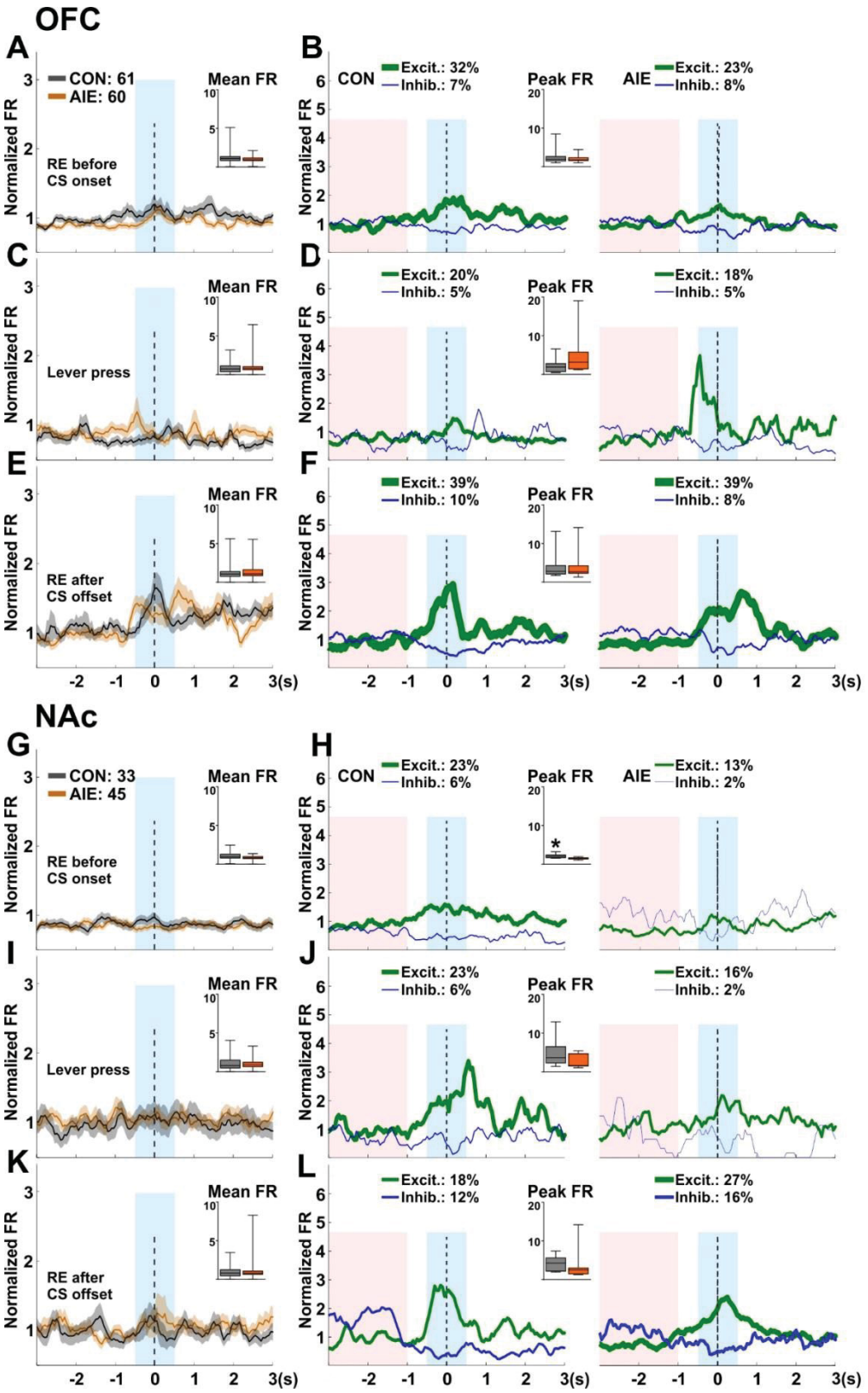

Supplemental Fig. S6: After changes in CS-US contingency, AIE group presented lower amplitude of the phasic excitation during receptacle entry before CS onset. Single-unit activity of OFC and NAc neurons were recorded during the reward omission session in sign-tracking rats. Neuronal population activity data (**A, C, E, G**) are normalized to the whole session firing rate and presented as mean firing rate (line) ± SEM (shading) for CON (gray) and AIE (orange) groups. Number of recorded cells: OFC= 60 cells on CON and 61 cells on AIE, NAc= 33 cells on CON and 45 cells on AIE. Inset: box plots show the mean firing rate in the target

window (blue box). Phasic firing patterns (**B, D, F, H**) for neurons that showed significant changes (excitations: green, inhibitions: blue) in firing rate are shown for CON (left graphs) and AIE (right graphs) groups, with line thickness reflecting the proportion of neurons exhibiting that phasic activity (non-phasic cells are not shown). Inset: box plots show the amplitude of excitation during the target window (blue box) compared to the baseline period (red box) for each phasic excitatory cell. Figures **A** to **L** represents OFC and NAc neuronal population activity and phasic activity during the first receptacle entry 30 s before the CS onset, first lever press, and first receptacle entry after CS offset. No statistical group difference was observed on OFC or NAc neuronal population activity (P's>0.05). On the neuronal phasic activity analysis, a significant group difference was observed on NAc for the amplitude of the phasic excitatory activity during the first receptacle entry 30 s before the CS onset **(H)**. CON group displayed a higher amplitude of the phasic excitation compared to AIE group (P=0.02). No additional statistical difference was observed on the percentage of neurons presenting phasic excitation, neither on the amplitude of the phasic excitatory activity in both OFC and NAc (P's>0.05). *significant group difference on the amplitude of the phasic excitatory activity (P<0.05). For statistical details see Supplemental Table 4.

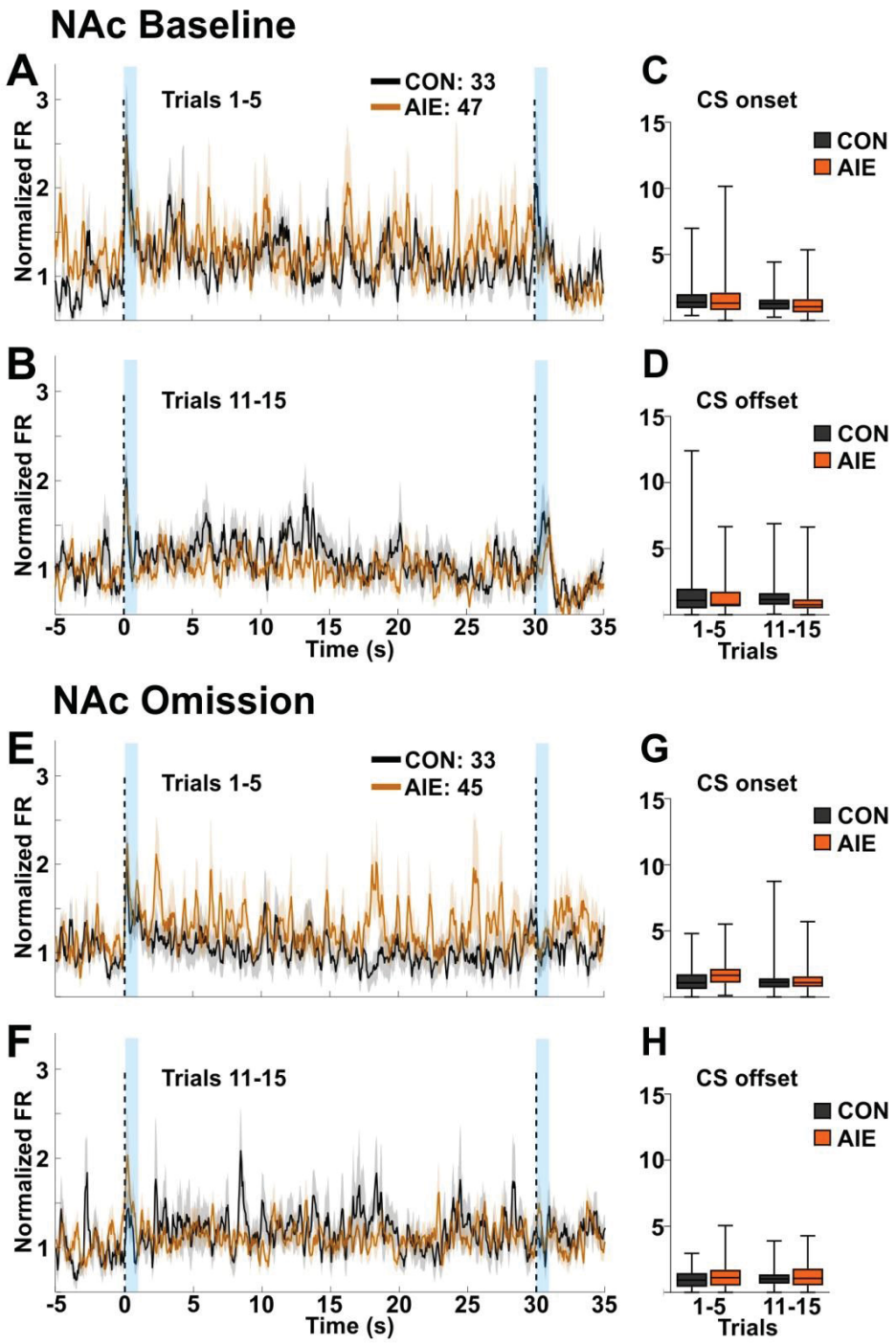

Supplemental Fig. S7: No significant difference was observed in NAc activity across the recording sessions. Single-unit activity on NAc in response to CS onset and CS offset (dashed lines) was acquired during trials 1 to 5 and trials 11 to 15 in both baseline and omission session. Figures **A, B, E,** and **F** represent NAc neuronal population activity around the 30 second CS period for trials 1-5 and 11-15 during the baseline session and omission session. Neuronal activity was normalized to the whole session firing rate and presented as mean firing rate (line) ± SEM (shading) for CON (gray) and AIE (orange) groups. Figures B, D, F, and H represent the mean firing rate in the target window (blue box) during first and late trials. Figures **C** and **D** demonstrated the NAc activity after CS onset and CS offset on baseline session: no significant main effects or interaction between factors was observed (P's>0.05). Figures **G** and **H** demonstrated the NAc activity after CS onset and CS offset on omission session: no significant main effects or interaction between factors was observed (P's>0.05). For statistical details see Supplemental Table 5.

Supplemental Material

Supplemental Table 1

I. Behavioral data during Pavlovian conditioning approach. Last 5 days of training phase (all animals)		
Variable	**P**	**MWU (U)**
LP	0.29	159
Lever latency	0.19	150
Lever probability	0.13	143
ES	0.61	179
Receptacle probability	0.97	196
Variable	**P**	**T-test (T)**
Receptacle latency	0.61	0.53
II. ST-GT score calculation		
Variable	**P**	**MWU (U)**
ST-GT score	0.21	152

Supplemental Table 2

I. Behavioral data during Pavlovian conditioning approach sessions (baseline and omission session)

Only ST animals					
Variable	**Effect**	**P**	**Exp(B)**	**CI Lower**	**CI Upper**
LP	Exposure	0.56	1.267	0.561	2.859
	Session	0.43	1.426	0.591	3.443
	Exp*Session	0.88	0.885	0.376	3.110
Lever latency	Exposure	0.98	0.948	0.005	190.2
	Session	0.12	0.009	0.001	3.425
	Exp*Session	0.88	0.585	0.000	1055
Lever probability	Exposure	***0.08***	0.910	0.818	1.012
	Session	**<0.001**	1.255	1.123	1.404
	Exp*Session	0.19	1.099	0.954	1.266
Receptacle latency	Exposure	0.46	3.749	0.113	124.8
	Session	***0.09***	0.034	0.001	1.786
	Exp*Session	0.83	1.678	0.012	238.8
Receptacle probability	Exposure	***0.08***	0.870	0.741	1.021
	Session	**<0.001**	1.514	1.289	1.778
	Exp*Session	0.88	0.985	0.801	1.212
Variable	**Effect**	**P**	**F**	**CI Lower**	**CI Upper**
Elevation score	Exposure	**0.01**	1.485	3.369	24.63
	Session	**0.03**	0.815	1.399	38.20
	Exp*Session	**0.02**	5.323	2.140	34.64
RE 30 s before CS onset	Exposure	0.24	1.412	2.795	10.19
	Session	**<0.001**	50.08	13.98	25.66
	Exp*Session	0.21	1.623	4.580	18.82
RE during CS onset	Exposure	0.65	0.210	2.797	12.88
	Session	**<0.001**	31.95	5.937	4.372
	Exp*Session	0.65	0.202	5.449	8.442

Supplemental Table 3

I. Behavioral data acquired in different stages of baseline and omission session (average of trials 1-5 and 11-15) was compared between CON-exposed versus AIE-exposed animals.

		PCA baseline				Reward omission			
Variable	**Effect**	**P**	**Exp(B)**	**CI Lower**	**CI Upper**	**P**	**Exp(B)**	**CI Lower**	**CI Upper**
Lever presses	Exposure	0.16	1.178	0.937	1.481	0.44	0.811	0.474	1.389
	Time	0.15	0.823	0.630	1.074	**<0.001**	0.564	0.404	0.789
	Exp*Session	0.55	0.557	0.778	1.592	**0.02**	1.969	1.071	3.622
Lever latency	Exposure	0.53	0.942	0.779	1.138	0.56	0.930	0.726	1.192
	Time	0.12	0.821	0.636	1.058	**<0.01**	0.649	0.459	0.918
	Exp*Session	0.25	1.213	0.872	1.688	0.92	1.022	0.636	1.644
Lever probability	Exposure	0.65	0.970	0.850	1.108	0.97	0.992	0.582	1.694
	Time	0.34	0.947	0.845	1.062	**<0.001**	1.842	1.296	2.618
	Exp*Session	0.51	1.048	0.910	1.207	0.73	0.905	0.507	1.615
ES	Exposure	0.42	7.395	0.052	1052	0.33	7.139	0.129	394.0
	Time	***0.06***	145.5	0.763	27768	**<0.01**	0.001	0.002	0.088
	Exp*Session	**0.03**	0.001	0.001	0.677	0.75	2.512	0.008	772.5
Receptacle latency	Exposure	0.77	1.014	0.922	1.115	0.22	1.057	0.966	1.155
	Time	0.67	1.021	0.927	1.124	0.32	1.053	0.951	1.166
	Exp*Session	0.72	0.948	0.861	1.110	0.60	0.969	0.861	1.090
Receptacle probability	Exposure	0.85	1.052	0.611	1.811	0.45	1.322	0.639	2.734
	Time	0.45	0.780	0.407	1.495	0.19	1.702	0.762	3.800
	Exp*Session	0.78	1.135	0.452	2.853	0.39	0.646	0.235	1.774

Supplemental Table 4

I. Neuronal population data analyzed on baseline session. Mean firing rate acquired during the events on interest was compared between CON-exposed versus AIE-exposed animals.				
	OFC		NAc	
Variable	P	MWU (U)	P	MWU (U)
CS onset	**0.05**	1298	0.65	729
CS offset	**0.02**	1253	0.21	647
LP	0.65	1566	0.14	626
First RE after CS onset	0.35	977	**<0.01**	223
RE before CS onset	0.73	1585	0.93	766
RE after CS offset	0.53	1537	0.23	653
II. Neuronal population data analyzed on omission session. Mean firing rate acquired during the events on interest was compared between CON-exposed versus AIE-exposed animals.				
CS onset	**0.04**	1436	0.53	680
CS offset	0.56	1719	0.50	676
LP	0.23	1598	***0.08***	574
RE before CS onset	0.48	1693	0.77	713
RE after CS offset	0.49	1697	0.96	738
III. Comparison between peak of firing rate presented by phasic excited cells on the baseline session on CON-exposed versus AIE-exposed animals.				
CS onset	>0.99	58	0.11	68
CS offset	0.35	73	0.81	33
LP	0.94	51	0.67	31
First RE after CS onset	0.44	35	0.81	12
RE before CS onset	0.30	121	0.35	29
RE after CS offset	0.46	260	0.92	95
IV. Comparison between peak of firing rate presented by phasic excited cells on the omission session on CON-exposed versus AIE-exposed animals.				
CS onset	0.78	108	0.37	61
CS offset	0.28	43	0.71	7
LP	0.21	19	0.29	13
RE before CS onset	0.65	120	**0.02**	6
RE after CS offset	0.97	274	0.10	18
IV. Comparison between the percentage of phasic excited neurons on baseline session on CON-exposed versus AIE-exposed animals.				
Variable	**P**	**Chi-square**	**P**	**Chi-square**
CS onset	0.20	1.608	0.33	0.926
CS offset	***0.09***	2.813	0.58	0.300
LP	0.11	2.503	0.58	0.300
First RE after CS onset	0.58	0.303	**<0.001**	17.65
RE before CS onset	0.81	0.052	0.79	0.068
RE after CS offset	0.13	2.274	0.10	2.699
V. Comparison between the percentage of phasic excited neurons on omission session on CON-exposed versus AIE-exposed animals.				
CS onset	**0.04**	4.027	0.48	0.488

CS offset	0.60	0.264	0.56	0.335
LP	0.56	0.327	0.75	0.094
RE before CS onset	0.28	1.158	0.21	1.538
RE after CS offset	0.39	0.724	0.37	0.772

Supplemental Table 5

I. Neuronal population analysis on different stages of baseline and omission session (average of trials 1-5 and 11-15) was compared between CON-exposed versus AIE-exposed animals.

		Baseline				Omission			
Variable	**Effect**	**P**	**Exp(B)**	**CI Lower**	**Upper**	**P**	**Exp(B)**	**CI Lower**	**Upper**
II. OFC neuronal population activity (mean firing rate) was compared across session and exposure.									
CS onset	Exposure	**0.01**	1.500	1.085	2.075	**0.04**	1.392	1.013	1.913
	Time	0.44	1.141	0.815	1.596	0.86	1.031	0.733	1.450
	Exp*Session	0.43	0.835	0.531	1.314	0.59	0.886	0.564	1.391
CS offset	Exposure	***0.08***	1.359	0.957	1.931	0.85	0.969	0.693	1.355
	Time	1.00	1.000	0.761	1.315	0.79	0.957	0.683	1.340
	Exp*Session	0.57	0.887	0.582	1.352	0.76	1.076	0.670	1.730
II. NAc neuronal population activity (mean firing rate) was compared across session and exposure.									
CS onset	Exposure	0.55	0.890	0.611	1.302	0.21	1.288	0.860	1.929
	Time	0.33	1.208	0.824	1.771	0.23	1.297	0.845	1.992
	Exp*Session	0.68	1.112	0.671	1.845	0.67	0.887	0.517	1.530
CS offset	Exposure	0.38	0.840	0.567	1.242	0.65	0.658	0.722	1.677
	Time	0.83	1.043	0.696	1.564	0.90	0.906	0.611	1.548
	Exp*Session	0.87	1.045	0.606	1.804	0.77	0.772	0.499	1.677

3.2 Nucleus accumbens neurons encode initiation and vigor of reward approach behavior

David Levcik[1, 4, *], Adam H. Sugi[1,2,3*], José A. Pochapski[1,2], Gabriel Baltazar[1,2,3], Laura N. Pulido[1,2], Cyrus Villas-Boas[1], Marcelo Aguilar-Rivera[5], Romulo Fuentes-Flores[6], Saleem M. Nicola[7,8], Claudio Da Cunha[1,2,3 #]

1. Laboratório de Fisiologia e Farmacologia do Sistema Nervoso Central, Universidade Federal do Paraná, 81531-980, Curitiba, Brazil. Tel +55(41)3361-1717, dacunha.claudio@gmail.com
2. Department of Pharmacology, Universidade Federal do Paraná, Curitiba, Brazil.
3. Department of Biochemistry, Universidade Federal do Paraná, Curitiba Brazil.
4. Institute of Physiology of the Czech Academy of Sciences, Videnska 1083, 142 20, Prague, Czech Republic.
5. Department of Bioengineering, University of California, 9500 Gilman Drive MC 0412, La Jolla, San Diego, 92093, USA.
6. Departamento de Neurociencia, Facultad de Medicina, Universidad de Chile, Av. Independencia 1027, Independencia 8380453, Santiago, Chile.
7. Department of Neuroscience, Albert Einstein College of Medicine, 1300 Morris Park Ave, Bronx, New York, 10461 USA.
8. Department of Psychiatry, Albert Einstein College of Medicine, New York, USA.

* Both authors presented equally important contributions.
# Corresponding author email address: dacunha.claudio@gmail.com

• Number of pages: 30
• Number of figures, tables, multimedia, and 3D models: 9, 2, 0, 0
• Number of words for abstract, introduction, and discussion: 250, 549, 1496
• Conflict of interest statement: The authors declare no competing financial interests.
• Acknowledgments: The financial support of the grants CNPq (432061/2018-5, 306855/2017-8, 465346/2014-60, 314654/2014-3), AZV 17-30833A, and GACR 20-00939S, is acknowledged.

Abstract

The nucleus accumbens (NAc) is considered an interface between motivation and action, with NAc neurons playing an important role in promoting reward approach. However, the encoding by NAc neurons that contribute to this role remains unknown. Here, we trained male rats to find rewards in an 8-arm radial maze. The activity of 62 neurons, mostly in the shell of the NAc, were recorded while rats ran towards each reward place. General linear model (GLM) analysis showed that variables related to the vigor of the locomotor approach, like speed and acceleration, and the fraction of the approach run completed were the best predictors of the firing rate for most NAc neurons. Nearly 23% of the recorded neurons, here named locomotion-off cells, were inhibited during the entire approach run, suggesting that reduction in firing of these neurons promotes initiation of locomotor approach. Another 24% of the neurons presented a peak of activity during acceleration followed by a valley during deceleration (peak-valley cells). Together, these neurons accounted for most of the speed and acceleration encoding identified in the GLM analysis. Cross-correlations between firing and speed indicated that the spikes of peak-valley cells were followed by increases in speed, suggesting that the activity of these neurons drives acceleration. In contrast, a further 19% of neurons presented a valley during acceleration followed by a peak just prior to or after reaching reward (valley-peak cells). These findings suggest that these three classes of NAc neurons control the initiation and vigor of the locomotor approach to reward.

Significance Statement

Deciphering the mechanisms by which the NAc controls the vigor of motivated behavior is critical to better understand and treat psychiatric conditions in which motivation is dysregulated. Manipulations of the NAc profoundly impair subjects' ability to spontaneously approach reward-associated locations, preventing them from exerting effort to obtain reward. Here, we identify for the first time specific activity of NAc neurons in relation to spontaneous approach behavior. We discover three classes of neurons that could control initiation of movement and the speed vs. time trajectory during locomotor approach. These results suggest a prominent but heretofore unknown role for the NAc in regulating the kinematics of reward approach locomotion.

Introduction

Since the early anatomical and physiological studies that established the nucleus accumbens (NAc) as a limbic-motor interface (Mogenson et al., 1980), a consensus view has emerged that a major function of NAc neurons is to promote the vigorous pursuit of rewards (Nicola, 2007; Salamone and Correa, 2012; Nicola, 2016). Manipulations of the NAc, and particularly of its dopamine input, impair performance of high-effort operant tasks while leaving lower-effort tasks relatively unaffected (Salamone et al., 1999), bias animals to choose the less effortful option in T-maze tasks (Salamone et al., 1994; Cousins et al., 1996; Hauber and Sommer, 2009), and reduce the probability of engaging in locomotor approach responses to reward-predictive cues (Nicola, 2010; Ambroggi et al., 2011). Consistent with these observations, many NAc neurons are excited by reward-predictive cues (Nicola et al., 2004; Gmaz et al., 2018), and these excitations predict the vigor of the approach response – specifically, the firing is greater when the latency to initiate approach will be shorter and the speed of approach greater (McGinty et al., 2013; Morrison et al., 2017). This form of encoding likely causally contributes to vigorous performance of cued approach tasks (du Hoffmann and Nicola, 2014; Caref and Nicola, 2018).

Although NAc cue-evoked firing responses compellingly link reward prediction to effort exertion, most paradigms that have revealed an effect of NAc manipulations on effort-based performance have not involved presentation of explicit predictive cues (Cousins et al., 1996; Aberman and Salamone, 1999; Salamone et al., 1999; Hauber and Sommer, 2009). For example, NAc disruption selectively impairs high-effort operant task performance by preventing the subject from approaching the operandum after pauses in performance, which are more frequent in higher-effort than lower-effort operant tasks (Nicola, 2010). These observations suggest that NAc neurons control spontaneous approaches to rewarded locations. The NAc neuronal activity underlying this form of effort exertion remains poorly understood. One challenge is to identify the onset of spontaneous approach events, which is difficult when standard operant chambers are used because short-distance spontaneous approaches are similar to the frequent non-approach movements exhibited by rodents when they are not engaged in the task. In contrast, approach movements are readily identifiable in maze or runway tasks in which subjects must move long distances (e.g. 1 m or greater) to rewarded locations. Although NAc neuronal activity has been measured in such tasks (Shibata et al., 2001; Mulder et al., 2004; Mulder et al., 2005; German and Fields, 2007; Khamassi et al., 2008; van der Meer and Redish, 2009; van der Meer et al., 2010), the relationship between neuronal activity and locomotor vigor has not been systematically investigated, despite anecdotal reports that the speed of locomotion is reported by NAc neurons (Sjulson et al., 2018).

To clarify how NAc neurons represent the vigor of spontaneous locomotion, we recorded from NAc neurons as rats performed an 8-arm radial maze task in which 3 arms were consistently rewarded with either the same or different chocolate milk reward values. We found that speed and proximity to the rewarded target were prominently encoded by many NAc neurons during reward approach, and that neuronal activity predicted speed approximately 100 ms in advance. In addition we found 3 classes of neurons with different patterns of activity that could control when the approach run starts as well as the timing of acceleration and deceleration.

Materials and Methods

Subjects

We used 5 adult male Wistar rats that were three months old at the beginning of the experiment. The rats came from the breeding colony of the Federal University of Parana State and were housed in groups of 4 per cage during behavioral training and individually after surgery. The rats were maintained in a temperature-controlled room (22 ± 2 °C) with a 12-hr light/dark cycle (lights on at 7:00 am). Access to water was allowed for one hour per day, and access to food was restricted to maintain the rats' body weight at 90% of their free-feeding weight (290 - 340 g). All experimental procedures were in agreement with the Brazilian and International legislation for animal care (Law N° 11.794 of October 8, 2008; EC Council Directive of November 24, 1986; 86/609/EEC). The project was approved by the Animal Care and Use Committee of the Federal University of Parana State and efforts were made to minimize the number of animals used, and their suffering and discomfort during the experimental procedures.

Apparatus

We used a stainless steel eight-arm radial maze, which had a surface covered with black contact paper, for behavioral training. Each arm (62 cm x 13 cm) and the central platform (an octagon with a 30 cm diameter) were elevated 60 cm above the floor. The walls of all arms were 5 cm high. One or four drops (25 µl per drop) of chocolate milk were delivered at the ends of reward arms before the start of each trial. A white curtain was installed around the maze and several salient visual cues (black felt geometrical shapes) were attached to it and remained in the same locations throughout behavioral training and experiments. Four light bulbs (15 W) were spaced equally on a metal frame (70 × 70 cm) above the center of the maze. This metal frame also served as a support for a motorized commutator (Plexon, USA), a camera (Allied Vision Technologies GmbH, Germany) connected to the main computer, and an amplifier (Plexon, USA). An OmniPlex D Neural Data Acquisition system (Plexon, USA) was located in the same room. Metal mesh was installed on the walls of the experimental room and grounded to create a Faraday cage.

Behavioral procedures

All rats were handled (5 min/day) by the experimenter for three consecutive days before the start of behavioral pre-training. During pre-training, rats were habituated to the maze and the chocolate milk reward by placing them at the end of one arm and letting them drink the chocolate milk from the reward receptacle.

After the pre-training phase, rats were trained to collect drops of chocolate milk consistently located at the ends of the same three arms of an eight-arm radial arm maze (Fig. 1A). The positions of these three reward arms were counterbalanced among rats and were chosen in a pseudorandom manner so that two adjacent arms were never baited. In the same-reward group (n = 2), all reward arms (X, Y and Z) contained 4 drops of chocolate milk (100 µl) in 100% of trials. In the different-reward group (n = 3), one of the reward arms contained four drops (100 µl) of chocolate milk in 100% of trials (high reward, H arm), another reward arm contained four drops (100 µl) in 66.7% of trials (medium reward, M arm), and the last reward arm contained one drop (25 µl) in 100% of trials (low reward, L arm). The arm that was less preferred by the rats at the end of the pre-training phase was assigned as the H arm, and the most preferred arm was assigned as the L arm. The rewarded locations, and the reward amounts and probabilities, remained constant for a given rat throughout training and experiments.

In both same-reward and different-reward groups, a fourth arm was consistently used as a resting platform, where the rats were placed and restricted between trials. The other four arms were used as starting positions (S1 - S4, Fig. 1A). The rats underwent nine trials per day. Two starting positions were alternated in a pseudorandom order, one used three times and the other two times. Each trial finished when all rewards were collected or after 5 min elapsed. The rats were trained five days per week until they reached the following criteria in three consecutive training days: a) no more than 20% reference memory errors (entering a non-reward arm); b) the high reward arm (4 drops, 100% probability) is the last choice in no more than 20% of trials; and c) the low reward arm (1 drop, 100% probability) is the first choice in no more than 20% of trials. Criteria b and c were applied only to the different-reward group. The rats took 40 to 50 training days to achieve these criteria.

Afterwards, rats underwent surgery to implant recording electrodes. After recovery, they were re-trained to the pre-surgery level of performance, which took approximately seven days. During these re-training sessions and the following test sessions, 12 trials per session were carried out.

Arm preference analysis

To show potential preferences for particular reward arms among individual rats, we compared the total number of first reward arm choices from all recording sessions to the chance level (total number of trials/3 – because we used three reward arms; Fisher’s exact test).

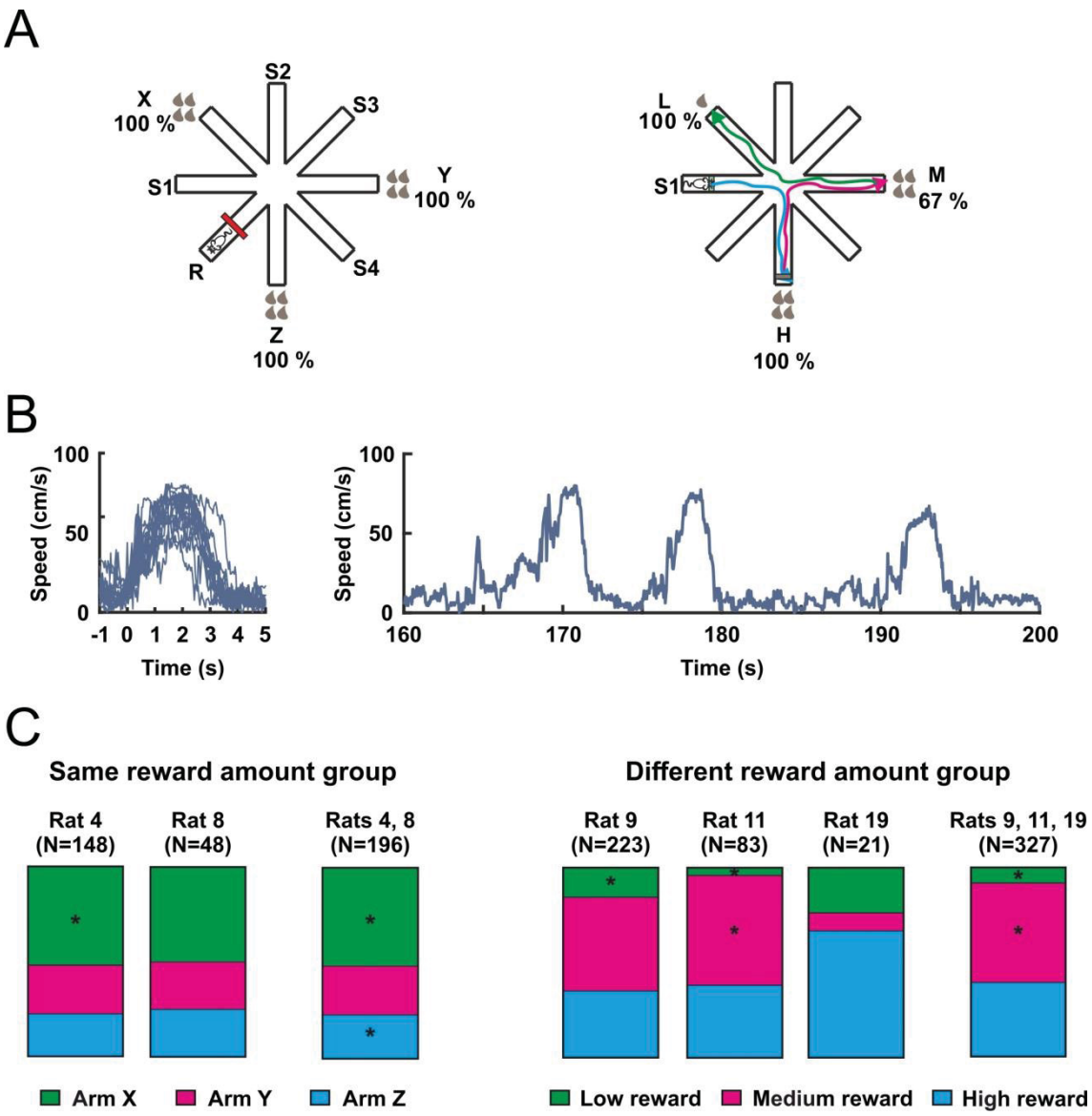

Figure 1: The eight-arm radial maze task. (A) Rats were trained to find drops of chocolate milk in the ends of the 3 baited arms. Two rats were trained to find the same reward amount (4 drops) with 100% probability (left) and the other three rats a different reward amount with a different probability (middle) in the end of the three reward arms. Each brown drop represents 25 µl of chocolate milk. The probabilities of reward occurrence are displayed next to each reward arm. Arms X, Y, and Z had equal reward value, and arms L, M, and H had low, medium, and high reward values, respectively. The red line represents an obstacle that was placed in the middle of the resting arm between trials to keep the rat restricted in the distal half of the starting arm. S1, S2, S3 and S4 indicate the starting arms. (B) Superimposed changes in speed during all runs of an individual session (left). Changes in speed during three subsequent runs (right). (C) Bars show the fraction of trials in which subjects entered the indicated arm first. * $P < 0.01$, compared to random choice (Fisher test).

Surgery

The rats were anesthetized with isoflurane (2%), placed in a stereotaxic frame (David Kopf, USA), and a customized microdrive with 2 × 4 stereotrode arrays (17 µm Ni-Chrome wire with insulation; A-M Systems, USA) was chronically implanted unilaterally above NAc shell at the following coordinates: AP +1.2 to +2.2 mm from bregma, ML +0.6 to +1.0 mm from midline, DV −5.0

mm from dura. The coordinates were determined according to the Paxinos and Watson Atlas (2007). Six anchoring stainless steel screws were placed in the skull to attach the implant using acrylic dental cement. One of the screws also served as a ground. After surgery, enrofloxacin (20 mg/kg; i.m.) was injected, neomycin gel was applied to the tissue around the implant, and ibuprofen (50 mg/500 ml) was added to the drinking water for the three following days. The rats were allowed to recover for seven days after the surgical procedures.

Electrophysiological recording

After one week of recovery, the stereotrodes were lowered in 40 µm increments (up to 160 µm/day) until single-unit activity was reliably detected and isolated. All stereotrodes were previously gold-plated with a nanoZ impedance tester (Multi Channel Systems, USA) to impedances between 100 − 300 kOhms. Two light-emitting diodes attached to the 16-channel headstage (20 x gain) signaled the position of the animal and allowed video tracking (30 frames/s) with the Cineplex system (Plexon, USA). Neural activity was amplified (1000 x), filtered (300 − 6000 Hz) and sampled at 40 kHz with the OmniPlex D Neural Data Acquisition system (Plexon, USA) to acquire and record single unit activity.

Spike sorting

Recorded spikes were manually sorted offline into clear clusters of putative cells with Offline Sorter software (Plexon, USA). To be accepted for spike sorting, spike amplitudes had to be at least three standard deviations higher than the background activity. Clusters were based on waveform properties identified through principal component analysis. Inter-spike interval histograms were calculated, and those clusters with similar waveform shape that showed a clearly recognizable refractory period (> 1.5 ms) were considered as originating from a single neuron.

Neuronal activity analysis

A test session consisted of 12 trials. In each trial, the rats should visit the three reward arms. The rats usually approached the reward areas of the three reward arms only once. Each approach was defined as a run – when the rat ran from the distal end of one arm towards the reward area of a reward arm (Fig. 1A). Trained rats performed few visits to non-reward arms, and only data from approaches to reward arms were analyzed. For most analyses, the time window analyzed for each run extended from 1 s before locomotion onset to 1 s after the locomotion end. Taking advantage of the fact that the animals' behavior across runs was generally consistent, locomotion onset was defined as the first time point in which the speed of the animal reached 20 cm/s before the peak speed of the run (Fig. 1B). Locomotion end was set as the first point at which the speed dropped below 10 cm/s. We restricted our analysis to stereotyped trajectories to the reward defined by an efficiency criterion, which was

calculated as the ratio of the distance traveled in the run to the length of the ideal path (from the end of one arm to the reward area of another arm). Incomplete runs, i.e. the rat enters the arm but does not reach the end of it, result in ratios <1. To eliminate most such runs, and runs in which the animal deviated substantially from a direct trajectory to the end of the reward arm, runs with high efficiency (ratio < 0.8) or low efficiency (ratio > 1.2) were discarded.

General linear model (GLM)

The goal of the multiple regression analysis was to evaluate which performance-related parameters can be used to predict neuronal firing rate. A general linear model (GLM) was calculated with the firing rate (spikes/100-ms bin) as the dependent variable and 12 parameters as predictors (independent variables; Tab. 1). Pearson correlations (r) among pairs of predictor variables were calculated and, for the pairs that showed r > 0.8, one of them was excluded (e.g. time and fraction of the run; Fig. 2).

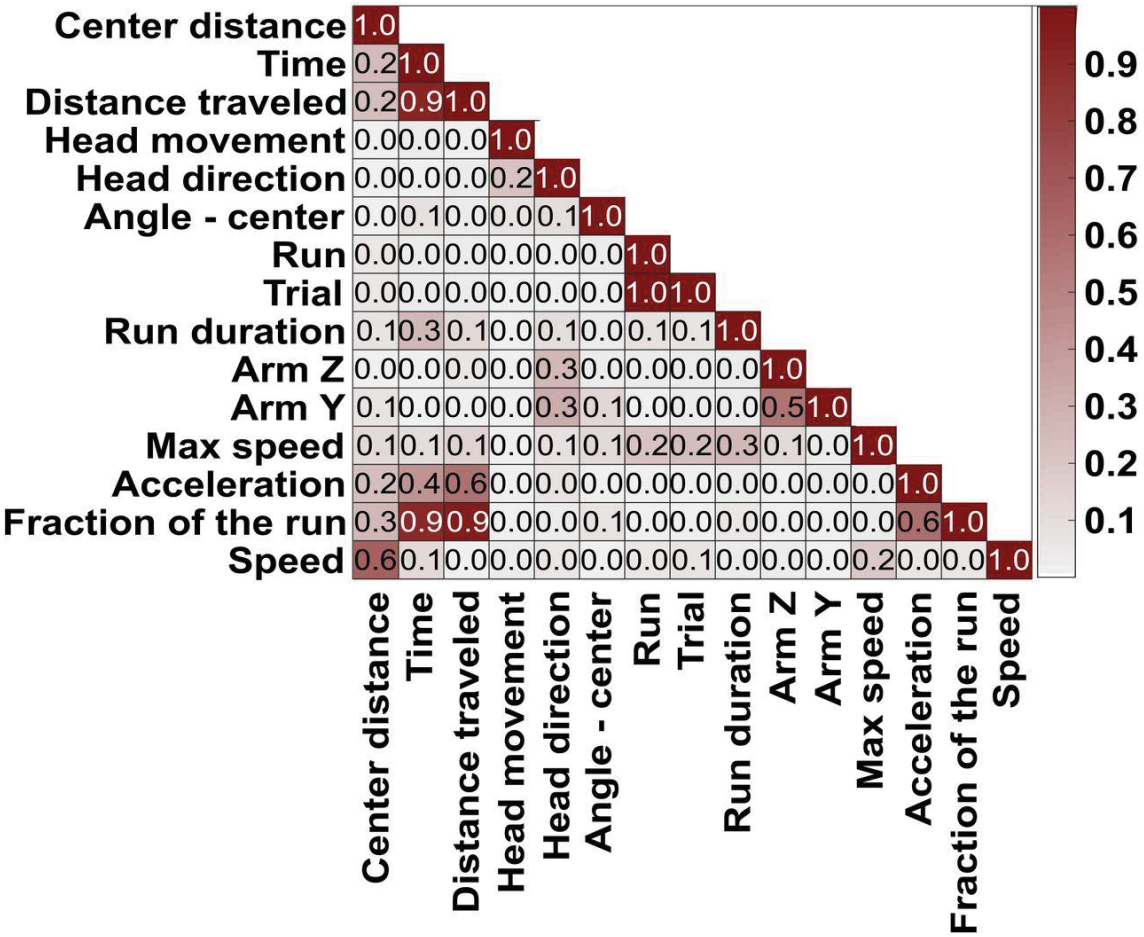

Figure 2: Correlation table for predictor variables considered for use in the GLM encoding model. For the pairs with high correlation (r > 0.8), one of the pairs was chosen to be included in the model.

Different continuous variables were extracted from the coordinates tracked in the recorded videos. The rat's locations were tracked at 30 frames

per second. However, to match the neuronal data that were binned at 100 ms, an interval of 3 frames was used (3 frames = 100 ms interval). Firing rate, speed and acceleration were smoothed by a sliding average window of 300 ms (Kropft et al., 2015; Rueda-Orozco and Robbe 2015). The β values were calculated with the MATLAB glmfit function. The multiple regression assumed a normal distribution for the data and the identity link function was used to estimate the β value for each parameter.

The GLM followed the equation:

$$Y(t) = \beta 0 + \beta 1 \boldsymbol{x} 1(t) + \beta 2 \boldsymbol{x} 2(t) + \ldots + \beta n \boldsymbol{x} n(t) + \varepsilon$$

where Y(t) is the predicted firing rate at time t, βn is the weight of the predictor n, xn(t) is the value of the predictor n at time t, and ε is the error term. For each neuron, the model was trained and tested by the fivefold cross validation method (Engelhard et al., 2019) as follows. The data from all the runs (speed, acceleration, firing rate, etc.) were divided into 5 parts with the same number of runs. The runs used in each part were randomly selected. The model was trained and tested five times with 4/5 of the total data, and the ability of the model to predict the remaining 1/5 of the data was assessed by correlating the predicted data to the actual data. Always, a different combination of the data was used as training and test data (Fig. 3).

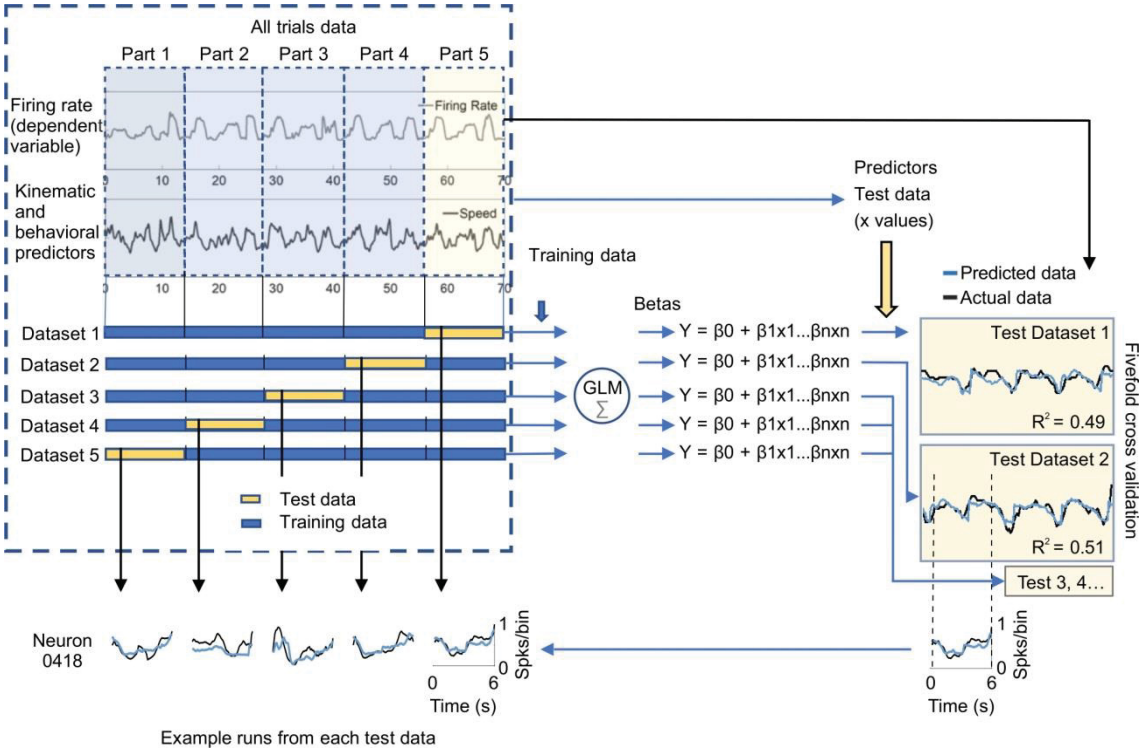

Figure 3: Fivefold cross validation method for evaluating the GLM encoding model. Data (firing rate and predictor variables) from a whole session were divided into five parts (datasets). Each dataset had the same number of runs (selected randomly). Four of the five datasets were used as training datasets to calculate the β values for each predictor. Then, using the predictors data from the remaining dataset (the test dataset) as input to the encoding model, predicted firing rates (Y) were calculated. The predicted firing rates were compared to the actual firing rates from the test data set. The variance explained by the GLM was calculated as the r^2 of the

correlation between the predicted and actual data. This process was repeated 5 times, with each dataset used only once as test data. The variance explained by the model was the mean of the 5 r^2 values (r^2mean).

The mean of the r^2 values obtained from the five correlations (r^2mean) was considered the mean fraction of variance explained by the full model (FM, the model with all predictors included). The significance of the model was evaluated by comparing the r^2mean to the distribution of r^2mean values generated by models trained with shuffled neuronal data (100 shuffled models per neuron, n = 62 neurons). Neurons for which the model explained the actual data better than the 99th percentile of the shuffled models were classified as having their firing rates significantly explained by the encoding model.

Contribution of each predictor to the GLM

To evaluate which variables had a significant contribution to the full model (FM), only neurons significantly explained by the FM were analyzed. To calculate the contribution of each of the variables (var) to the FM, the FM was compared to the full model less the selected variable (FM – var). The fraction of the variance of the FM explained by each variable was calculated as:

$C = 1 - R^2FM/FM - var,$

in which C is the fraction of the contribution of the variable to the FM and $R^2FM/FM - var$ is the r^2 of the correlation between the output of the FM and the output of the FM – var. Next, we tested whether the percent of the variance explained after each variable was removed (C*100) was significantly different from the percent of variance explained by the FM. Log(C*100), but not C*100, passed the D'Agostino & Person test of normality (D'Agostino, 1986). Therefore, log(C*100) was used for t-tests in this analysis. The contribution of a variable was considered significant if $P < 0.01$.

Cross-correlogram analysis

The aim of this analysis was to test whether changes in firing rate preceded or followed changes in the animal's speed. First, based on each neuron's Pearson's correlation between speed and firing rate, we divided neurons into two groups, those with positive correlations between firing rate and speed, and those with negative correlations. Only neurons with correlations higher or lower than the 99.5th percentile of a bootstrapping distribution of Pearson's correlations were included in these groups (1000 correlations of shuffled spike times and speed were generated for each neuron). For each of the included neurons, the average speed before and after each spike (bins of 33 ms) was calculated to generate a normalized (z-scored) cross-correlogram. Finally, the time of the peak of each cross-correlogram was identified and then compared to zero (one-sample t-test).

The two Gaussians model (2G)

The 2G model used fraction of time as the only independent variable. Time during the run was normalized by dividing the periods from locomotion onset to the peak of speed and from the peak of speed to locomotion end into 10 bins each. On average, the bin width was ~150 ms. The time windows starting 1.05 s before locomotion onset to locomotion onset, and from locomotion end to the 1.05 s after locomotion end, were each divided in 7 bins (150 ms each). The firing rate during each bin was calculated and z-transformed.

$$Y_{(t)} = G1_{(t)} + G1_{(t)} + \mathrm{BL}$$

where *Y(t)* is the predicted firing rate at time *t*, G1 is the Gaussian equation for the peak of the curve, G2 is the equation for the valley of the curve, and BL is the baseline activity.
The Gaussian equations (G(t)) used were:

$$G1_{(t)} = H1e^{-\pi(\frac{X_{(t)}-F1}{W1})^2} \quad G2_{(t)} = -H2e^{-\pi(\frac{X_{(t)}-F2}{W2})^2}$$

where H, F, and W are constants with the following meaning: H represents the amplitude of the Gaussian curve, which reflects the height (H1) and depth (H2) of the activity peak and the valley, respectively. F is the bin where the Gaussian is centered. Therefore, F1 is the bin in which the neuron is most active, and F2 is the bin in which the neuron is least active. W is the standard deviation of each Gaussian, which reflects the durations of the activation peak (W1) and valley (W2). For each neuron, data from all runs were randomly split in two pools. One data pool was used to adjust these constants and the other pool was used to test the prediction power of the model. 2G constants were adjusted by using the Generalized Reduced Gradient (GRG) engine solver of Microsoft Excel to minimize the sum of the square roots of the difference between the firing rate recorded in each fraction of time and the firing rate predicted by the 2G model. Next, the r and P for the correlation between the firing rate predicted by the 2G model and the firing rate activity calculated with the other data pool was calculated. The 2G model was considered to significantly predict activity of a neuron when $P < 0.01$.

Data and code accessibility

The spike-train data, behavioral data and custom MATLAB code used for the data analysis of this study will be made available from the corresponding author upon reasonable request.

Histology

After completion of recording procedures, electrolytic microlesions (12 μA negative current between one wire of each stereotrode and the ground, 30 s duration) were made at the tips of all stereotrodes using the nanoZ (Multi Channel Systems, USA). The next day, the rats were deeply anesthetized with ketamine (75 mg/kg; i.p.) and xylazine (10 mg/kg; i.p.), and then transcardially

perfused with 300 ml saline followed by 300 ml 4% paraformaldehyde. The brains were removed and 40 µm slices were processed for cresyl violet staining. The final locations of the electrodes were verified.

Results

Behavioral task performance

Five rats were trained in one of two versions of the 8-arm radial maze task, the same-reward (n=2) and the different-reward version (n=3) (Fig. 1A). After extensive training (40 − 50 days), the rats rarely visited the non-reward arms. Furthermore, after consuming the reward in one arm, rats only occasionally revisited the arm in the same trial. Therefore, for each trial only the three approach runs towards the end of the reward arms were considered, while the runs to non-reward arms were not analyzed. Because travelled distances from the starting location to the reward location were long and constant, speed varied from locomotion start to locomotion end in a very stereotyped way (Fig. 1B). Each run consisted of a single acceleration to peak speed followed by a deceleration to locomotion end at the reward location (i.e., along the way to the end of the run, rats did not stop and restart, or slow down and re-accelerate). This consistent pattern of speed variation during each run allowed us to evaluate the relationship between kinematic variables and neuronal activity. Unlike most tasks used to study approach behavior, no start cue was provided and each run was therefore self-initiated.

The two versions of the 8-arm radial maze used in this study were chosen to test whether differences in expected value and arm preference were encoded by NAc neurons. We used the number of times each arm was visited first in each trial as a preference score. Fisher test was used to compare the number of trials each rat first entered each arm versus the number of times they were expected to enter if they had no preference (i.e., 1/3 of the trials). One of the two rats trained under the same-reward version entered significantly more times in arm X ($P < 0.01$) as first choice but did not show preference for entering arm Y or Z as first choice (Fig. 1C). The other rat trained under the same-reward version did not show significant preference for entering any of the reward arms ($P > 0.15$). The three rats trained under the different-reward version showed on average a significant preference (vs. chance) for entering arm M (medium reward arm, baited with four drops of chocolate milk in 2/3 of the trials and no reward in ⅓ of trials, $P < 0.001$), significantly less preference for entering arm L (low reward arm, baited with one drop of chocolate milk in all trials, $P < 0.001$), and no preference for entering arm H (high reward arm, baited with four drops of chocolate milk in all trials, $P = 0.14$). This suggests that a reward of low magnitude decreased the rats' preference, but their preference was not affected by a lower reward probability. The rats' overall preference for entering arm M first rather than arm H may be explained by the pre-training

procedure, in which the arm that was least preferred when the three arms were baited with the same reward was assigned as arm H and the most preferred arm was assigned as arm L in the subsequent training stage.

Speed and fraction of the run are the best predictors of NAc firing rate during approach behavior

Sixty-two NAc neurons were recorded while trained rats performed the radial arm maze tasks (Tab. 2). To examine how NAc neurons encode reward and kinematic parameters of locomotion, we considered the set of variables shown in Table 1. Many of these were calculated from video tracking data and changed from moment to moment within a single run (e.g., speed, distance traveled); others were constant throughout each run but changed across runs (e.g., trial number, maximum speed during the run). We tested whether the firing rate of each neuron could be predicted with a general linear model (GLM) that used all these parameters as predictive variables. Before running the GLMs, we examined the correlation between pairs of variables and found that fraction of the run, time and distance travelled were strongly correlated with each other ($r > 0.8$, Fig. 2). We therefore eliminated time and distance travelled from the GLM analysis. In addition, fraction of the run and acceleration were correlated, but less strongly ($r = 0.6$). Therefore, we conducted three separate GLM analyses for each neuron, one including both variables and the other two including either fraction of the run or acceleration. We refer to these three GLMs as full models (FMs).

	Variable type	In GLM	Unit or value	Description
Speed	Continuous	Yes	cm/s	Movement speed of the animal during the task
Fraction of the run*	Continuous	Yes	from 0 to 1	Fraction of the total distance traveled during the reward approach
Acceleration	Continuous	Yes	cm^2/s	Acceleration of the animal during the task
Max speed	Constant	Yes	cm/s	Maximum speed reached during the run
Arm Y	Dummy	Yes	1 or 0	1 if the animal is approaching reward arm Y
Arm Z	Dummy	Yes	1 or 0	1 if the animal is approaching reward arm Z
Run duration	Constant	Yes	s	Total duration of the run
Trial	Constant	Yes	from 1 - 12	Number of the trial in a session of 12 trials
Run	Constant	No	from 1 - 36	Number of the run in a session of 12 trials
Angle - center	Continuous	Yes	degrees (0 - 360)	Angle formed by the center of the maze and the animals location
Head direction	Continuous	Yes	degrees (0 - 360)	Animal's head direction
Head movement	Continuous	Yes	degrees (-360 to +360)	Changes in head direction (counter-clockwise or clockwise)
Distance traveled*	Continuous	No	cm	Distance traveled since the locomotion onset of each run
Time*	Continuous	No	s	Time since the locomotion onset of each run
Center distance	Continuous	Yes	cm	Distance between the animal location and the center of the maze

*The values of these variables are reseted (to zero) at the beginning of each new run

Table 1. Description of individual variables considered for use as predictors in the GLM encoding model. Variable types include Continuous (continuous variables that could change throughout each run), Constant (continuous variables that were constant throughout each run, but could change across runs), and Dummy (0 or 1). Variables marked Yes under In GLM were included in the GLMs; those marked No were not. “Arm Y” and “Arm Z” were both 0 in cases where the animal entered Arm X. For rats in the different-reward group, Arms X, Y and Z refer to Arms L, M and H, respectively.

We first assessed the validity of the GLM that included both fraction of the run and acceleration using a five-fold validation method (see Engelhard et al. 2019). For each neuron, we computed the r^2mean: the mean of the five r^2 values from the correlations between the modeled firing rates (obtained from running the GLM on ⅘ of the data) and the remaining ⅕ of the actual firing rate data (Fig. 3). Representative examples comparing actual firing rate with the firing rate predicted by the FM are shown in Fig. 4B. The average r^2 across the 39 neurons (r^2mean ± SEM) was 0.15 ± 0.014. We then ran the model 1000 times for each neuron on shuffled data sets and obtained the r^2mean value from each shuffled data run. The number of neurons per rat with variance explained by the FMs is shown in Table 2. FMs predicted the changes in the firing rate of 39 units (~63% of the neurons) with a r^2mean greater than the correlation predicted by 99% of the models using shuffled data (Fig. 4A). In the model in which the variable acceleration was excluded, 39 cells (63%) passed this criterion (Fig. 4-1) and in the model in which the variable fraction of the run was excluded 36 cells (58%) passed this criterion (Fig. 4-2). Therefore, in the majority of neurons, our GLMs predicted firing rates much better than chance, and in these neurons the models were able to account for approximately 15% of the variance in firing rate.

	Rat #04	Rat #08	Rat #09	Rat #11	Rat #19	**Total**	**%**
Number of recorded neurons	18	4	25	11	4	**62**	**100**
Number of neurons with signifcant GLM result	17	1	12	9	1	**40**	**65**
Number of locomotion-off cells	3	2	7	1	1	**14**	**23**
Number of peak-valley cells	10	0	4	1	0	**15**	**24**
Number of valley-peak cells	2	1	4	5	0	**12**	**19**
Number of unclassified cells	3	1	10	4	3	**21**	**34**
Total	18	4	25	11	4	**62**	**100**

Table 2: Summary of recorded cells in individual rats.

To determine which independent variables accounted for the most variance in firing rate, for each neuron we ran the GLM with one variable excluded, and repeated this with each variable. Removing variables that account for the most variance in firing rate should result in the largest reduction in total variance explained. Removing only two individual variables, speed and fraction of the run, significantly decreased the r^2mean across neurons ($P < 0.01$, t-test, Fig. 4C, D). Removing acceleration had an effect that did not reach significance after correction for multiple comparisons (Fig. 4D); however, when the variable fraction of the run (which was correlated with acceleration, $r = 0.6$) was excluded from the model, removing acceleration caused a significant decrease in r^2mean (Fig. 4-2). Furthermore, when acceleration was excluded from the model, removing the variable fraction of the run caused an even higher decrease in r^2mean (Fig. 4-1). This suggests that part of the predictive information carried by the variable fraction of the run that is encoded by the NAc neurons is the change in acceleration during the run.

Finally, to confirm that speed and fraction of the run strongly influence firing, we ran GLMs that included only these two independent variables. These models predicted the firing rate of 38 (61%) of the neurons with a r^2mean greater than the coefficient generated in 99% of models using shuffled data. Thus, our GLM analysis reveals that at least two kinematic variables (speed as well as the progression of the animal along the run and/or acceleration) are most strongly predictive of NAc firing activity, whereas other variables (e.g., those related to the animal's choice of arm to enter) are not consistently related to firing activity of the NAc neurons.

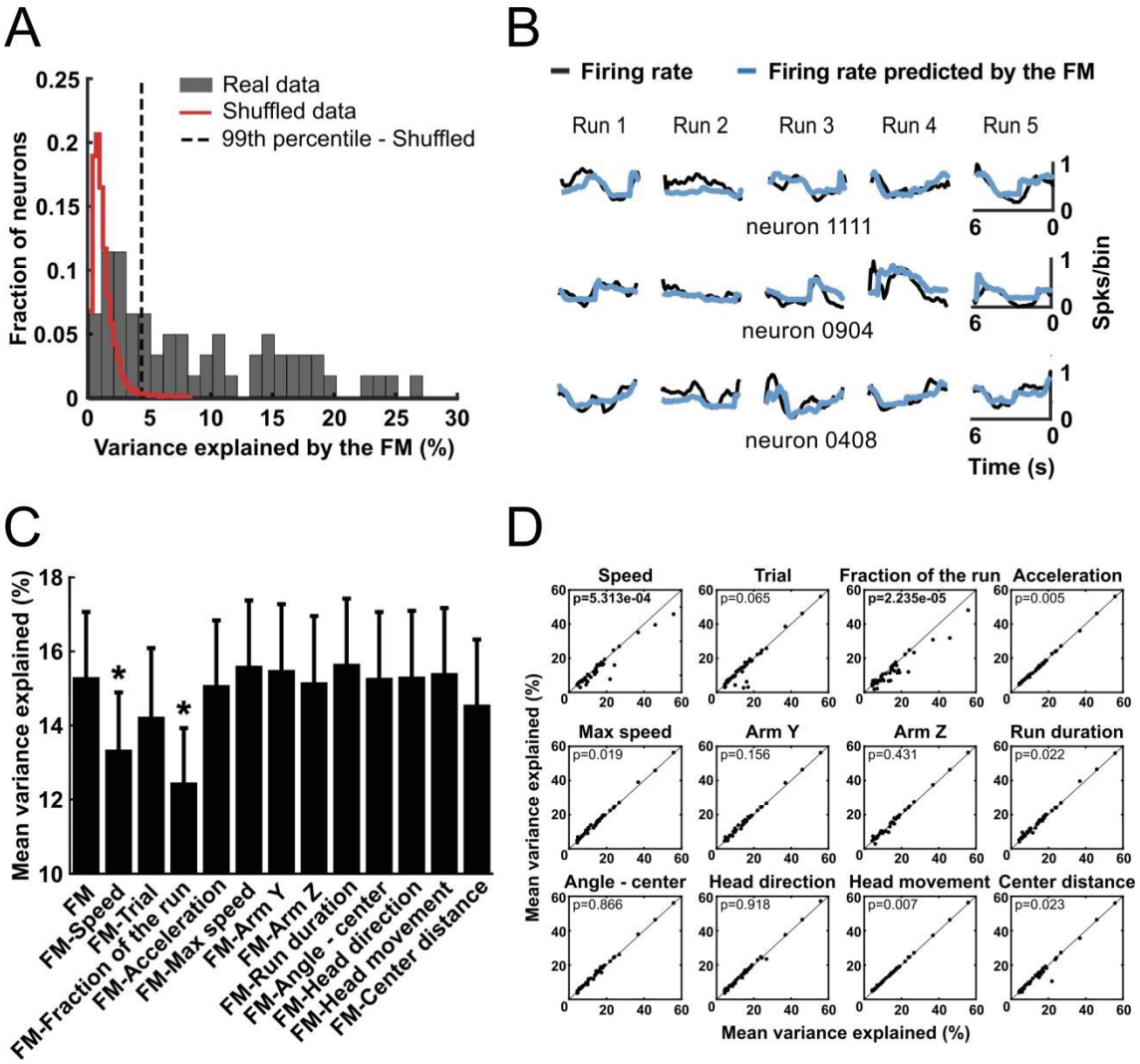

Figure 4: Generalized linear models (GLM) were used to predict activity of NAc neurons based on behavioral variables. **(A)** Distribution of the variance explained by a GLM full model (FM) that used all variables shown in (C) as predictors. Red line delimits the distribution of the variance explained by a GLM calculated with shuffled neuronal data (100 shuffled models per neuron). Neurons on the right of the dashed line (99th percentile of the shuffled models distribution) were classified as significantly explained by the GLM (63% of recorded neurons). In this and subsequent graphs, variance explained is depicted as a percent (100 x r^2mean). **(B)** Neuronal activity during 5 runs towards the ends of reward arms predicted by the GLM (blue line) compared to the real data (black line) for three individual neurons. **(C)** Percentage of mean variance explained (mean ± SEM of r^2mean across neurons). Only data from the neurons with activity significantly predicted by the FM (full GLM model) were included. The mean variance

explained by the FM is shown in the first column. The other columns show the activity explained by the FM models excluding the indicated variable. * $p < 0.01$, paired t-test (after Bonferroni correction) comparing the indicated model with the FM. **(D)** Comparison of mean variance explained by the FM (X-axis) and by the FM after excluding the indicated variable (Y-axis) for all neurons (black dots) explained significantly by the FM.

Although our GLM analysis showed that the arm variable (the arm the animal entered) was not necessary to predict the firing rate of most recorded neurons, we further tested whether arm choice affected neuronal activity in different phases of the approach behavior. First, for each neuron, we pooled data from all runs towards the same arm. The mean firing rate was calculated during four phases: the pre-locomotion phase (the 3 seconds before locomotion start), the acceleration phase (from locomotion start to the speed peak time), the deceleration phase (from the peak speed time to locomotion end), and the post-locomotion phase (the 3 seconds after locomotion ended). Runs with inter-trial intervals shorter than 6 s were excluded. We then compared firing rate in these phases with two-way ANOVA taking the phases as repeated measures and the target arm as the other independent variable (Fig. 6-2). The phase factor was significantly different for 44 out of 62 neurons. The arm factor was significantly different for only three neurons, and the interaction between these factors was significant for eight neurons ($P < 0.01$). The fraction of neurons that showed significant arm or interaction effects in rats trained under different rewards in the three reward arms was not significantly different from rats trained under the same-reward condition (Fisher test, $P < 0.01$). This finding reinforces the hypothesis that most of the recorded neurons did not encode the arm choice or reward expectation. Based on this finding and also because the GLM analysis indicated that encoding of the arm entered was weak or non-existent (Fig. 4), in the subsequent analyses data from all runs were pooled. This approach is further justified by our observation (described above) that arm H was not strongly preferred by the group of rats receiving different rewards in different arms.

Three distinct activity patterns

A neuron whose firing is related to the variable fraction of the run could encode a number of biologically-relevant parameters that themselves vary according to the fraction of the run completed, such as reward proximity and acceleration. Another possibility is that the fraction of the run neurons reach a peak at a specific relative location along the approach trajectory, which could occur at locomotion onset, locomotion offset, or any point in between. To explore these possibilities we first constructed z-normalized histograms of each neuron's activity aligned to locomotion onset, peak of acceleration, peak of speed, peak of deceleration and locomotion end. These histograms are plotted as heat maps sorted by the time at which the peak activity occurred (Fig. 5A). Some neurons seemed to be inhibited during the runs, an observation we confirmed with paired t-tests comparing the firing rate during the runs with the

firing rate during the inter-run intervals. Fourteen neurons were significantly inhibited during the locomotion phase ($P < 0.01$) and were named Locomotion-Off (LO) cells. An example neuron's raster and histogram are shown in Fig. 6A1,2, and histograms of all LO cells are shown in Fig. 7A. These histograms show that LO cells tended to be inhibited beginning just prior to locomotion onset, continue to be inhibited throughout the run, and abruptly recover from the inhibition just after locomotion offset.

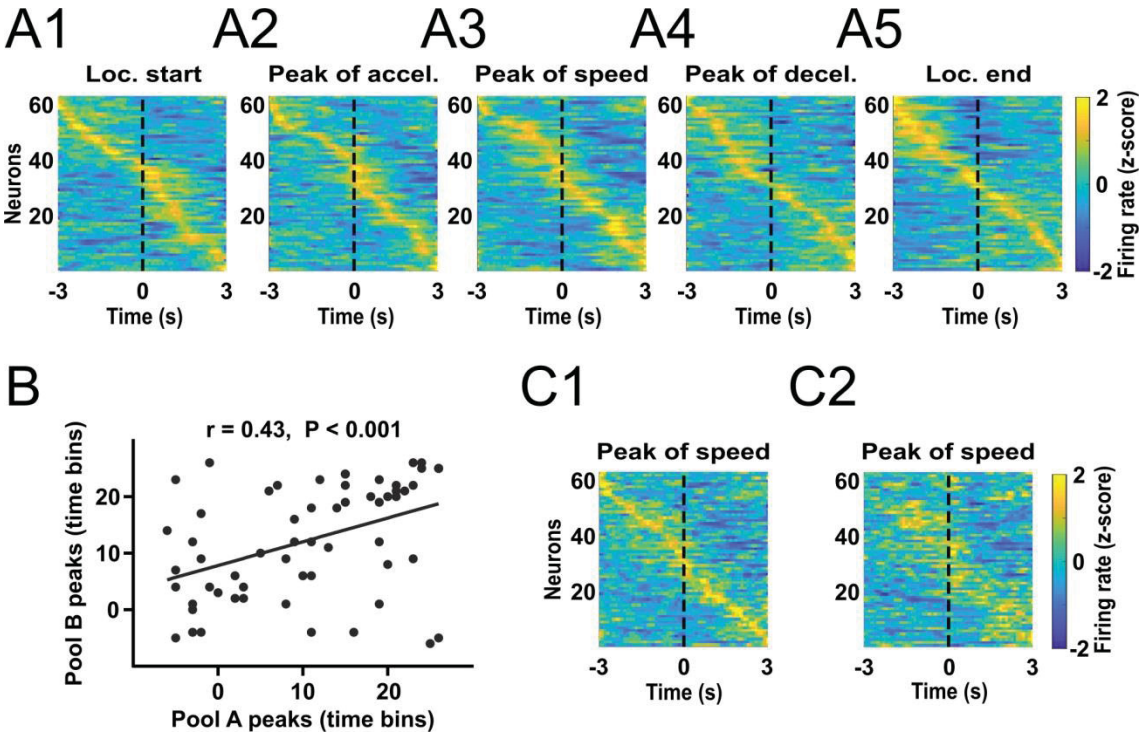

Figure 5: Different neuron peak activity at different bins of time. **(A)** Averaged firing rate zscore Histograms from all runs of all recorded neurons aligned to locomotion start (A1), peak of acceleration (A2), peak of speed (A3), peak of deceleration (A4), locomotion end (A5). **(B, C)** Firing rate z-score data from all runs were aligned to the peak of speed and split into two pools counterbalanced for the trial order and visited arm. The time bin in which the activity of each neuron peaked was calculated separately for the two pools and plotted against each other. Statistical results are from the Pearson test for correlation. **(C)** Neurons were sorted by the peak of activity calculated with the first data pool (C1). The activities of the same neurons calculated with data from the second data pool is shown in the same order as for the first data pool (C2).

Fig. 5A shows that many of the remaining neurons exhibited activity peaks at various times from before locomotion start to after locomotion end. Consequently, the distribution of the histogram peaks sorted by time from the alignment event formed a diagonal line, particularly when activity was centered on the peak of speed (roughly the midpoint of the run). To assess whether this diagonal was the result of each neuron's firing consistently reaching a peak at about the same time across runs relative to the peak of speed, we split the data from each neuron into two pools counterbalanced by trial order and target arm. Peak speed-aligned histograms of the activity of all neurons calculated with the first data pool, sorted by the time of peak of activity, are shown in Fig. 5C1; and

the histograms calculated with the second data pool, sorted in the same order as the first pool, are shown in the Fig. 5C2. We found that the times of the peak bins determined from the two data pools were correlated (Fig. 5B, $r = 0.43$, $p < 0.0001$). We also found that for 37 (60%) neurons, the firing rates in each time bin within individual runs were also correlated between data pools ($P < 0.01$). These results demonstrate that each individual neuron exhibits peaks at consistent times, and that the times during the run at which these peaks occur vary widely across neurons.

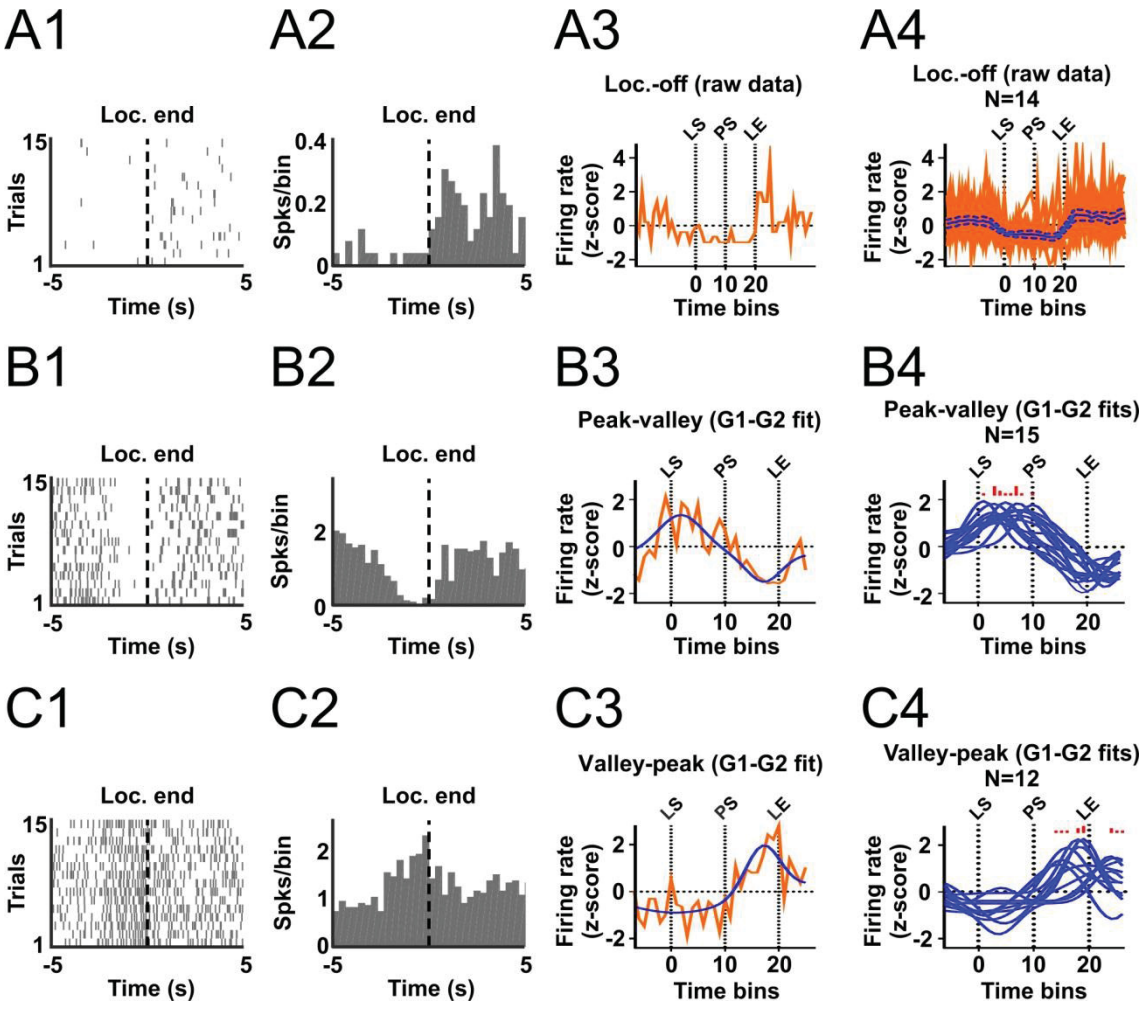

Figure 6: Classification of LO, PV and VP cells. **A1** and **A2** show rasters and histograms aligned to locomotion end for an example LO cell. **A3** shows the time-normalized histogram for this neuron, and **A4** shows time-normalized histograms for all LO cells superimposed (red traces) and the mean ± SEM (blue trace and blue dashed traces). **B** and **C** show similar plots for PV (**B**) and VP (**C**) neurons. The blue traces in **B3, B4, C3** and **C4** show individual neurons' 2G model results. The red histograms superimposed above **B4** and **C4** indicate the time at which each neuron's peak firing occurs according to its 2G model. LS, PS, and LE correspond to locomotion start, peak of speed, and locomotion end, respectively.

Intriguingly, neurons that showed an activity peak in the first part of the approach run (before reaching peak speed; i.e., during acceleration) tended to show a valley in the second part of the run (after peak speed; i.e., during deceleration), and vice-versa (Fig. 5A). We hypothesized that a large subset of

neurons exhibited the Peak-Valley (PV) pattern of activity because they reach activity peaks and valleys exclusively during acceleration and deceleration, respectively. Similarly, we hypothesized that neurons exhibiting the complementary Valley-Peak (VP) pattern reached activity peaks and valleys exclusively during deceleration and acceleration, respectively. To test these hypotheses, we first had to account for the fact that the durations of the acceleration and deceleration phases were not identical across runs, which means that if firing peaks occurred at a specific fraction of the acceleration or deceleration phase, the peaks would occur at different absolute time points in different runs. Therefore, we time-normalized the firing rate data. In each run, the acceleration period was divided into 10 bins of the same size, and the firing rate in each bin was calculated. The deceleration period was also divided into 10 bins. The approximate average width of the adjusted bins was 150 ms. In addition, 7 bins of 150 ms each were included prior to locomotor start and after locomotor end. Next, the firing rates from all runs were averaged per bin and z-transformed. Finally, we modeled the peak-valley and valley-peak patterns as the sum of two Gaussian curves (2G model, see Methods and Fig. 6-1 for details).

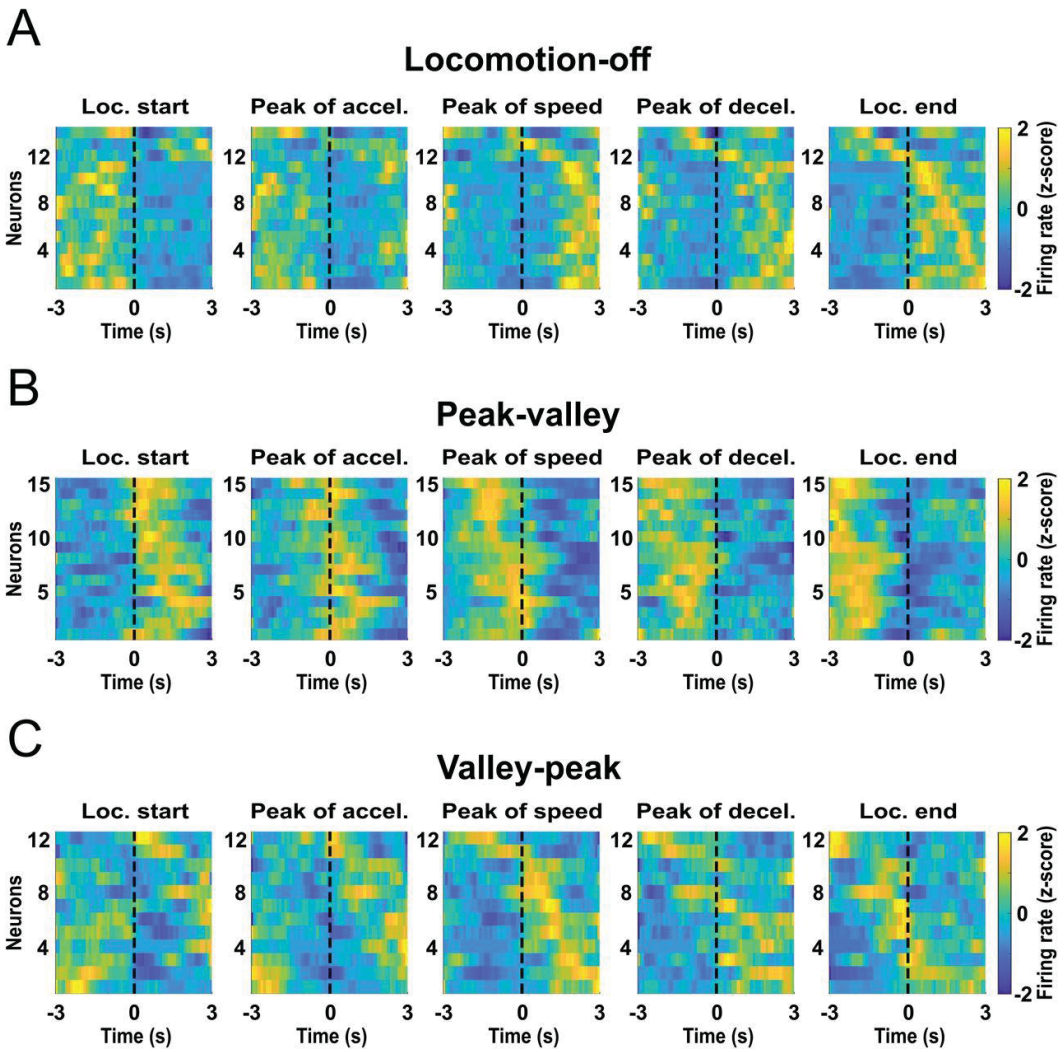

Figure 7: LO (A), PV (B) and VP (C) cells exhibit peak activity at different kinematic stages of the reward approach run. Histograms show firing rates aligned to locomotion start, peak o acceleration, peak of speed, peak of deceleration, and locomotion end. Data were z-scored and the colors in each row show the average across runs for an individual neuron.

To validate the 2G model, we split the firing rate data from all runs of each neuron into two pools. The first data pool was used to calculate the average activity per bin and the second data pool was used to train the 2G model. Next, we examined whether the activity per bin calculated with the first data pool was significantly correlated with the activity predicted by the 2G model (Pearson correlation, $P < 0.01$). Fifteen PV cells (24%) and 12 VP cells (19%) passed this criterion (Fig. 6B,C). Note that the peak firing rate of PV cells occurred exclusively during the acceleration phase (Fig. 6B4, 7B), whereas the firing rate peak of VP cells occurred mostly during the deceleration phase, although some neurons peaked after locomotion end (Fig. 6C4, 7C). LO cells were not modelled with the 2G model, but we plotted the time-normalized firing rates of these neurons in the same way as for the PV and VP cells in Fig. 6A4.

These firing modes further refine the GLM results (Fig. 4C,D) showing that speed and fraction of the run (or acceleration) explain a portion of the variance in firing rate. To examine how LO, PV and VP cells encode speed and acceleration, we plotted the simple correlation coefficients relating firing rate and speed against the normalized times at which the peak firing of each neuron occurred (Fig. 8A), and similarly for the firing rate vs acceleration correlation coefficients (Fig. 8B). PV cells tended to have the strongest positive correlation coefficients for both speed and acceleration, whereas LO neurons had the strongest negative coefficients for speed. VP cells tended to have the strongest negative correlation coefficients for acceleration whereas their coefficients for speed were more widely distributed across negative and positive values.

To further confirm these findings based on individual neuronal data, we determined, for each class of neurons (LO, PV, VP, and non-categorized), the mean GLM β values for speed and acceleration (Fig. 8C, E), as well as the mean r values for simple correlations between speed or acceleration and firing rate (Fig. 8D, F). The results show that PV cells encode speed most strongly, with mean positive coefficients that were significantly different from 0 ($P < 0.01$, one-sample t test, Fig. 8C, D). In contrast, VP cells did not exhibit consistently negative or positive coefficients for speed, whereas LO cells tended to exhibit negative correlations (Fig. 8C, D). On average, PV cells had significantly positive firing vs acceleration correlations, whereas VP cells' acceleration correlations were significantly negative (Fig. 8F). These results were recapitulated in the GLM β values for acceleration, although they did not reach significance (Fig. 8E). On average, the correlation coefficients for fraction of the run were also significant (and the GLM β values tended to significance) for the 3 classes of cells (Fig. 8G, H). For PV and VP cells, the signs of the fraction of the

run coefficients were the opposite of those for acceleration, as expected given that acceleration occurs early in the run and deceleration occurs later.

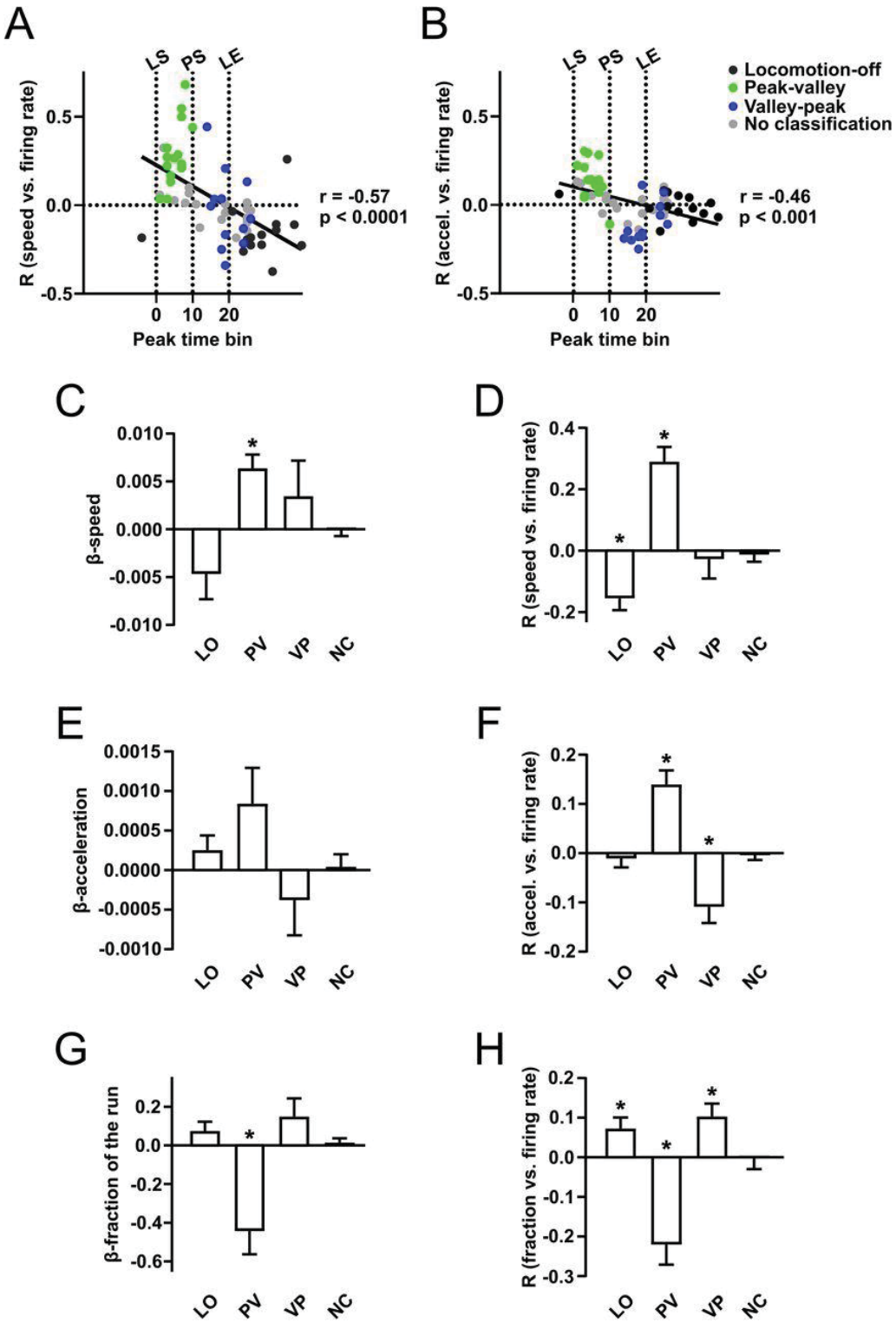

Figure 8: Neurons in each class defined by the 2G analysis share common correlates to predictors in the GLM analysis. The r values for the correlation between speed and firing rate (**A**) and for acceleration and firing rate (**B**) are plotted against the normalized time at which the neuron exhibits peak firing activity. The time of peak is negatively correlated with both r values; the indicated P values are from Pearson's correlations. Points are color-coded according to classification from the 2G analysis. In **C**, **E** and **G**, the mean ± SEM weights (β values) from the

GLM for the variables speed (C), acceleration (E), and fraction of the run (G) are shown separately for LO, PV, VP and non-categorized neurons. Similarly, in **D**, **F** and **H**, mean ± SEM r values for simple correlations between these variables and firing rate are shown. * P < 0.01, one-sample t-test comparison to 0.

Together, these results indicate that the encoding of acceleration and/or fraction of the run revealed by the GLM is largely the result of PV and VP cells' firing peaks and valleys, whereas encoding of speed is largely due to PV cells' positive correlations of firing with speed and LO cells' with negative correlations.

Activity of speed-correlated neurons precedes increases in speed

Our finding that the activity of NAc neurons is correlated with approach speed is in agreement with the hypothesis that NAc neurons promote vigorous reward seeking (Nicola, 2007; Salamone and Correa, 2012; Nicola, 2016). If the firing of these neurons is causal to increased speed of reward approach, then increases in speed should reliably follow the activation of these neurons. We tested this prediction with a cross-correlation analysis in which we plotted speed versus time aligned to each spike. Neurons were sorted according to the correlation between speed and firing rate (Fig. 9A1). On average, the speed of the positively-correlated neurons peaked 146 ms after the action potential (P = 0.0017, t test for difference from 0, Fig. 9B). In contrast, the peak of the cross-correlograms of the negatively-correlated neurons were not significantly different from the spike times (P = 0.35, Fig. 9B). As suggested by Fig. 8, PV cells were the class with the strongest correlation between firing and speed. To verify that the firing of these neurons preceded an increase in speed, we constructed heat maps of LO, PV and LO cells' firing-speed cross-correlations. These plots show that only PV cells consistently exhibited cross-correlogram speed peaks after the spike (Fig. 9A2). Notably, the cross-correlogram speed minimum tended to follow the spike in VP cells. These results are consistent with the possibility that the firing of PV cells causes an increase in the speed during the acceleration phases, whereas the firing of some VP cells causes a decrease in speed during the deceleration phase.

Place-related activity

Alterations in the firing rate of NAc neurons prior to arrival at a reward place have been previously reported (Martin and Ono, 2000; Miyazaki et al., 1998). To test whether the speed or run fraction encoding we identified could be accounted for by location or reward prediction encoding, we performed several analyses. First, we included variables related to location in the GLM described in Fig. 2 including head direction, head movement, angle of the arm and distance from the center of the arm. In the population of neurons as a whole, none of these variables were found to contribute significantly to the model's predictive power (Fig. 4C). Second, we asked whether any of the recorded neurons could be classified as place cells according to the criterion used by

Yeshenko et al. (2004). Five PV and two LO neurons passed the criterion. However, their tentative firing fields were mainly located on the central platform, the neurons were quite active on other parts of the maze, and their firing fields were quite small compared to those of CA1 place cells recorded on a similar radial eight-arm maze (Xu et al., 2019).

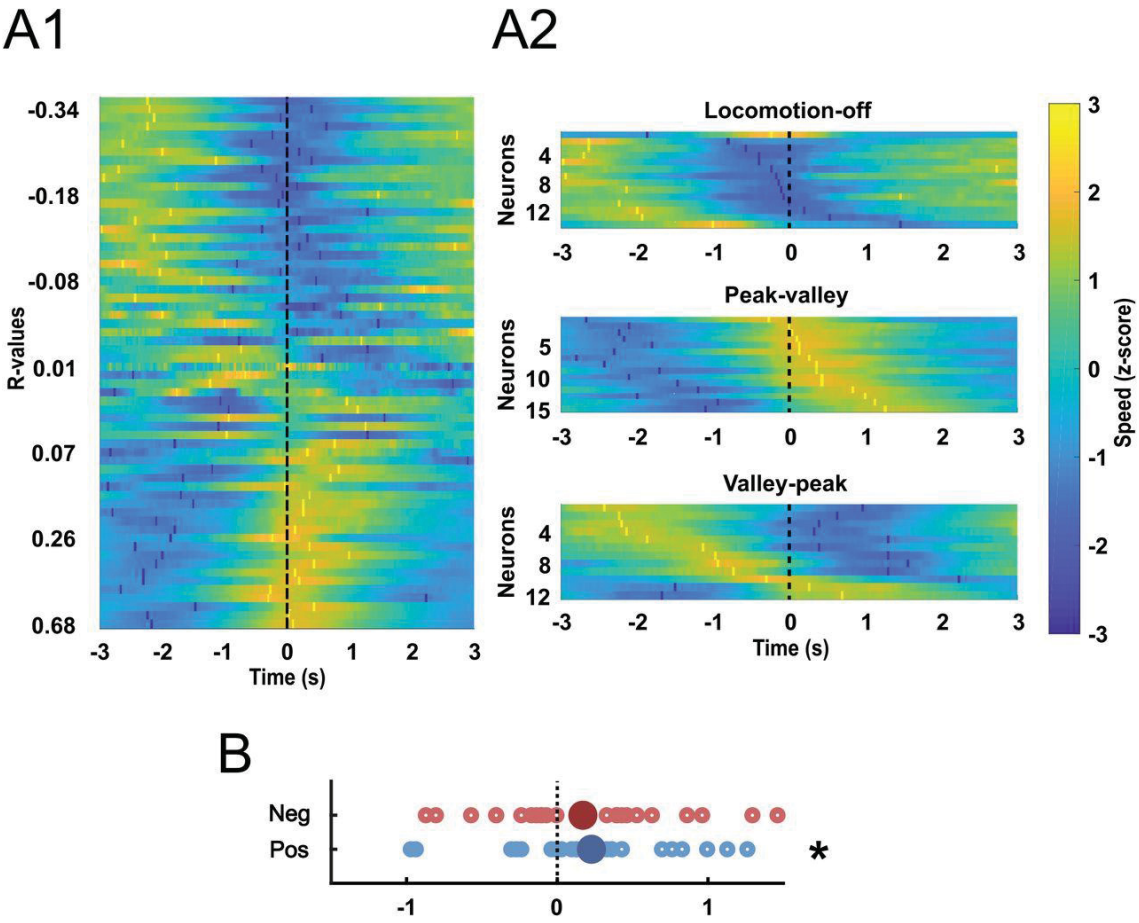

Figure 9: Spike-speed cross-correlations. **A1**, Each row contains a histogram of the average z-score (colors) of speed aligned to the spikes of an individual neuron. The bright yellow and dark blue markers indicate peaks and valleys of the cross-correlogram, respectively. Neurons in the heat map were sorted according to the Pearson's correlation coefficient (r) for speed vs firing rate. All 62 neurons are shown. **A2**, Cross-correlograms are shown separately for LO, PV and LO cells, sorted according to the time at which the crosscorrelogram peak speed occurred. **B,** The time at which the lowest cross-correlogram speed occurred is shown for neurons that had negative correlations with speed (top, red points), and the time at which the highest cross-correlogram speed occurred is shown for neurons that had positive correlations with speed (bottom, blue points). Only data from the neurons with significant positive (blue) or negative (red) correlations with speed are shown. * P = 0.04, one-sample t test compared to 0.

Neuronal classification based on electrophysiological properties

We sorted the recorded neurons into tentative populations of medium spiny neurons (MSNs) and interneurons based on average firing rate and peak width, similar to previous studies (e.g. Berke et al., 2004; Yamin et al., 2013). We classified 34 neurons (55%) as putative MSNs, 8 neurons (13%) as putative

interneurons, and 20 neurons (32%) as cells with no clear classification (Fig. 6-3A). 9/14 LO, 3/15 PV, and 8/12 VP cells were classified as MSNs. 1/14 LO, 3/15 PV, and 2/12 VP cells were classified as interneurons. 4/14 LO, 9/15 PV, and 2/12 VP cells showed no clear classification (Fig. 6-3B).

Histology

Most of the recorded neurons were in the NAc shell, but a few of them were in the NAc core or in the border between the dorsal and ventral striatum (Fig. 6-4). We found no evidence that the different classes of neurons were anatomically clustered.

Discussion

The present study clarifies how NAc neurons represent the vigor of spontaneous approaches to rewarded locations. Rats had to run long distances (~1.5 m) to approach each reward, which allowed us to determine how firing changes during large increases and decreases in approach speed. Firing reflected the animal's speed as well as its progression towards the movement target but not location of the movement target or predicted reward value. Our results suggest that NAc neurons govern the kinematics of approach behavior - when to speed up and when to slow down, and by how much - but, in our task, NAc neurons do not contribute to deciding which target to approach.

We included a broad range of variables related to approach vigor, navigation, and timing in each neuron's GLM. Only three - speed, fraction of the run completed and acceleration - were found to contribute significantly to the variance in firing rate of the population of NAc neurons (although because acceleration and fraction of the run were correlated, acceleration was found to contribute to variance only when fraction of the run was excluded from the GLMs). Because these variables are related to vigor and kinematics, we conclude that the primary function of NAc neurons in this task is to control the time course of increases and decreases in speed rather than the direction of locomotion.

NAc neurons did not encode kinematic parameters in a uniform way, but rather fell into three classes defined by the trajectory of their firing rates during runs. First, we noted that correlation coefficients relating firing and speed were widely distributed across both positive and negative values. Many neurons with negative coefficients were found to be continuously inhibited during locomotion (LO cells, Figs. 6A, 7A, 8C, D), similar to previously-identified NAc neurons that are inhibited throughout appetitive and consummatory behaviors (Taha and Fields, 2006). However, in LO cells, firing resumed just after locomotion offset even though animals presumably engaged in reward consumption at that point. As suggested previously (Taha and Fields, 2006), the inhibitions of LO cells may gate appetitive behaviors or trigger locomotor approach.

In contrast, many neurons with positive speed coefficients were not continuously excited during locomotion, but rather exhibited firing peaks during acceleration and valleys during deceleration (PV cells, Figs. 6B, 7B, 8A-F). These neurons also tended to exhibit positive correlations with speed/acceleration and negative correlations with fraction of the run completed (Fig. 8E-H). Intriguingly, their firing peaks were distributed throughout the acceleration phase (Figs. 6B4, 8A, B) and did not align precisely to the peak of acceleration (Fig. 7B). These results suggest that PV cells each report that the animal is at a different point along the acceleration trajectory, information that could be used to control the precise timing of the speed increase during the run. This possibility is supported by our cross-correlation results showing that an increase in speed followed a spike in all but one PV cell (Fig. 9A2). This temporal relationship held for most neurons with positive correlations between firing and speed (Fig. 9A1), strengthening the hypothesis that a major role of NAc neurons is to increase the vigor of approach.

The third category of neurons, VP cells, were complementary to PV cells in that VP cells exhibited a firing valley during acceleration. However, VP cells' peaks were not limited to the deceleration phase, but tended to occur just before or sometimes after locomotion offset (Figs. 6C4, 7B, 8AB). VP cells did not consistently encode speed (Fig. 8A, D), but did tend to show negative correlations with acceleration and positive correlations with fraction of the run completed (Fig. 8E-H) - a pattern opposite to that of PV cells. Thus, PV and VP cells together account for much of the fraction of the run and acceleration encoding identified by the GLM analysis, suggesting that together these neurons report the animal's relative position along the run. Alternatively, the fact that VP cells tend to fire most near locomotion offset may mean that these neurons are specialized for some aspect of reaching the end of the run, such as coming to a complete stop or preparing for reward consumption.

The GLM analysis yielded little evidence that NAc neurons participate in choosing which reward location to approach or determining the route to get there. In particular, the arm entered variables reflect both movement target and, in some animals, the reward that can be expected, but the firing of few, if any, neurons was influenced by these variables (Fig. 4C,D). Specifically, when the arm variables were removed from the GLMs, the remaining variables explained the variance in firing rate to the same extent as when the arm variables were included. Because this "leave one out" method assesses the contribution of variables to variance independent of whether the variable is positively or negatively correlated, negative results in the cross-neuron analysis are not simply due to existence of roughly equivalent numbers of positively- and negatively-correlated neurons. Rather, variables other than speed, fraction of the run and acceleration did not strongly contribute to the variance of any neurons (Fig. 4D and Extended Figs. 4-1C, 4-2C).

The near absence of representation of navigation and reward parameters contrasts with previous studies showing that NAc neurons integrate reward and

spatial information in maze tasks (Floresco et al., 1996; Shibata et al., 2001; Mulder et al., 2004; Mulder et al., 2005; German and Fields, 2007; Ito et al., 2008; Khamassi et al., 2008; van der Meer and Redish, 2009; van der Meer et al., 2010; Lansink et al., 2012) and that the NAc may be required for spatial navigation towards large rewards (Albertin et al., 2000). However, our rats were overtrained and likely approached reward locations (particularly the second and third in each trial) in a sequence of habit-like stimulus-action chains (Graybiel, 1995); i.e., they used a praxic or taxic approach strategy as opposed to a navigational strategy (O'Keefe and Nadel, 1978; Nicola, 2016). Consequently, spatial navigation processing may have been offline or muted, potentially explaining why we found little evidence for location or movement target encoding (McDonald and White, 1993; but see Miyoshi et al., 2012).

Our observation of robust anticipatory speed encoding provides a potential mechanism to explain previous observations indicating a role for NAc neurons in promoting vigorous reward seeking. Approach speed is an important component of vigor (Floresco, 2015; Shadmehr et al., 2016; Salamone et al., 2016), and increasing dopaminergic (Mogenson et al. 1993; Wu et al. 1993) or glutamatergic activity (Maldonado-Irizarry & Kelley 1994) in the NAc increases locomotor activity and invigorates reward seeking (Berridge 2007). Moreover, free-run operant tasks with higher effort requirements are especially susceptible to disruption by interference with NAc dopamine transmission (Salamone et al., 1999). These effects are due to increased latency to return to the operandum after a pause in which the animal moves away from it (Nicola, 2010). One possibility is that dopamine promotes the firing of NAc PV cells, which exhibit the most robust positive correlations between firing rate and speed, and whose firing tends to be followed by an increase in speed. The activity of these neurons could then trigger initiation of locomotor approach by reaching a threshold. PV cells could express the D1 receptor as activation of this receptor tends to have excitatory effects (Andre et al., 2010); because VP cells tend to be inhibited during acceleration, they may express D2 receptors, causing them to be inhibited by dopamine. Recordings from identified D1 and D2 NAc neurons are needed to address these hypotheses.

Consistent with the idea that PV cells drive locomotor initiation, previous studies showed that the magnitude of NAc neuronal excitations in response to reward-predictive cues predicts both the latency to initiate approach locomotion and the speed of approach (Morrison et al., 2017; McGinty et al., 2013). These cue-evoked excitations are brief (typically well under 1 s) and precede initiation of movement. Although this time course contrasts with our observation of speed encoding during locomotion, the previous studies used smaller operant chambers in which locomotor events were brief and higher speeds could not be attained. Thus, it is possible that neurons exhibiting cue-evoked excitations are the same as the PV cells identified here. Alternatively, because cue-evoked excitations are greater when the subject is closer to reward (Morrison 2014, 2017), it is possible that these neurons are VP cells because VP cells tend to

exhibit bursts as the animal reaches the rewarded location. Further comparative work is needed to assess whether encoding of kinematic parameters occurs in the same neuronal populations across tasks, and whether similar encoding occurs during locomotion that is not directed towards reward.

Our results demonstrate that NAc neurons' activity during free-run reward approach is most consistent with control by these neurons over approach kinematics - when to speed up and when to slow down, and by how much. Future studies should use tasks requiring cognitive map-based navigation to assess how encoding of kinematics is related to forms of activity that contribute to deciding where to go and how to get there.

Acknowledgments

The financial support of the grants CNPq (432061/2018-5, 306855/2017-8, 465346/2014-60), AZV 17-30833A, and GACR 20-00939S, is acknowledged.

References

Aberman JE, Salamone JD (1999) Nucleus accumbens dopamine depletions make rats more sensitive to high ratio requirements but do not impair primary food reinforcement. Neuroscience 92:545–552.

Albertin SV, Mulder AB, Tabuchi E, Zugaro MB, Wiener SI (2000) Lesions of the medial shell of the nucleus accumbens impair rats in finding larger rewards, but spare reward-seeking behavior. Behav Brain Res 117:173–183.

Ambroggi F, Ghazizadeh A, Nicola SM, Fields HL (2011) Roles of nucleus accumbens core and shell in incentive-cue responding and behavioral inhibition. J Neurosci 31:6820–6830.

Andre VM, Cepeda C, Cummings DM, Jocoy EL, Fisher YE, Yang XW, Levine MS (2010) Dopamine modulation of excitatory currents in the striatum is dictated by the expression of D1 or D2 receptors and modified by endocannabinoids. Eur J Neurosci 31:14–28.

Berridge KC (2007) The debate over dopamine's role in reward: the case for incentive salience. Psychopharmacology 191:391-431.

Berke JD, Okatan M, Skurski J, Eichenbaum HB (2004) Oscillatory entrainment of striatal neurons in freely moving rats. Neuron 43:883–896.

Caref K, Nicola SM (2018) Endogenous opioids in the nucleus accumbens promote approach to high-fat food in the absence of caloric need. Elife 7.

Cousins MS, Atherton A, Turner L, Salamone JD (1996) Nucleus accumbens dopamine depletions alter relative response allocation in a T-maze cost/benefit task. Behav Brain Res 74:189–197.

RB D'Agostino RB. Tests for Normal Distribution. In: Goodness-Of-Fit Techniques edited by RB D'Agostino and MA Stephens, Macel Dekker, 1986.

du Hoffmann J, Nicola SM (2014) Dopamine invigorates reward seeking by promoting cueevoked excitation in he nucleus accumbens. J Neurosci 34:14349–14364.

Engelhard B, Finkelstein J, Cox J (2019) Specialized coding of sensory, motor and cognitive variables in VTA dopamine neurons. Nature 570:509–513.

Floresco SB (2015) The Nucleus Accumbens: An Interface Between Cognition, Emotion, and Action. Annual Rev of Psychology 66:25-52.

Floresco SB, Seamans JK, Phillips AG (1996) Differential effects of lidocaine infusions into the ventral CA1/subiculum or the nucleus accumbens on the acquisition and retention of spatial information. Behav Brain Res 81:163–171.

German PW, Fields HL (2007) Rat nucleus accumbens neurons persistently encode locations associated with morphine reward. J Neurophysiol 97:2094–2106.

Gmaz JM, Carmichael JE, van der Meer MA (2018) Persistent coding of outcome-predictive cue features in the rat nucleus accumbens. Elife 7.

Graybiel AM (1995) Building action repertoires: Memory and learning functions of the basal ganglia. Curr Opin Neurobiol 5:733–741.

Hauber W, Sommer S (2009) Prefrontostriatal circuitry regulates effort-related decision making. Cereb Cortex 19:2240–2247.

Ito R, Robbins TW, Pennartz CM, Everitt BJ (2008) Functional interaction between the hippocampus and nucleus accumbens shell is necessary for the acquisition of appetitive spatial context conditioning. J Neurosci 28:6950–6959.

Khamassi M, Mulder AB, Tabuchi E, Douchamps V, Wiener SI (2008) Anticipatory reward signals in ventral striatal neurons of behaving rats. Eur J Neurosci 28:1849–1866.

Kropff E, Carmichael JE, Moser M, Moser, EI (2015) Speed cells in the medial entorhinal cortex. Nature 523:419-424.

Lansink CS, Jackson JC, Lankelma JV, Ito R, Robbins TW, Everitt BJ, Pennartz CM (2012) Reward cues in space: commonalities and differences in neural coding by hippocampal and ventral striatal ensembles. J Neurosci 32:12444–12459.

Maldonado-Irizarry CS, Kelley AE (1994) Differential behavioral effects following microinjection of an NMDA antagonist into nucleus accumbens subregions. Psychopharmacology 116:65-72.

Martin PD, Ono T (2000) Effects of reward anticipation, reward presentation, and spatial parameters on the firing of single neurons recorded in the subiculum and nucleus accumbens of freely moving rats. Behav Brain Res 116:23–38.

McDonald RJ, White NM (1993) A triple dissociation of memory-systems - hippocampus, amygdala, and dorsal striatum. Behav Neurosci 107:3–22.

McGinty VB, Lardeux S, Taha SA, Kim JJ, Nicola SM (2013) Invigoration of reward-seeking by cue and proximity encoding in the nucleus accumbens. Neuron 78:910–922.

Miyazaki K, Mogi E, Araki N, Matsumoto G (1998) Reward-quality dependent anticipation in rat nucleus accumbens. Neuroreport 9:3943–3948.

Miyoshi E, Wietzikoski EC, Bortolanza M, Boschen SL, Canteras NS, Izquierdo I, Da Cunha C (2012) Both the dorsal hippocampus and the dorsolateral striatum are needed for rat navigation in the Morris water maze. Behav Brain Res 226:171–178.

Mogenson GJ, Jones DL, Yim CY (1980) From motivation to action: functional interface between the limbic system and the motor system. Prog Neurobiol 14:69–97.

Mogenson GJ, Brudzynski SM, Wu M, Yang CY, Yim CCY (1993) From motivation to action: a review of dopaminergic regulation of limbic to nucleus accumbens to ventral pallidum to pedunculopontine nucleus circuitries involved in limbic-motor integration. In: Limbic motor circuits and neuropsychiatry (1st Ed), pp193–236. Boca Raton: CRC Press.

Morrison SE, Nicola SM (2014) Neurons in the nucleus accumbens promote selection bias for nearer objects. J Neurosci 34:14147-62.

Morrison SE, McGinty VB, Du Hoffmann J, Nicola SM (2017) Limbic-motor integration by neural excitations and inhibitions in the nucleus accumbens. J Neurophysiol 118:2549–2567.

Mulder AB, Tabuchi E, Wiener SI (2004) Neurons in hippocampal afferent zones of rat striatum parse routes into multi-pace segments during maze navigation. Eur J Neurosci 19:1923–1932.

Mulder AB, Shibata R, Trullier O, Wiener SI (2005) Spatially selective reward site responses in tonically active neurons of the nucleus accumbens in behaving rats. Exp Brain Res 163:32–43.

Nicola SM (2007) The nucleus accumbens as part of a basal ganglia action selection circuit. Psychopharmacology 191:521–550.

Nicola SM (2010) The flexible approach hypothesis: unification of effort and cue-responding hypotheses for the role of nucleus accumbens dopamine in the activation of reward-seeking behavior. J Neurosci 30:16585–16600.

Nicola SM (2016) Reassessing wanting and liking in the study of mesolimbic influence on food intake. Am J Physiol Regul Integr Comp Physiol 311:R811–R840.

Nicola SM, Yun IA, Wakabayashi KT, Fields HL (2004) Cue-evoked firing of nucleus accumbens neurons encodes motivational significance during a discriminative stimulus task. J Neurophysiol 91:1840–1865.

O'Keefe J, Nadel L (1978) The hippocampus as a cognitive map. Oxford: Clarendon Press.

Paxinos G, Watson C (2007). The Rat Brain in Stereotaxic Coordinates (6th Ed). San Diego: Elsevier Academic Press.

Rueda-Orozco PE, Robee D (2015) The striatum multiplexes contextual and kinematic information to constrain motor habits execution. Nat Neurosci 18:453-60.

Salamone JD, Correa M (2012) The mysterious motivational functions of mesolimbic dopamine. Neuron 76:470–485.

Salamone JD, Cousins MS, Bucher S (1994) Anhedonia or anergia? Effects of haloperidol and nucleus accumbens dopamine depletion on instrumental response selection in a Tmaze cost/benefit procedure. Behav Brain Res 65:221–229.

Salamone JD, Aberman JE, Sokolowski JD, Cousins MS (1999) Nucleus accumbens dopamine and rate of responding: neurochemical and behavioral studies. Psychobiology 27:236–247.

Salamone JD, Yohn SE, López-Cruz L, Miguel NS, Correa M (2016) Activational and effortrelated aspects of motivation: neural mechanisms and implications for psychopathology. Brain 139:1325-1347.

Shadmehr R, Huang HJ, Ahmed AA (2016) A Representation of Effort in Decision-Making and Motor Control. Curr Biol 26:1929-1934.

Shibata R, Mulder AB, Trullier O, Wiener SI (2001) Position sensitivity in phasically discharging nucleus accumbens neurons of rats alternating between tasks requiring complementary types of spatial cues. Neuroscience 108:391–411.

Sjulson L, Peyrache A, Cumpelik A, Cassataro D, Buzsaki G (2018) Cocaine place conditioning strengthens location-specific hippocampal coupling to the nucleus accumbens. Neuron 98:926–934.

Taha SA, Fields HL (2006) Inhibitions of nucleus accumbens neurons encode a gating signal for reward-directed behavior. J Neurosci 26:217–222.

van der Meer MA, Redish AD (2009) Covert expectation-of-reward in rat ventral striatum at decision points. Front Integr Neurosci 3:1.

van der Meer MA, Johnson A, Schmitzer-Torbert NC, Redish AD (2010) Triple dissociation of information processing in dorsal striatum, ventral striatum, and hippocampus on a learned spatial decision task. Neuron 67:25–32.

Wu M, Brudzynski SM, Mogenson GJ (1993) Functional interaction of dopamine and glutamate in the nucleus accumbens in the regulation of locomotion. Can J Physiol Pharmacol 71:407–413.

Xu H, Baracskay P, O'Neill J, Csicsvari J (2019) Assembly responses of hippocampal CA1 place cells predict learned behavior in goal-directed spatial tasks on the radial eight-arm maze. Neuron 101:119–132.

Yamin HG, Stern EA, Cohen D (2013) Parallel processing of environmental recognition and locomotion in the mouse striatum. J Neurosci 33:473–484.

Yeshenko O, Guazzelli A, Mizumori SJ (2004) Context-dependent reorganization of spatial and movement representations by simultaneously recorded hippocampal and striatal neurons during performance of allocentric and egocentric tasks. Behav Neurosci 118:751–769.

Supplemental data

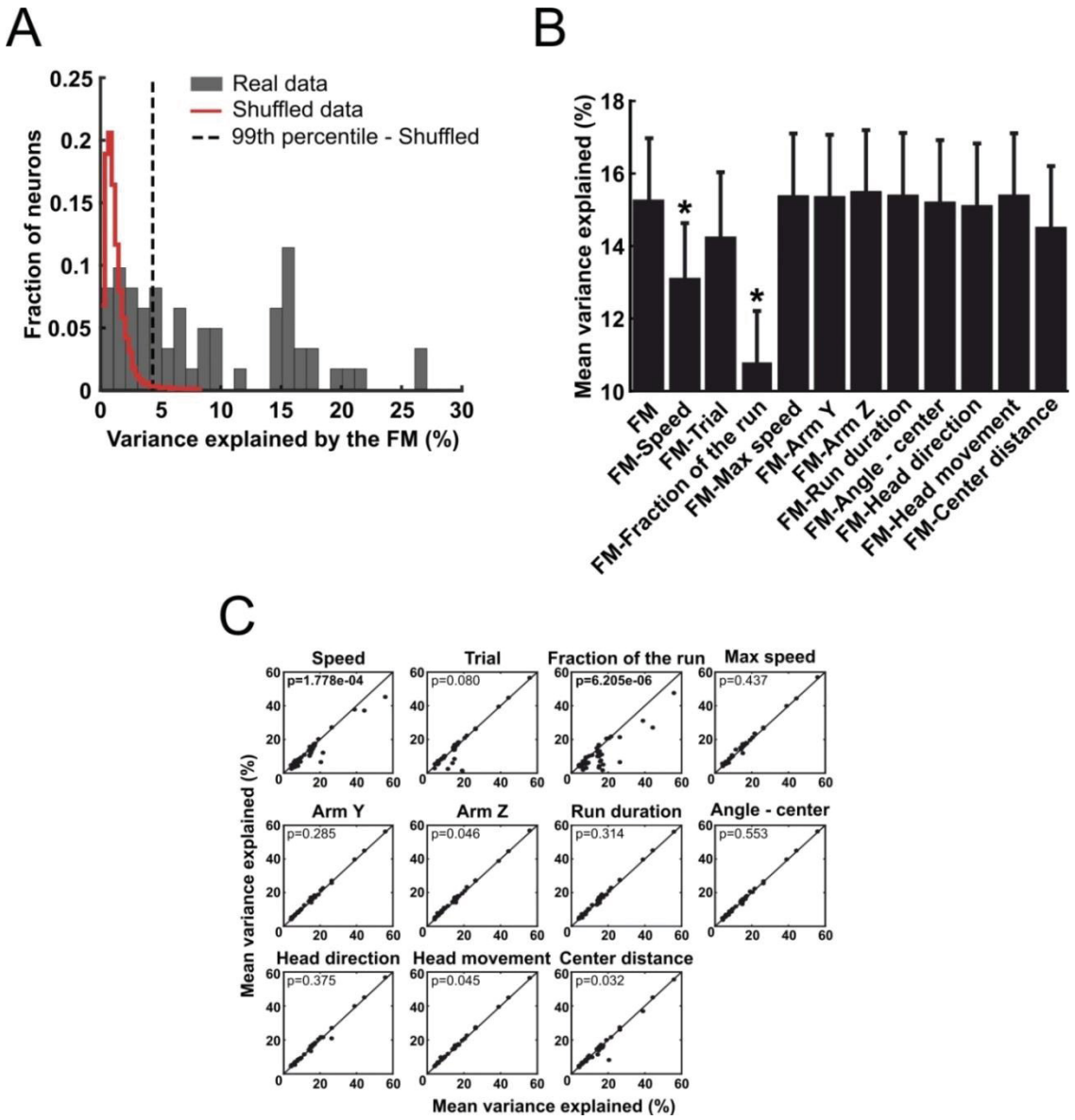

Figure 4-1: Generalized linear models (GLM) without the acceleration variable. **(A)** Distribution of the variance explained by a GLM full model (FM) that used all variables shown in (B) as predictors. Red line delimits the distribution of the variance explained by a GLM calculated with shuffled neuronal data (100 shuffled models per neuron). Neurons to the right of the dashed line (99th percentile of the shuffled models distribution) were classified as significantly explained by the GLM (63% of recorded neurons). In this and subsequent graphs, variance explained is depicted as a percent (100 x r^2 mean). **(B)** Percentage of mean variance explained (mean ± SEM of r^2mean across neurons) of the firing rate of neurons with activity significantly explained by the FM. The mean variance explained by the FM is shown in the first columns. The other columns show the variance explained by the FM excluding the indicated variable. * $p < 0.01$, paired t-test (after Bonferroni correction) comparing the indicated model to the FM. **(C)** Comparison of mean variance explained by the FM (X-axis) and by the FM excluding the indicated variable (Y-axis) for all neurons (black dots) explained significantly by the FM.

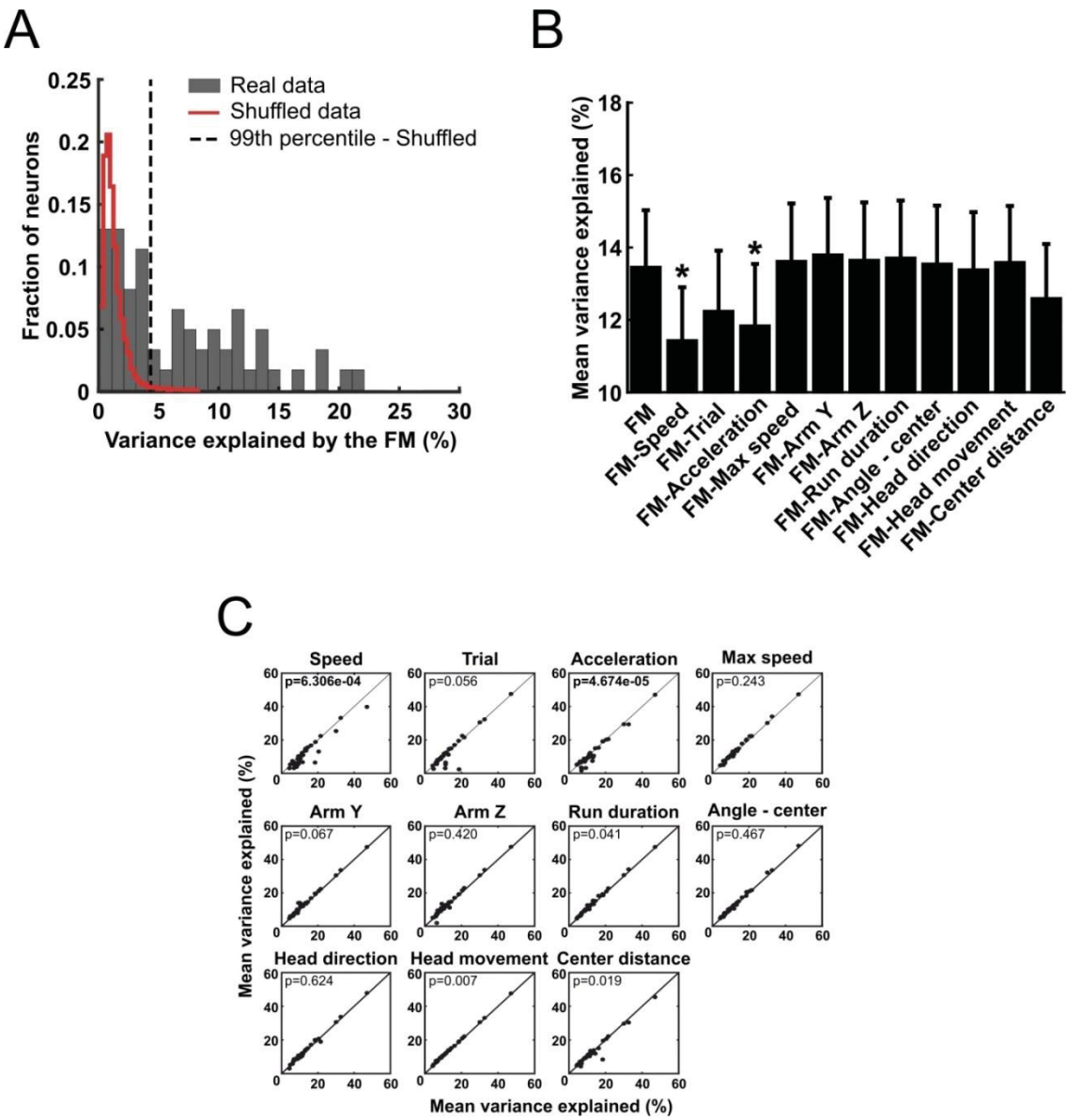

Figure 4-2: Generalized linear models (GLM) without the fraction of the run variable. Panels are as described for Fig. 4-1, except that these GLM predicted the changes in the firing rate of 58% of the neurons.

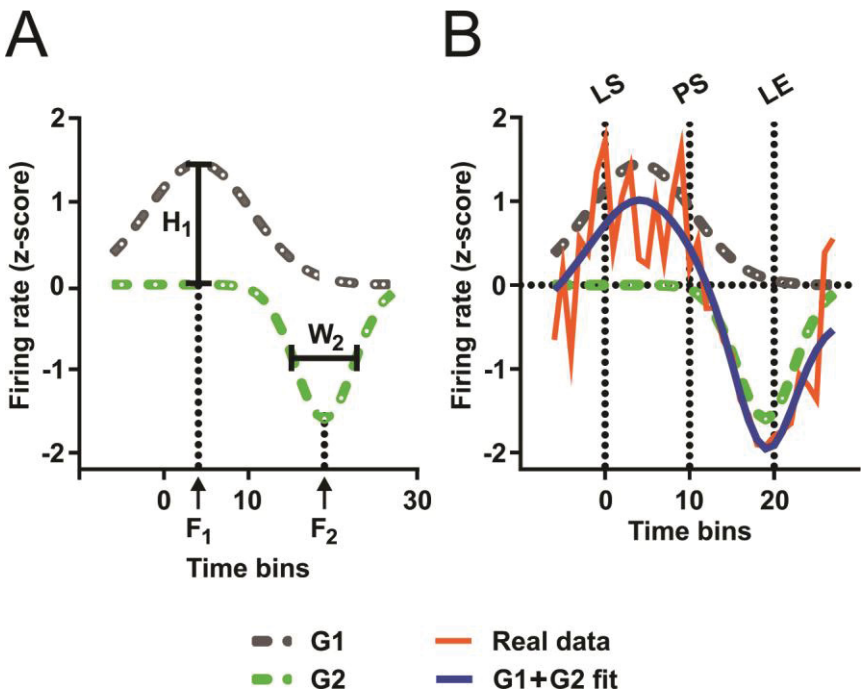

Figure 6-1: The sum of two Gaussians (2G) model. A non-linear model that consists of the sum of two Gaussian curves was used to model the firing rate during the approach run. The panel A shows the two modeled Gaussian curves, and the panel B shows the same two curves as well as the mean firing rate data (z-score) and the sum of the two Gaussian curves. The only predictor used in this model is the fraction of time. The period of time from the locomotion start (LS) to the peak of speed (PS) was divided into 10 bins, and the time from the peak of speed and the locomotion end (LE) was also divided into 10 bins. These bins were ~150 ms each. The 7 bins preceding locomotion start (LS) and following locomotion end (LE) were 150 ms each. Changes in z-scored firing rate as function of normalized time (Y(t)) was modelled as

$$Y_{(t)} = G1_{(t)} + G1_{(t)} + \mathrm{BL}$$

where G1 was the equation for the peak part of the curve, G2 was the equation for the valley part of the curve and BL was the baseline activity. The Gaussian equations (G(t)) used were:

$$G1_{(t)} = H1e^{-\pi(\frac{X_{(t)}-F1}{W1})^2} \quad G2_{(t)} = -H2e^{-\pi(\frac{X_{(t)}-F2}{W2})^2}$$

,

where H, F, and W are constants with the following meaning: H represents the amplitude of the Gaussian curve, which reflects the height (H1) and depth (H2) of the activity peak and the valley, respectively. F is the bin where the Gaussian is centered. Therefore, F1 is the bin in which the neuron is most active, and F2 is the bin in which the neuron is least active. W is the standard deviation of each Gaussian, which reflects the durations of the activation peak (W1) and valley (W2).

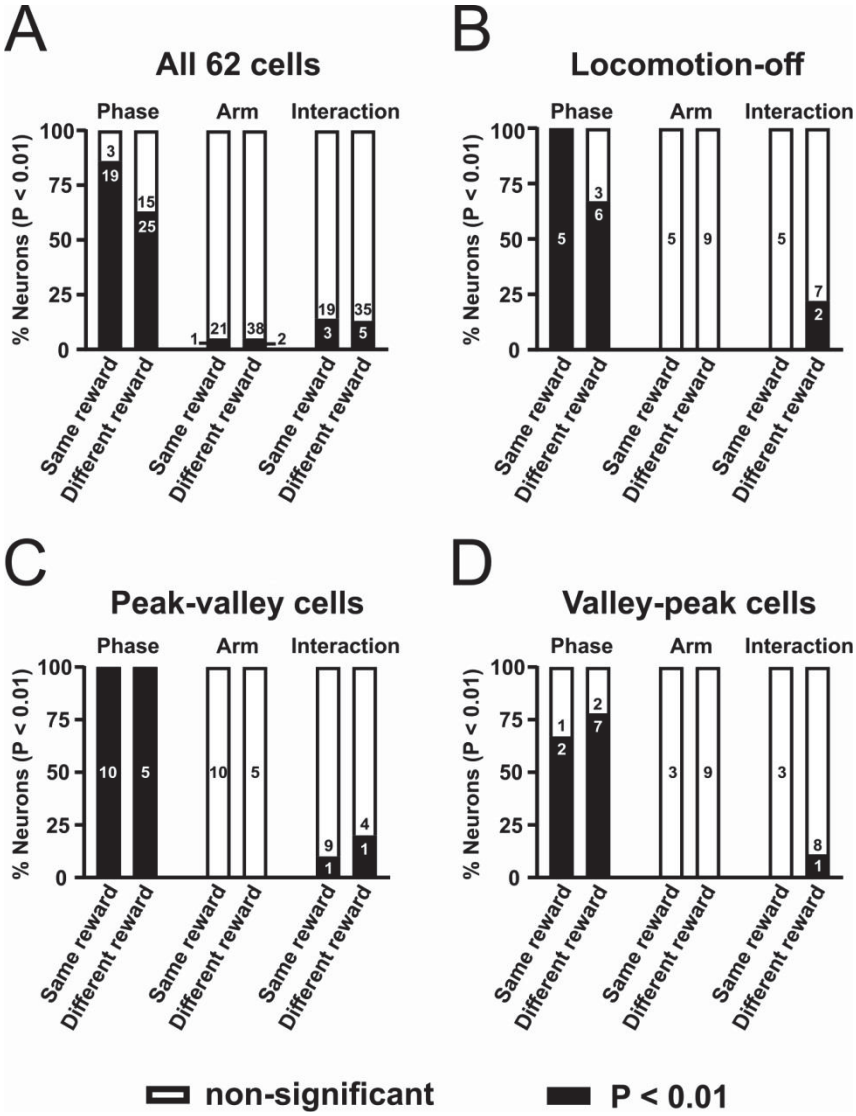

Figure 6-2: Effects of the target arm and the phases of the approaches run on the firing rate. The firing rates were scored during the 3 s before the approach run and during the acceleration and deceleration phases of the runs. Independent repeated measures (phases) ANOVAS were run for each neuron. Bars represent the percent of neurons with significant phase factor, significant arm factor, and significant interaction phases ($P < 0.01$). The absolute number of neurons in each category is printed inside the bars. No significant difference between the number of neurons with significant effects from rats that were trained with the same and rewards in the 3 arms was found ($P > 0.01$, Fisher test).

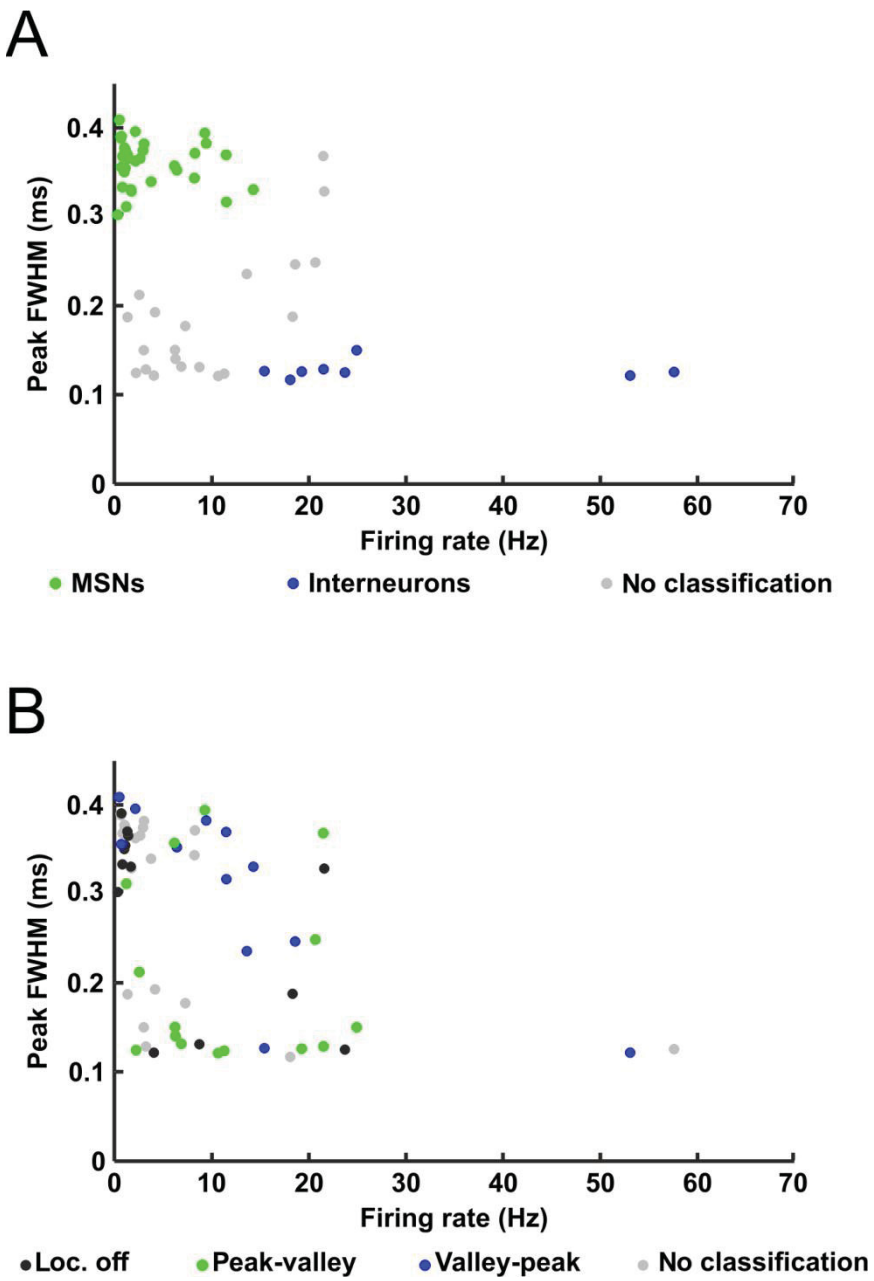

Figure 6-3: Separation of recorded cells into clusters of tentative MSNs (blue), interneurons (red), and neurons with no classification (gray).

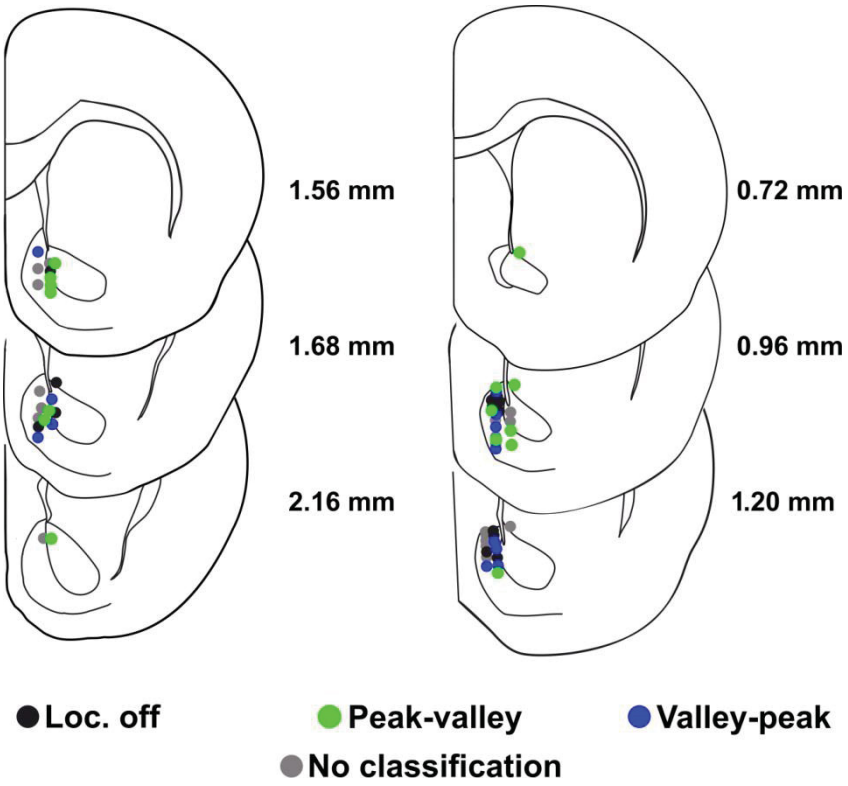

Figure 6-4: Placement of tips of recording electrodes. Neurons located outside of the nucleus accumbens were excluded from the analysis.

Behavioural Brain Research 395 (2020) 112858

Contents lists available at ScienceDirect

Behavioural Brain Research

journal homepage: www.elsevier.com/locate/bbr

Evidence that haloperidol impairs learning and motivation scores in a probabilistic task by reducing the reward expectation

Bernadete Negrelli[1], José Augusto Pochapski[1], Cyrus Antonio Villas-Boas, Letícia Ferreira Jessen, Mayra Aline Lopes Teixeira, Claudio Da Cunha*

Universidade Federal do Paraná (UFPR) – Departamento de Farmacologia, 81531- 980, Curitiba, Brazil

ARTICLE INFO

Keywords:
Dopamine
Haloperidol
Cognition
Motivation
Perseverative behaviors

ABSTRACT

Activation of midbrain dopamine neurons in response to positive prediction errors and reward predictive cues is proposed to "energize" reward seeking behaviors and approach responses to places where the reward is expected. In the present study, we tested the effect of the D2-dopamine receptor antagonist haloperidol on response latencies to enter two arms of a Y-maze with different reward probabilities. Adult male Wistar rats were trained to explore the Y-maze with sucrose pellets placed 30% of times at the end of one arm and 70% of times at the opposite arm. Therefore, the reward expectation was different among arms, and was updated in the trials when the reward was omitted. After training, rats received 0.05, 0.10, 0.15 mg/kg haloperidol, or saline 30 min before the test session. In the last, but not in the first trials, haloperidol caused a dose-dependent increase in arm choice latency and response latency. Saline, but not haloperidol, treated rats presented significantly longer response latencies for the 30% compared to the 70% reward probability arm. Haloperidol also caused a dose-dependent decrease in the number of entries in the 70% reward probability arm, increased the number of non-responses, and caused a dose-dependent increase in the number of re-entries in the 30% reward probability arm after non-rewarded trials. Control experiments suggested that haloperidol did not cause motor impairment or satiation, but rather impaired learning and motivation scores by reducing the reward expectation.

1. Introduction

Striatal dopamine is proposed to affect approach behavior toward a reward-delivery place by causing invigoration of reward seeking [1], increasing the incentive salience of reward-related cues [2], reinforcing the approach response [3,4] and/or by encoding positive prediction errors [5]. The mechanisms of these functions are related to the differential roles of the medium spiny neurons that connect the striatum with the output structures of the basal ganglia. The striatonigral neuron constitutes the direct efferent pathway and the striatopallidal neuron gives rise to the indirect pathway. The striatonigral neuron expresses D1-like receptors (D1R) including the D1 dopamine receptor and the D5 dopamine receptor. On the other hand, the striatopallidal neuron expresses D2-like receptors (D2R) including the D2, D3, and D4 dopamine receptors [6].

Activation of medium spiny neurons by cortical, limbic, and thalamic glutamatergic neurons is modulated by dopamine. Dopamine has higher affinity for D2R than for D1R. Therefore, D2R are more tonically activated than D1R by basal dopamine levels and are more sensitive to the effects of dopamine pauses, which signals a negative reward prediction error, while D1R are more sensitive to dopamine bursts, which signals a positive reward prediction error [7–9]. Strong activation of the dopamine neurons basically promotes potentiation of corticostriatal synapses onto the direct pathway and learning from rewarding outcomes, while weak dopamine receptor activation promotes potentiation of corticostriatal synapses onto the indirect pathway and learning from aversive outcomes [10,11]. Reward-related cues also promote bursts of dopamine release [7], which makes these cues more attractive - a phenomenon known as incentive salience [2]. In addition, the bursts of dopamine invigorate or energize the approach response by increasing the wanting or motivational state [1,2].

Activation of D1R is proposed to promote Go responses and the reduction in the occupation of D2 receptors is proposed to promote NoGo responses. However, D2R are not completely occupied by basal levels of dopamine. Therefore, the dopamine bursts are also able to enhance D2R signaling [8,9], thus participating in the psychomotor activation evoked by rewarding-related stimuli. Nevertheless, although there is evidence that both neurons of the direct and indirect pathways

* Corresponding author.
E-mail address: dacunha.claudio@gmail.com (C. Da Cunha).
[1] Both authors contributed equally to this manuscript.

https://doi.org/10.1016/j.bbr.2020.112858
Received 28 April 2020; Received in revised form 11 July 2020; Accepted 3 August 2020
Available online 15 August 2020

are activated during the expression of Go-directed responses [12], few studies addressed the role of the activation of D2R in the reward-motivated behaviors such as appetitive approach behavior [3].

In the present study, we tested the effect of blocking D2R with haloperidol in rats trained to expect a high and low probability of reward when approaching one or the other target arms of a Y-maze. The goal was to test how such D2R blockage affects the choice and response latencies of approach responses when the reward expectation is low or high.

2. Materials and methods

2.1. Animals

One hundred and nine adult male Wistar rats from the vivarium of the Federal University of Paraná (UFPR) were used. Animals weighed 220-290 g at the beginning of the experiments. Rats were maintained in a temperature-controlled room (22 ± 2 °C) on a 12/12 light/dark cycle (lights on at 7 a.m.) with water ad libitum until the behavioral training started. All possible efforts were made to minimize the number of animals used and their discomfort during experimental procedures. All procedures were approved by the Animal Care and Use Committee of the UFPR (protocol number 1014) and conducted in accordance with the Brazilian law (11.7948 October 2008) and the National Institutes of Health Guidelines for the Care and Use of Laboratory Animals.

2.2. Y-maze probabilistic reinforcement task

The maze was made of wood and painted in black. Each arm was 15 cm wide, 30 cm long, and the walls were 30 cm high. One of the arms was used as the start area and the left and right arms had manually operated guillotine doors (Fig. 1). Rats were trained in a Monday to Friday schedule. The protocol consisted of 5 phases.

Phase 1 started on a Monday and consisted of the first 3 days of food restriction. Rats were housed in groups of 3 per home cage and the amount of food was adjusted to maintain their weight in 90-95% of the weight one day before the food restriction started. Food restriction was maintained until the end of the experiment, but during phase 1, in addition to standard food, 30 sucrose pellets (mean weight of 0.1 g per pellet) were placed in each home cage.

Phase 2 consisted of a 2-day habituation to the Y-maze (Fig. 1) starting on a Thursday. On each daily habituation session, rats were placed in the start area with the doors of the two target arms open and allowed to freely explore the maze for 10 min and eat the 2 pellets that were previously placed in the maze, one at the end of each target arm. When the pellet of one arm was eaten, it was replaced as soon as the rat left that arm. On average each rat ate 4 pellets per session.

In **Phase 3,** which started on the following Monday and lasted 5 days, rats learned to approach the reward area to eat the pellet previously placed in reward area of the arm that was open. This schedule was used to prevent rats from developing a preference for the first arm they were reinforced, as we observed in a pilot study. It consisted of one session per day in which free choices were given only on the 5th trial of each block. Each session consisted of 6 blocks of 5 trials each. In the first 4 trials of each block, each rat was placed in the start arm with both doors closed. Only one door was open to give access to the arm baited with one pellet. Which arm (right or left) was open was counterbalanced in a pseudorandom order, but rats were reinforced with one pellet independently of the open arm. After the rat had eaten the pellet it was placed in the entry arm and a new trial started immediately afterwards. Therefore, in the first 4 trails of each block rats had no choice but to enter the open arm. A free choice was given every 5th trial of the blocks. The two doors were opened at the same time and the two arms were baited with 1 sucrose pellet. Immediately after entering one of the arms and eating the sucrose pellet the rat was placed back into the entry arm. Therefore, in the free choice trial, rats were also reinforced independently of which arm they had chosen to enter, but they were not allowed to go from one arm to the other arm in the same trial. In **Phase 4** free choices were given in all trials and rats were trained on a probabilistic reinforcement schedule. This phase started on a Monday and lasted 4 days with one session per day, each session consisting of 5 blocks of 10 trials. In each trial the rat was placed in the start area and allowed to enter one of the arms, but only one arm was baited. 70% of times one of the arms was baited and 30% of times the other arm was baited, in a pseudorandom sequence. The arms that were baited 30% and 70% of times were the same in all sessions for the same rat. The arm baited 30% and 70% of times were counterbalanced among rats.

Test day was carried out on the following day. Rats were assigned to 4 groups, which received i.p. saline or 0.05, 0.10, or 0.15 mg/kg haloperidol (Johnson & Johnson, New Brunswick, NJ), respectively. These doses are lower than those described to cause catalepsy [13] and were chosen based on previous studies [14–16]. Thirty minutes later, rats were given 50 trials in which both arms were opened simultaneously giving the rats free choice to enter the 30% or the 70% rewarded arm. Two other independent groups of rats were submitted to the same protocol, but on the test day, they received i.p. saline or 0.15

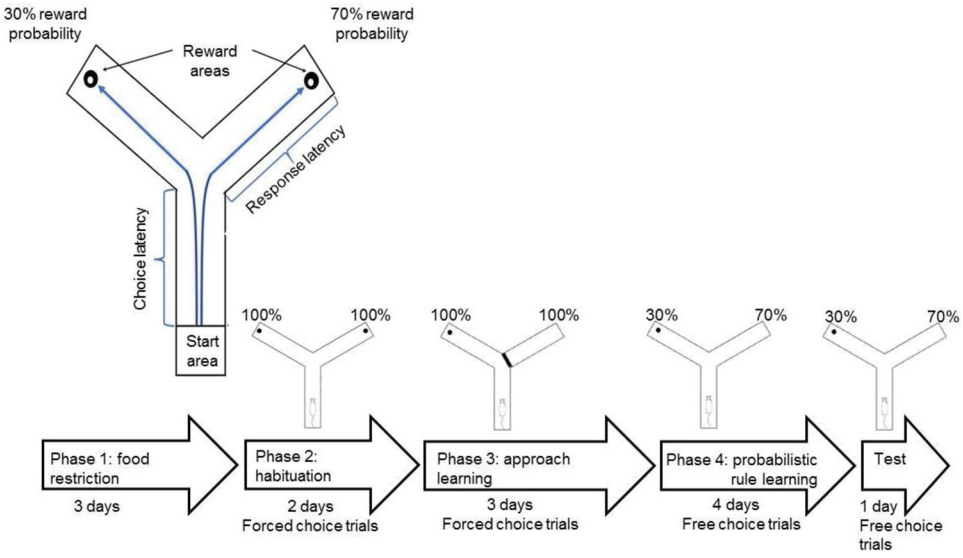

Fig. 1. Illustrative sketch of the Y-maze and the behavioral task protocol.

mg/kg haloperidol 60 min before the test. The goal of this experiment was to test whether the effect of haloperidol achieved a plateau after 30 min. The half-life of haloperidol clearance is around 1.5 hr [17]. Since this session lasted no more than 40 min (20 min in average), the effect of haloperidol did not decrease more than 50% of the peak effect for both groups that received the injection 30 and 60 min before the test. Sessions were recorded by a video camera placed above the maze. Videos were analyzed in slow motion and the number of times each rat entered each arm was scored. Latency to enter the chosen arm with forepaws (choice latency) and latency to reach the end of that arm (response latency) were also scored (Fig. 1).

2.3. Satiety test

Other 4 groups of 12 rats each were kept under food restriction for 3 days. In the 2 days before the test, sucrose pellets were placed in the rats' home box to avoid neophobia. One day before the test day the rats were left for 10 min individually in a home cage box without bedding for a habituation session. On the test day, saline or 0.15 mg/kg of haloperidol were administered 30 or 60 minutes before and each rat was placed in the same box for 20 minutes, where they had free access to 20 g of sucrose pellets. After the rat was removed, the uneaten sucrose pellets were weighed.

2.4. Statistics

Only the percentage of entries in the arm with high probability of reward data passed D'agostino-Pearson test of normality. Therefore, we used parametric statistics to analyze this set of data (ANOVA followed by Holm-Sidak test). Kruskal-Wallis ANOVA followed by Dunn's test or Mann-Whitney test were used to analyze non-parametric data. Differences were considered significant if $p < 0.05$.

3. Results

Haloperidol treatment caused a dose-dependent reduction in the number of entries in the arm with a higher probability of reward (Fig. 2A, $H = 10.0$, $p < 0.05$, Kruskal-Wallis ANOVA). Dunn's post-hoc showed a significant difference between the group treated with 0.15 mg/kg haloperidol and the control group ($p < 0.05$).

After a non-rewarded trial in the arm with lower reward probability, saline-treated rats mostly avoided re-entering that same arm in the next trial (Fig. 2B). This behavior contrasted with the behavior of the rats treated with 0.15 mg/kg haloperidol rats which did this choice significantly more times ($H = 10.3$, $p < 0.05$ Kruskal-Wallis ANOVA; $p < 0.05$ Dunn's test). In addition, in a significantly higher number of trials, the rats treated with 0.15 mg/kg haloperidol did not enter one of the arms, compared to the saline group (Fig. 2C, $H = 16.9$, $p < 0.001$, Kruskal-Wallis ANOVA; $p < 0.01$, Dunn's test).

Fig. 3 shows that haloperidol caused significant increases in the latencies to choose which arm to enter (choice latency) and to run from the entry of the arm to the reward area (response latency). Data were pooled by blocks of 10 trials and analyzed by Kruskal-Wallis ANOVA followed by Dunn's test. Fig. 3A shows significant effects for choice latency ($H = 121$, $p < 0.001$), response latency in the 30% reward probability arm (Fig. 3B, $H = 99.6$, $p < 0.001$), and response latency in the 70% reward probability arm (Fig. 3C, $H = 133$, $p < 0.001$). Dunn's test showed significant differences ($p < 0.05$) only between 0.15 mg/kg and saline groups. When data of all trials were pooled, Kruskal-Wallis ANOVA showed significant effects for choice latency (Fig. 3D, $H = 30.7$, $p < 0.001$), response latency in the 30% reward probability arm (Fig. 3E, $H = 26.8$, $p < 0.001$), and response latency in the 70% reward probability arm (Fig. 3F, $H = 31.6$, $p < 0.001$). Compared to the saline group, Dunn's post-hoc test showed significant increases in the choice latencies of the 0.15 mg/kg haloperidol treated group (Fig. 3D $p < 0.001$), response latency in the 30% reward arm of the 0.10 and 0.15 mg/kg haloperidol treated groups (Fig. 3E, $p < 0.01$), and response latencies in the 70% reward arm of the 0.05, 0.10, and 0.15 mg/kg haloperidol treated groups (Fig. 3F, $p < 0.05$).

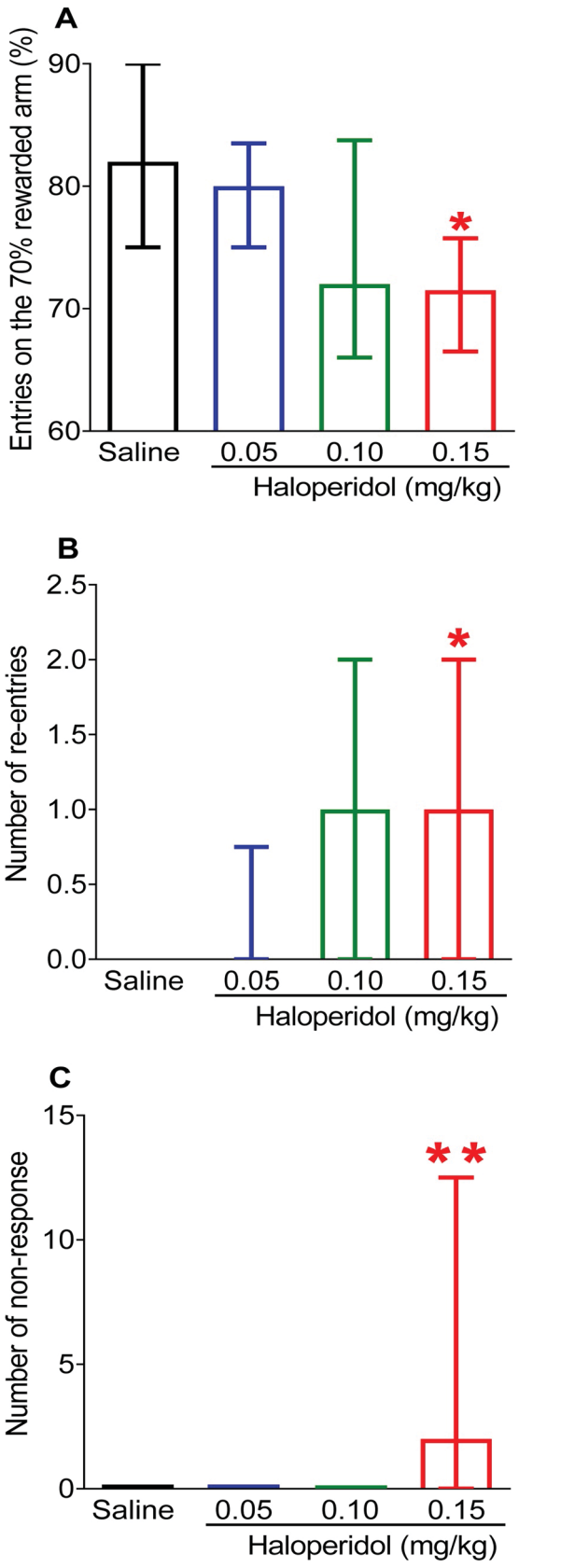

(caption on next page)

Fig. 2. Effect of haloperidol on number of entries in the Y-maze arm with higher probability of reward. After extensive training, rats were given either saline or haloperidol and submitted to a 50-trial test session. One of the arms was reinforced 70% of times and the other arm was reinforced 30% of times. Data are expressed as median with interquartile range percent of times rats entered the 70% reinforced arm (A), number of times rats re-entered the 30% reinforced arm after a non-rewarded trial (B), and number of trials in which rats did not leave the start area (non-responses, C). * $P < 0.05$ and ** $P < 0.01$ compared to haloperidol saline group, Kruskal-Wallis ANOVA followed by the Dunn's test. N = 12 rats per group.

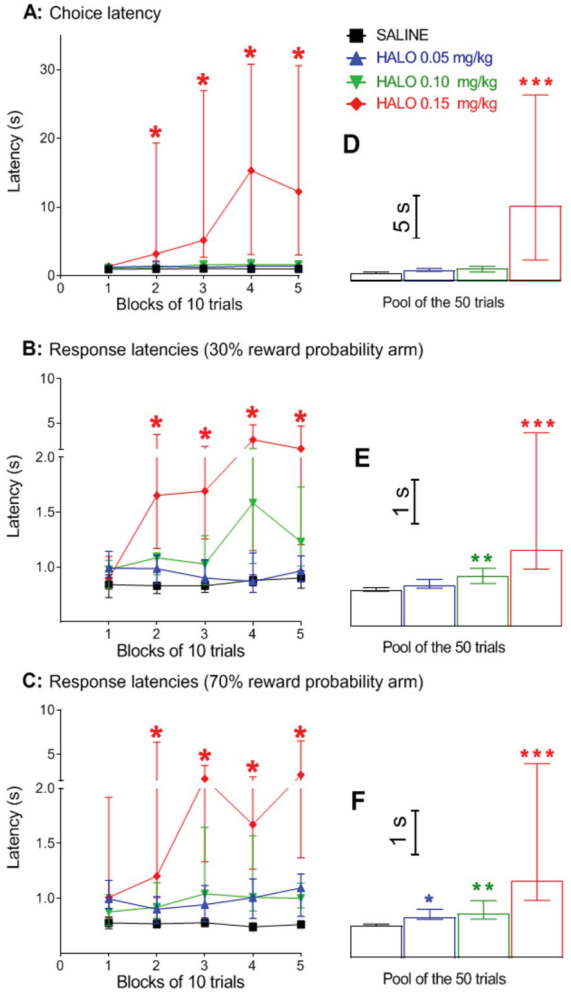

Fig. 3. Effects of haloperidol on choice and response latencies. After 4 days of training, rats were given either saline or haloperidol and submitted to a 50-trial test session in the Y-maze. One of the arms was reinforced 70% of times and the other arm was reinforced 30% of times. (A) Latency to enter one of the arms after the start door was opened (choice latency). (B) Latency to arrive at the reward area after entering the arm with a 30% reward probability (response latency). (C) Latency to arrive at the reward area after entering the arm with a 70% reward probability. Data are expressed as median (interquartile range). In the graphics shown in the left column (A, B, and C) data were averaged in blocks of 10 trials. In the graphics shown in the right column data of all trials were averaged. N = 12 rats per group. * $P < 0.05$, ** $P < 0.01$ and *** $P < 0.001$ compared to saline, Dunn's multiple comparisons test after Kruskal-Wallis ANOVA.

Note that the administration of 0.15 mg/kg haloperidol affected response and choice latencies in blocks 2-5, but not in block 1 (Fig. 3). This delayed response suggests a build-up of the drug in the brain that had a more pronounced motoric effect with time. Haloperidol was injected 30 min before the test session started and each block of trials

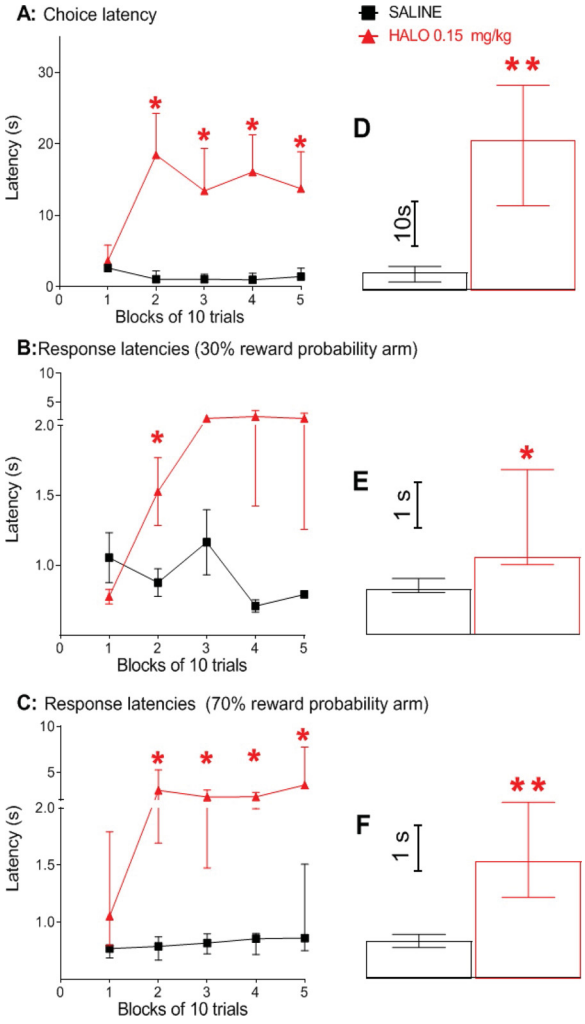

Fig. 4. Effects of haloperidol administration 1 hour before the beginning of the test session on choice and response latencies. After 4 days of training, rats were given either saline or haloperidol 1 hour prior to a 50-trial test session in the Y-maze. One of the arms was reinforced 70% of times and the other arm was reinforced 30% of times. (A) Choice latency (time to enter one of the arms after the start door was opened). (B) Response latency (time to arrive in the reward area after entering the arm with 30% reward probability). (C) Response latency for the 70% reward probability arm. Data are expressed as median (interquartile range). In the graphics shown in the left column, data was polled in blocks of 10 trials. In the graphics shown in the right column data of all trials were pooled. Saline group, N = 7 rats per group, 0.15 mg/kg haloperidol group, N = 6. * $P < 0.05$, ** $P < 0.01$ compared to saline, Mann Whitney test.

lasted nearly 30 min. Therefore, if this hypothesis were correct, the effects of the administration of haloperidol 60 min before the test session should have decreased the choice and response latencies in all the 5 blocks of trials. However, Fig. 4 shows that the administration of 0.15 mg/kg haloperidol caused a significant increase in the choice and response latencies only in blocks 2-5, but not in block 1, even when administered 60 min before the onset of the test session. Significant differences among these groups were observed for choice latency (Fig. 4A, $p < 0.05$, Mann-Whitney tests), response latency in the 30% reward probability arm (Fig. 4B, $p < 0.05$, Mann-Whitney tests), and response latency in the 70% reward probability arm (Fig. 4C, $p < 0.05$, Mann-Whitney tests). When data of all trials were pooled, Mann-Whitney tests showed significant effects for choice latency (Fig. 4D, $p < 0.01$), response latency in the 30% reward probability arm (Fig. 4E, $p < 0.05$), and response latency in the 70% reward probability arm (Fig. 4F, $p < 0.01$).

An alternative hypothesis to explain the delayed effect of haloperidol on choice and response latencies is that instead of causing a sedative/motoric effect, it causes a decrease in the motivation to approach the reward area. Motivation is expected to decrease after the first trials because rats will be more tired to run. Motivation also depends on rat hunger. In order to test whether haloperidol increased response latencies by causing quicker satiation of hunger 2 other independent groups of rats were treated with saline or 0.15 mg/kg haloperidol and 30 min later they were allowed to eat all sucrose pellets they wanted. The same experiment was repeated with 2 other groups of rats, but saline or 0.15 mg/kg haloperidol were injected 60 min before the test. The rats that received saline 30 min or 60 min before the test ate 2.40 ± 0.13 g and 2.07 ± 0.10 g of sucrose, respectively (data expressed as mean ± SEM; N = 12 per group). The rats that received 0.15 mg/kg haloperidol 30 min or 60 min before the test ate 2.37 ± 0.18 g of sucrose and 2.15 ± 0.17 g of sucrose, respectively (N = 12 per group). No significant difference among groups was observed for the amount of sucrose pellets eaten ($F(3,46) = 1.12$, $p > 0.05$. One-way ANOVA). Therefore, the reason why haloperidol-treated rats approached the reward area of the arms more slowly compared to saline-treated rats was not hunger satiation 30 or 60 min after the drug administration.

Fig. 2A shows that in the free choice test session, saline-treated rats have chosen to enter the 70% reward probability arm nearly 80% of times and entered the 30% reward probability arm only 20% of times. This finding suggests that the rat reward expectation was higher when it chose to enter the arm with higher reward probability. In addition, Fig. 4A and B show that the saline-treated rats ran more quickly to the reward area of the 70% probability reward arm compared to the 30% reward arm ($p < 0.05$ Mann-Whitney test).

In this probabilistic task the reward expectation was constantly updated according to the prediction error that occurs in every trial. Because reward expectation is not 100%, any time rats entered a baited arm a positive prediction error occurred: to be rewarded is 0.7 or 0.3 better than expected when they entered the 30% or 70% reward probability arm, respectively. We tested whether these changes in reward expectation affected motivation by comparing response latencies in the next trial after the rewarded and reward omission trials. Fig. 5B and C show that rats presented longer response latency after they entered the 30% reward probability trial compared to a reward omission in the same arm ($p < 0.05$, Mann-Whitney test). In addition, latency to enter the 30% reward probability arm in the next trial was also longer compared to the latencies to enter the 70% reward probability arm, independently of the previous trial in the 70% reward probability arm to have been rewarded or not ($p < 0.05$, Mann-Whitney test). Two things were different after a rat entered a 30% probability arm and was rewarded: (i) a big positive prediction error (+0.7) occurred; (ii) the reward probability in the next trial increased - because the reward probability is fixed in the 30% per session, each time this arm is not rewarded the probability that it will be rewarded in the next trial increases. This increase in reward expectation may explain why saline-treated rats ran more quickly to this arm in the next trial.

Finally, Fig. 5 shows that all doses of haloperidol abolished the response latency difference between 30% and 70% rewarded arms. In addition, as also shown in Fig. 4C, haloperidol caused a dose dependent increase in the response latencies. Kruskal-Wallis ANOVA of these data showed significant effects among groups for Fig. 5A (30% reward probability arm: $H = 22.3$, $p < 0.001$; 70% reward probability arm: $H = 3.15$, $p < 0.001$), Fig. 5B (30% reward probability arm: $H = 24.5$, $p < 0.001$; 70% reward probability arm: $H = 28.4$, $p < 0.001$), and Fig. 4C (30% reward probability arm: $H = 30.7$, $p < 0.001$; 70% reward probability arm: $H = 29.5$, $p < 0.001$). Dunn's post-hoc test showed a significant dose-dependent increase in response latencies (see Figs. 5A, 4B, and 5C).

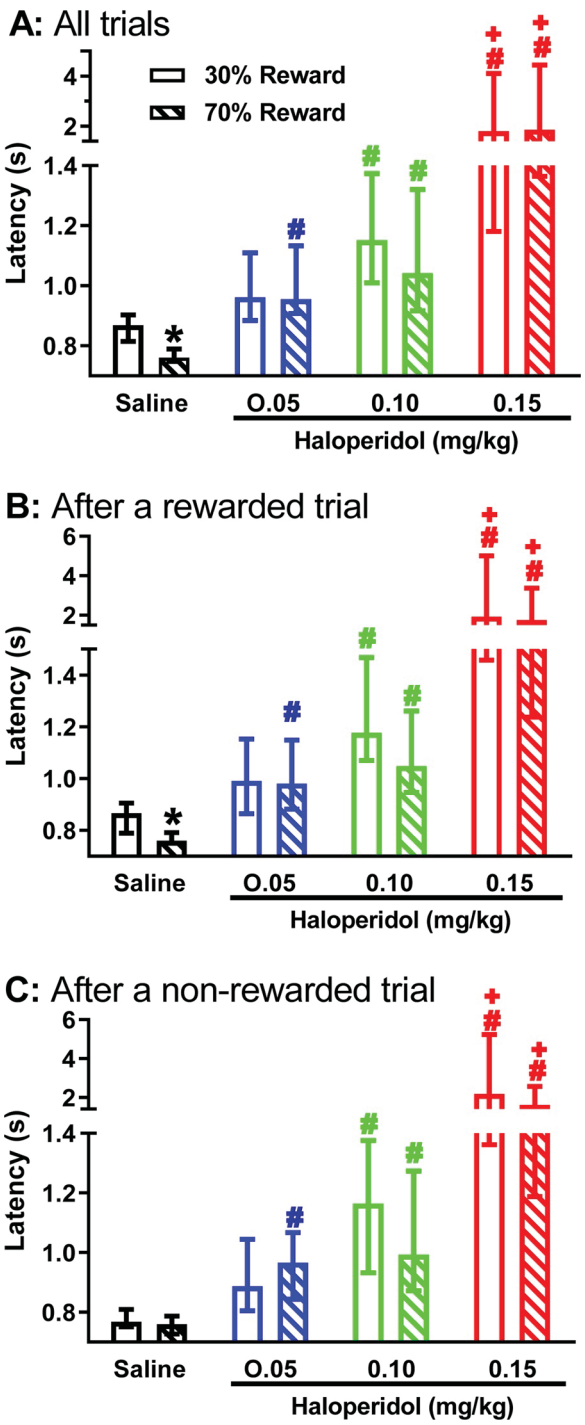

Fig. 5. Effect of reward probability and haloperidol on the response latencies. After 4 days of training, rats were given either saline or haloperidol and submitted to a 50-trial test session in the Y-maze. One of the arms was reinforced 70% of times and the other arm was reinforced 30% of times. Data of all trials were pooled and split in the latency for the response latency for the 70% or 30% arm. Bars represent median values and error bars represent interquartile range. N = 12 rats per group. * P ≤ 0.05 compared to 70% in the same group (Mann-Whitney test); # P ≤ 0.05, compared to the saline group (Dunn's test after Kruskal-Wallis ANOVA); + P ≤ 0.05, compared to 0.05 haloperidol group (Dunn's test after Kruskal-Wallis ANOVA).

4. Discussion

In the present study, we found that the D2 dopamine receptor antagonist haloperidol administered systemically to rats 30 min before the

test caused a dose-dependent increase in choice and response latencies in the Y-maze probabilistic reinforcement task. Activation of D1 receptors depolarizes the Go neurons while activation of postsynaptic D2 receptors hyperpolarizes the NoGo neurons of the dorsal striatum [10,11]. Because haloperidol is a dopamine receptor antagonist with higher affinity for D2-Rs compared to D1-Rs [18], it is tempting to explain the longer response latencies observed in the haloperidol-treated rats as resulting from blockade of D2-Rs and consequent activation of the NoGo neurons. The striatopallidal medium spiny NoGo neuron expresses D2-Rs while the striatonigral spiny Go neuron expresses D1-Rs [10]. According to this hypothesis, haloperidol could have increased the approach responses latencies by modulating the motoric effect of the Go/NoGo striatal neurons. However, this haloperidol effect was observed in the last, but not in the first, trials of the test session. One can suspect that this happened because haloperidol was injected i.p. 30 min before the test and the effect on locomotion might have the peak later. We tested this hypothesis by injecting haloperidol 60 min before the test and, again, longer latencies were not observed in the first, but in the following trials. Therefore, the effect of haloperidol on the approach latency was not caused by motoric impairment. Furthermore, motoric impairment (e.g. catalepsy) has been reported to occur only with doses of haloperidol higher than the doses used in the present study [13,19].

If haloperidol is not causing a motor impairment, by which mechanism did it reduce locomotion speed? Was it by decreasing motivation? While some authors explain the reduction of locomotor activity in an open field as a motor impairment [20,21], others propose that this effect is caused by a reduction in motivation. Similar to what we observed in the present study, previous studies have shown that the effect of low doses of haloperidol on locomotor activity was evident only in the last part of an open field session [22,23]. As reported in these studies, when control rats were exposed to an open field for the first time, a progressive decline in locomotor activity was observed, suggesting a decrease in the motivation to explore the environment. Coherently, when re-tested in the same environment, control rats exhibited reduced locomotor activity from the beginning to the end of the session. However, when the same rats were tested in a novel environment, they behaved as in the first open field session, showing high locomotor activity at the beginning of the session, followed by a progressive decline. In these studies, rats treated with a lower dose of haloperidol did not differ from controls at the beginning of the session: they presented high locomotor activity. However, locomotor activity decreased sharply, and, at the end of the session, haloperidol treated rats were significantly slower than controls. When re-tested in the same open field, haloperidol treated rats showed locomotor activity lower than controls from the beginning to the end of the session. These findings cannot be explained by a motoric or attentional effect of haloperidol and support the hypothesis that haloperidol decreases motivation to explore familiar environments.

This reasoning is in agreement with the hypothesis that haloperidol decreases locomotion by acting in the meso-cortico-limbic dopamine pathway, which is critical for motivation [1]. Also in agreement with this hypothesis, the longer latencies that we observed in haloperidol-treated rats in the last trials of the test session could be caused by a reduced motivation to approach the reward area. In the present study, the motivation to run towards the arm with a 70% reward probability was higher compared to the motivation to approach the 30% reward probability arm. Such motivational difference could be measured by the latency to approach the reward area: as predicted by the motivational hypothesis, saline-treated rats presented shorter latencies to approach the reward area of the 70% reward probability arm and haloperidol blocked this effect.

Motivation or wanting can also be measured by the effort to get a reward. The hypothesis that haloperidol reduces motivation to express previously rewarded responses is also supported by cost/benefit studies. A study by Salamone et al. (1994) reported that control rats tested in a T-maze preferred to climb a 44 cm barrier to enter an arm with four food pellets than entering the other arm which had no barrier but only two food pellets. On the other hand, rats treated with haloperidol did the opposite. In another study, rats were trained in a T-maze to climb progressively higher barriers to get progressively more food. Rats treated with haloperidol preferred to climb lower barriers to get smaller rewards. Treatment with amphetamine (which increases dopamine release) had the opposite effect and reverted the haloperidol effect [14]. In another study, control rats preferred to press a bar for preferred food than eating regular lab chow. Pre-feeding rats with lab chow reduced both bar-pressing for preferred food and feeding. Prefeeding also reduced bar-pressing in rats treated with haloperidol but increased the ingestion of regular chow. Another piece of evidence supporting the motivation hypothesis comes from the finding that treatment with haloperidol and other neuroleptics caused a progressive decrease of instrumental responses in a manner similar to the omission of primary reinforcers [24].

If the haloperidol effect can be explained by reduced motivation, it is important to discover by which mechanism this happens. A possible hypothesis is that haloperidol causes faster satiation by the sucrose pellets. We tested this hypothesis by measuring the amount of sucrose pellets saline- and haloperidol-treated rats consumed when they were given free access to all pellets they could for a period of time similar to the duration of the test session. Contrary to the satiation hypothesis, rats treated with the higher dose of haloperidol injected 30 or 60 min before the test ate nearly the same amount of sucrose pellets that saline-treated rats had eaten.

Therefore, if not by reducing satiation, by which mechanism could haloperidol have reduced motivation to approach the reward areas in the Y-maze? There is also solid evidence that reward predictive cues cause the release of dopamine in the ventral striatum in an amount that is proportional to reward expectation. It is also well established that activation of dopamine receptors in the ventral striatum is critical to “energize” reward seeking behaviors and the approach behavior to the reward area [1]. In the present study, such invigoration of the approach response could be measured by locomotion speed. Recent studies have shown that the locomotion speed is correlated with the activity of the Go-Neurons, as well as NoGo neurons and parvalbumin-positive fast-spiking interneurons (FSIs) [25,26]. Both the NoGo neurons and the FSIs express D2Rs which are sensitive to low doses of haloperidol. Therefore, the longer latencies observed in the haloperidol treated rats may result in an unrealistic low expectation that the reward is available at the end of the Y-maze arms. In other words, haloperidol may reduce the incentive salience or the wanting evoked by the environmental cues that trigger the approach response and control its vigor [1,2].

Another possible explanation is that the effect of haloperidol on the rat performance in this task resulted from an inability to evaluate whether the outcome in which arms to enter in each trial matched the expected reward. The mismatch between expected and obtained reward is called reward prediction error and it has been well established that it is encoded by the amount of dopamine in the dorsal and ventral striatum after the reward delivery or omission [27–31]. The phasic release of dopamine affects more the Go-neurons, which express D1-Rs, than the NoGo-Rs, which express D2-DRs. This happens because the basal level of dopamine saturates most of the striatal D2-Rs [8,9]. Therefore, mostly D1Rs will not be already saturated when the more dopamine is released in response to positive prediction errors. Therefore, in a control rat, activation of D1-Rs plays a key role in learning when an action is reinforced and D2-Rs are more important to learn to avoid an action when the expected reward is omitted. This prediction was confirmed in a study by Frank and co-workers (2004) who showed that Parkinsonian patients off medication were better at learning how to avoid choices that lead to negative outcomes than they were at learning from positive outcomes and that dopamine medication reversed this bias. This hypothesis is also supported by the finding that polymorphisms associated with transcription of D2Rs in humans are

predictive of avoidance-based decisions in a probabilistic task [32,33].

Therefore, because haloperidol has a higher affinity for D2-Rs, it is expected to impair the learning of avoiding non-reinforced choices. This reasoning can explain why haloperidol treated rats re-entered the non-rewarded arms that they had just visited, even after the trials in which the reward was omitted. On these occasions, the blockage of presynaptic neurons by haloperidol increased dopamine release giving a false message that the outcome was rewarding when it was indeed absent. This reasoning is also supported by a previous study that reported perseveration of nonreinforced behaviors in rats submitted to chronic treatment with haloperidol and tested in the Olton version of the 8-arm radial maze [34].

In summary, the present study suggests that haloperidol impairs the learning and performance of the probabilistic Y-maze task, not by causing a motor impairment or by reducing satiation. Instead, it suggests that haloperidol affects the motivation to approach the reward areas. This lack of motivation may be caused by an inability to update reward predictions and/or by a decrease in the incentive salience of environmental cues that signal the reward probability associated with each rewarded area.

Author Statement

Bernadete Negrelli contributed to this manuscript performing the experiment design, data collection, and data analysis. The author also contributed to the data discussion and manuscript writing.

José Augusto Pochapski contributed to this manuscript performing the experiment design, data collection, and data analysis. The author also contributed to the data discussion and manuscript writing.

Cyrus Antonio Villas-Boas contributed to this manuscript performing the experiment design, data discussion, and manuscript writing.

Letícia Ferreira Jessen contributed to this manuscript performing data collection and data analysis.

Mayra Aline Lopes Teixeira contributed to this manuscript performing data collection and data analysis.

Claudio da Cunha contributed to this manuscript performing the experiment design, data discussion, and manuscript writing.

Acknowledgements

This work was supported by CAPES (grant number 1478962) and CNPq.

References

[1] S. Ikemoto, C. Yang, A. Tan, Basal Ganglia Circuit Loops, Dopamine and Motivation: A Review and Enquiry, (2015), pp. 17–31, https://doi.org/10.1016/j.bbr.2015.04.018.Basal.
[2] K.C. Berridge, The debate over dopamine's role in reward: the case for incentive salience, Psychopharmacology (Berl) 191 (2007) 391–431, https://doi.org/10.1007/s00213-006-0578-x.
[3] J.D. Salamone, M. Correa, Motivational views of reinforcement: Implications for understanding the behavioral functions of nucleus accumbens dopamine, Behav. Brain Res. 137 (2002) 3–25, https://doi.org/10.1016/S0166-4328(02)00282-6.
[4] D.P. Covey, J.F. Cheer, Accumbal dopamine release tracks the expectation of dopamine neuron-mediated reinforcement, Cell Rep. 27 (2019) 481–490, https://doi.org/10.1016/j.celrep.2019.03.055 e3.
[5] P.W. Glimcher, Understanding dopamine and reinforcement learning: the dopamine reward prediction error hypothesis, Proc. Natl. Acad. Sci. U. S. A. 108 (2011) 15647–15654, https://doi.org/10.1073/pnas.1014269108.
[6] C.R. Gerfen, D.J. Surmeier, Modulation of striatal projection systems by dopamine, Annu. Rev. Neurosci. 34 (2011) 441–466, https://doi.org/10.1146/annurev-neuro-061010-113641.Modulation.
[7] W. Schultz, Behavioral dopamine signals, Trends Neurosci. 30 (2007) 203–210, https://doi.org/10.1016/j.tins.2007.03.007.
[8] J.K. Dreyer, C.M. Vander Weele, V. Lovic, B.J. Aragona, Functionally distinct dopamine signals in nucleus accumbens core and shell in the freely moving rat, J. Neurosci. 36 (2016) 98–112, https://doi.org/10.1523/JNEUROSCI.2326-15.2016.
[9] C. Yapo, A.G. Nair, L. Clement, L.R. Castro, J. Hellgren Kotaleski, P. Vincent, Detection of phasic dopamine by D1 and D2 striatal medium spiny neurons, J. Physiol. 595 (2017) 7451–7475, https://doi.org/10.1113/JP274475.
[10] D.J. Surmeier, S.M. Graves, W. Shen, Dopaminergic modulation of striatal networks in health and Parkinson's disease, Curr Opin Neurobiol. 29 (2014) 109–117, https://doi.org/10.1016/j.conb.2014.07.008.
[11] T.C. Jhou, P.J. Vento, Bidirectional regulation of reward, punishment, and arousal by dopamine, the lateral habenula and the rostromedial tegmentum (RMTg), Curr. Opin. Behav. Sci. 26 (2019) 90–96, https://doi.org/10.1016/j.cobeha.2018.11.001.
[12] G. Cui, S.B. Jun, X. Jin, M. Pham, S. Vogel, D.M. Lovinger, R.M. Costa, Concurrent activation of striatal direct and Indirect pathways during action initiation, Nature 494 (2013) 238–242, https://doi.org/10.1038/nature11846.
[13] A.S. Bazyan, V.M. Getsova, N.V. Orlova, Haloperidol catalepsy consolidation in the rat as a model of neuromodulatory integration, Neuroscience 99 (2000) 279–288, https://doi.org/10.1016/S0306-4522(00)00183-4.
[14] M.E. Bardgett, M. Depenbrock, N. Downs, M. Points, L. Green, Dopamine modulates effort-based decision making in rats, Behav. Neurosci. 123 (2009) 242–251, https://doi.org/10.1037/a0014625.
[15] J.D. Salamone, M.S. Cousins, S. Bucher, Anhedonia or anergia? Effects of haloperidol and nucleus accumbens dopamine depletion on instrumental response selection in a T-maze cost/benefit procedure, Behav. Brain Res. 65 (1994) 221–229, https://doi.org/10.1016/0166-4328(94)90108-2.
[16] J.D. Salamone, R.E. Steinpreis, L.D. McCullough, P. Smith, D. Grebel, K. Mahan, Haloperidol and nucleus accumbens dopamine depletion suppress lever pressing for food but increase free food consumption in a novel food choice procedure, Psychopharmacology (Berl) 104 (1991) 515–521, https://doi.org/10.1007/BF02245659.
[17] Y.F. Cheng, L.K. Paalzow, Linear pharmacokinetics of haloperidol in the rat, Biopharm. Drug Dispos. 13 (1992) 69–76, https://doi.org/10.1002/bdd.2510130106.
[18] P. Li, G.L. Snyder, K.E. Vanover, The international journal for in-depth reviews on current topics in medicinal chemistry dopamine targeting drugs for the treatment of schizophrenia: past, present, Curr. Top. Med. Chem. 16 (2016) 3385–3403, https://doi.org/10.2174/1568026616666160608.
[19] A. Campbell, R.J. Baldessarini, M.C. Cremens, Dose-catalepsy response to haloperidol in rat: effects of strain and sex, Neuropharmacology 27 (1988) 1197–1199, https://doi.org/10.1016/0028-3908(88)90018-4.
[20] G.J. Schaefer, R.P. Michael, Drug interactions on spontaneous locomotor activity in rats, Neuropharmacology 23 (1984) 909–914, https://doi.org/10.1016/0028-3908(84)90004-2.
[21] R. Carey, E. Damianopoulos, G. De Palma, 8-OH DPAT can restore the locomotor stimulant effects of cocaine blocked by haloperidol, Pharmacol. Biochem. Behav. 66 (2000) 863–872, https://doi.org/10.1016/S0091-3057(00)00290-2.
[22] M.R. Lynch, R.J. Carey, Environmental stimulation promotes recovery from haloperidol-induced extinction of open field behavior in rats, Psychopharmacology (Berl) 92 (1987) 206–209, https://doi.org/10.1007/BF00177916.
[23] L. De Angelis, C. Furlan, Within-session behavioral decrement of atypical antipsychotics: role of novelty, Drug Dev. Res. 42 (1997) 71–75, https://doi.org/10.1002/(SICI)1098-2299(199710)42:2<71:AID-DDR3>3.0.CO;2-M.
[24] R.A. Wise, J. Spindler, H. Dewit, gary J. Gerber, Neuroleptic-Induced "Anhedonia" in rats: pimozide blocks reward quality of food, Science (80-.) 201 (1978) 262–264, https://doi.org/10.1126/science.566469.
[25] W.C. Fobbs, S. Bariselli, J.A. Licholai, N.L. Miyazaki, B.A. Matikainen-Ankney, M.C. Creed, A.V. Kravitz, Continuous representations of speed by striatal medium spiny neurons, J. Neurosci. 40 (2020) 1679–1688, https://doi.org/10.1523/JNEUROSCI.1407-19.2020.
[26] N. Kim, H.E. Li, R.N. Hughes, G.D.R. Watson, D. Gallegos, A.E. West, I.H. Kim, H.H. Yin, A striatal interneuron circuit for continuous target pursuit, Nat. Commun. 10 (2019), https://doi.org/10.1038/s41467-019-10716-w.
[27] W. Schultz, Predictive reward signal of dopamine neurons, J. Neurophysiol. 80 (1998) 1–27, https://doi.org/10.1152/jn.1998.80.1.1.
[28] A.S. Hart, J.J. Clart, P.E.M. Phillips, Dynamic shaping of dopamine signals during probabilistic Pavlovian conditioning, Neurobiol Learn Mem. 117 (2015) 84–92, https://doi.org/10.1016/j.nlm.2014.07.010.
[29] P.N. Tobler, C.D. Fiorillo, W. Schultz, Adaptive coding of reward value by dopamine neurons, Science 307 (2005) 1642–1645, https://doi.org/10.1126/science.1105370.
[30] S.Q. Park, T. Kahnt, D. Talmi, J. Rieskamp, R.J. Dolan, H.R. Heekeren, Adaptive coding of reward prediction errors is gated by striatal coupling, Proc. Natl. Acad. Sci. U. S. A. 109 (2012) 4285–4289, https://doi.org/10.1073/pnas.1119969109.
[31] K.M.M.J. Diederen, T. Spencer, M.D.D. Vestergaard, P.C.C. Fletcher, W. Schultz, Adaptive prediction error coding in the human midbrain and striatum facilitates behavioral adaptation and learning efficiency, Neuron 90 (2016) 1127–1138, https://doi.org/10.1016/j.neuron.2016.04.019.
[32] M.J. Frank, L.C. Seeberger, R.C. O'Reilly, By carrot or by stick: cognitive reinforcement learning in Parkinsonism, Science (80-.) 306 (2004) 1940–1943, https://doi.org/10.1126/science.1102941.
[33] M.J. Frank, K. Hutchison, Genetic contributions to avoidance-based decisions: Striatal D2 receptor polymorphisms, Neuroscience 164 (2009) 131–140, https://doi.org/10.1016/j.neuroscience.2009.04.048.
[34] E.J. Hutchings, J.L. Waller, A.V. Terry, Differential long-term effects of haloperidol and risperidone on the acquisition and performance of tasks of spatial working and short-term memory and sustained attention in rats, J. Pharmacol. Exp. Ther. 347 (2013) 547–556, https://doi.org/10.1124/jpet.113.209031.

Final considerations and conclusion

How is motivation encoded in our central nervous system? Which neuronal mechanisms control these processes? What changes drugs of abuse can induce on these neuronal circuitries? These are of the questions that have been asked since the early times of the modern neuroscience field. Even although considerable progress was accomplished in the past decades, several questions remain unanswered as long as new questions arise.

Using electrophysiological recordings of the neuronal activity associated with behavioral and pharmacologic approaches, this thesis evaluated the neuronal activity control over motivated behavior and changes promoted by drugs of abuse. In summary, the studies included in this thesis demonstrate new evidence of the NAc neuronal control of motivated behavior. Our results demonstrate that NAc neurons encode the speed and acceleration of the animal during the approach to rewarded places. These findings also suggest encoding of the distance of the reward location by a subset of NAc neurons. Classical studies describe that NAc is the interface of motor and limbic circuits (Mogenson et al., 1980). Here in agreement with this classical concept, we demonstrated that this interface role performed by NAc neurons could be represented by the encoding of locomotion kinetics (speed and acceleration) and distance of reward locations. NAc is a component of a much broader circuit underlying control over motivated behavior, including PFC, VTA, hippocampus, amygdala, among others limbic and cortical structures. Drugs of abuse are described to promote changes in several components of this circuitry. In this thesis, we demonstrated that the early stages of neurodevelopment, such as adolescence, are a critical window to alcohol effects on NAc and OFC activity. We demonstrated robust long-term changes promoted by adolescent alcohol exposure on OFC encoding of conditioned stimulus. NAc neuronal activity during reward-motivated behavior was also altered by the alcohol exposure. The changes in neuronal activity were also associated with a decrease in goal-tracking behavior in these animals. These findings demonstrate neuronal and behavioral changes promoted by adolescent alcohol exposure that could increase the risk of developing alcohol use disorder in adulthood. In our last chapter, we focused on evaluating the role of D2 dopaminergic receptors on

motivated behavior. Dopaminergic receptors are strongly expressed on NAc, striatum, OFC, and other limbic and cortical structures. Previously approach-behavior was associated with the activation of D1, but not D2-dopaminergic receptor. However, this vision was challenged by posterior studies (Nicola 2004, 2007, Ikemoto, 2007). Using behavioral and pharmacologic approaches, we demonstrated that D2-dopaminergic receptor activity is required in the early stages of reward approach and motivated behavior. The three studies presented in this thesis demonstrate important new evidences on how NAc neurons could control motivation, and reward approach, the role of D2-dopaminergic receptors on this process and neuronal components of these circuits that are affected by alcohol exposure during adolescence.

These experiments were also particularly important for my professional and personal development. The opportunity to learn about *in vivo* single-unit electrophysiology and perform the data collection and analysis in the laboratory of Professor Donita L. Robinson, Ph.D., at the University of North Carolina at Chapel Hill, was an essential part of this process. Besides the behavioral and neuronal data presented in this thesis, additional data analyses are still in progress. We are further analyzing possible differences in OFC and NAc activity between sign-trackers and goal-trackers subjects and also evaluating the effects of naltrexone, a drug applied for alcoholism treatment, on the OFC and NAc neuronal activity. We expect in the near future to contribute with additional scientific articles from these already collected data.

Also, this period of *doutorado sanduíche* allowed the acquisition of experience and expertise to perform further electrophysiological studies in Professor Claudio da Cunha's laboratory at UFPR. The scientific article presented in the second chapter of this thesis was fully performed and analyzed in our laboratory at UFPR. The finding of this study, besides the scientific relevance, also present special personal significance, as this was the first *in vivo* electrophysiological experiment performed in our laboratory and also in our university. This is a final outcome from several years of extensive data collection and analysis from many scientists from our group and collaborators from 3 different continents.

Electrophysiological recordings of neuronal activity are a powerful approach for understanding neuronal mechanisms associated with behavioral

expression. It allows us to, on a time scale of milliseconds, acquire the neuronal activity data from an individual neuron and evaluate the subsequent behavior simultaneously. This technic can be applied in association with several behavioral tasks or different technics. For example, new methodological approaches, such as optogenetics, can be simultaneously performed with electrophysiological recordings. We expect to associate in future studies the optogenetics and single-unit electrophysiological recordings to further differentiation of structurally distinct neuronal populations, resulting in a distinct approach to better identification and classification of the neuronal activity.

The association of classical and new methodologic approaches is essential for the convergence of well-established concepts with the complexity of newly described mechanisms and functions. Besides the interesting and important findings observed in our studies, several questions remain unanswered as long as new questions arise. An expressive number of pathologies present disruptions on mechanisms underlying motivated behavior, and effective treatment are absent. A better understanding of mechanisms underlying motivated reward behavior under normal or pathological conditions is highly required. In this thesis, we provided pieces of evidence on neuronal circuits and mechanisms underlying the encoding of motivated behavior in normal and abnormal conditions.

References

ALAUX-CANTIN, S.; WARNAULT, V.; LEGASTELOIS, R.; et al. Alcohol intoxications during adolescence increase motivation for alcohol in adult rats and induce neuroadaptations in the nucleus accumbens. **Neuropharmacology**, v. 67, 2013.

AMBROGGI, F.; ISHIKAWA, A.; FIELDS, H. L.; NICOLA, S. M. Basolateral Amygdala Neurons Facilitate Reward-Seeking Behavior by Exciting Nucleus Accumbens Neurons. **Neuron**, p. 648–661, 2008.

AMODEO, L. R.; KNEIBER, D.; WILLS, D. N.; et al. Alcohol drinking during adolescence increases consumptive responses to alcohol in adulthood in Wistar rats. **Alcohol**, p. 43–51, 2017.

BAVA, S.; TAPERT, S. F. Adolescent Brain Development and the Risk for Alcohol and Other Drug Problems. Neuropsychol Rev, p. 398–413, 2010.

BEAULIEU, J.; GAINETDINOV, R. R. The Physiology , Signaling , and Pharmacology of Dopamine Receptors. **PHARMACOLOGICAL REVIEWS**, v. 63, n. 1, p. 182–217, 2011.

BERKE, J. D. What does dopamine mean ? **Nature Neuroscience**, 2018. Springer US.

BERRIDGE, K. C. Motivation concepts in behavioral neuroscience. **Physiology and Behavior,** v. 81, n. 2, p. 179–209, 2004.

BRADFIELD, L. A.; DEZFOULI, A.; HOLSTEIN, M. VAN; et al. Medial Orbitofrontal Cortex Mediates Outcome Retrieval in Partially Observable Task Situations. **Neuron**, v. 88, n. 6, p. 1268–1280, 2015.

BROADWATER, M. A.; LEE, S.; YU, Y.; et al. Adolescent alcohol exposure decreases frontostriatal resting-state functional connectivity in adulthood. **Addiction Biology**, 2017.

BURKE, K. A.; TAKAHASHI, Y. K.; CORRELL, J.; BROWN, P. L.; SCHOENBAUM, G. Orbitofrontal inactivation impairs reversal of Pavlovian learning by interfering with disinhibition of responding for previously unrewarded cues. **Eur J Neurosci**., v. 30, n. 10, p. 1941–1946, 2009.

CABALLERO, A.; GRANBERG, R.; TSENG, K. Y.; CHICAGO, N. Mechanisms contributing to Prefrontal Cortex Maturation during Adolescence. **Neurosci Biobehav Rev**., v. 70, p. 4–12, 2016.

CALIPARI, E. S.; JUAREZ, B.; MOREL, C.; et al. Dopaminergic dynamics underlying sex-specific cocaine reward. **Nature Communications**, 2017.

CARELLI, R. M.; DEADWYLER, S. A. A comparison of nucleus accumbens neuronal firing patterns during cocaine self-administration and water reinforcement in rats. **Journal of Neuroscience**, v. 14, n. 12, p. 7736–7746, 1994.

CARELLI, R. M.; IJAMES, S. G.; CRUMLING, A. J. Evidence that separate neural circuits the nucleus accumbens encode cocaine versus “natural” (water and food) reward. **Journal of Neuroscience**, v. 20, n. 11, p. 4255–4266, 2000.

CASEY, B.; JONES, R. M.; SOMERVILLE, L. H. Braking and Accelerating of the Adolescent Brain. **J Res Adolesc**, v. 21, n. 1, p. 21–33, 2011.

CHUNG, T.; CRESWELL, K. G.; BACHRACH, R.; CLARK, D. B.; MARTIN, C. S. Adolescent Binge Drinking. **Alcohol Research: Current Reviews**, v. 39, p. 5–15, 2015.

CODDINGTON, L. T.; DUDMAN, J. T. The timing of action determines reward prediction signals in identified midbrain dopamine neurons. **Nature Neuroscience**, v. 21, n. 11, p. 1563–1573, 2018.

COLEMAN, L. G.; HE, J.; LEE, J.; STYNER, M.; CREWS, F. T. Adolescent binge drinking alters adult brain neurotransmitter gene expression, behavior, brain regional volumes, and neurochemistry in mice. **Alcohol Clin Exp Res**, v. 35, n. 4, p. 671–688, 2011.

COLEMAN, L. G.; LIU, W.; OGUZ, I.; STYNER, M.; CREWS, F. T. Adolescent binge ethanol treatment alters adult brain regional volumes, cortical extracellular matrix protein and behavioral flexibility. **Pharmacol Biochem Behav**, p. 142–151, 2014.

COLEMAN, L.; LIU, W.; OGUZ, I.; STYNER, M.; CREWS, F. T. Adolescent binge ethanol treatment alters adult brain regional volumes, cortical extracellular matrix protein and behavioral flexibility.. Pharmacology, Biochemistry and Behavior, v. 116, p. 142–151, 2014.

COX, J.; WITTEN, I. B. Striatal circuits for reward learning and decision-making. **Nature Reviews Neuroscience**, v. 20, n. August, 2019.

CREWS, F.; HE, J.; HODGE, C. Adolescent cortical development: A critical period of vulnerability for addiction. **Pharmacology Biochemistry and Behavior**, v. 86, n. 2, p. 189–199, 2007.

CREWS, F. T.; BRAUN, C. J.; HOPLIGHT, B.; SWITZER, R. C.; KNAPP, D. J. Binge ethanol consumption causes differential brain damage in young adolescent rats compared with adult rats. **Alcoholism: Clinical and Experimental Research**, v. 24, n. 11, p. 1712–1723, 2000.

CREWS, F. T.; VETRENO, R. P.; BROADWATER, M. A.; ROBINSON, D. L. Adolescent Alcohol Exposure Persistently Impacts Adult Neurobiology and Behavior. **Pharmacol Rev**, p. 1074–1109, 2016.

DA CUNHA, C.; GOMEZ-A, A.; BLAHA, C. D. The role of the basal ganglia in motivated Behaviour. **Reviews in the Neurosciences**, v. 23, n. 5–6, p. 747–767, 2012.

DA CUNHA, C.; WIETZIKOSKI, E. C.; DOMBROWSKI, P.; et al. Learning processing in the basal ganglia: a mosaic of broken mirrors. **Behavioural brain research**, v. 199, n. 1, p. 157–70, 2009.

DANNENHOFFER, C. A.; KIM, E. U.; SAALFIELD, J.; et al. Oxytocin and vasopressin modulation of social anxiety following adolescent intermittent ethanol exposure. **Psychopharmacology**, v. 235, n. 10, p. 3065–3077, 2019.

DAY, J. J.; ROITMAN, M. F.; WIGHTMAN, R. M.; CARELLI, R. M. Associative learning mediates dynamic shifts in dopamine signaling in the nucleus accumbens. **Nature Neuroscience**, v. 10, n. 8, p. 1020–1028, 2007.

DAY, J. J.; WHEELER, R. A.; ROITMAN, M. F.; CARELLI, R. M. Nucleus accumbens neurons encode Pavlovian approach behaviors: Evidence from an autoshaping paradigm. **European Journal of Neuroscience**, v. 23, n. 5, p. 1341–1351, 2006.

DOBBS, L. K.; KAPLAN, A. R.; LEMOS, J. C.; et al. Dopamine Regulation of Lateral Inhibition between Striatal Neurons Gates the Stimulant Actions of Article Dopamine Regulation of Lateral Inhibition between Striatal Neurons Gates the Stimulant Actions of Cocaine. **Neuron**, v. 90, n. 5, p. 1100–1113, 2016.

DOREMUS-FITZWATER, T. L.; BARRETO, M.; SPEAR, L. P. Age-related differences in impulsivity among adolescent and adult Sprague-Dawley rats. **Behav Neurosci**., v. 126, n. 5, p. 735–741, 2012.

ENGELHARD, B.; FINKELSTEIN, J.; COX, J.; et al. variables in VTA dopamine neurons. **Nature**. Springer US.

ENGELHARD, B.; FINKELSTEIN, J.; COX, J.; et al. Specialized coding of sensory, motor and cognitive variables in VTA dopamine neurons. **Nature**, v. 570, n. 7762, p. 509–513, 2019.

FERNANDEZ, G. M.; SAVAGE, L. M. Adolescent binge ethanol exposure alters specific forebrain cholinergic cell populations and leads to selective functional deficits in the prefrontal cortex. **Neuroscience**, v. 361, p. 129–143, 2017.

FLAGEL, S. B.; AKIL, H.; ROBINSON, T. E. Individual differences in the attribution of incentive salience to reward-related cues: Implications for addiction. **Neuropharmacology**, v. 56, n. Suppl 1, p. 139–148, 2009.

FLAGEL, S. B.; WATSON, S. J.; ROBINSON, T. E.; AKIL, H. Individual differences in the propensity to approach signals vs goals promote different adaptations in the dopamine system of rats. **Psychopharmacology**, v. 191, n. 3, p. 599–607, 2007.

FLORES-BARRERA, E.; VIZCARRA-CHACÓN, B. J.; BARGAS, J.; TAPIA, D.; GALARRAGA, E. Dopaminergic modulation of corticostriatal responses in medium spiny projection neurons from direct and indirect pathways. **Frontiers in Systems Neuroscience**, v. 5, n. MARCH 2011, p. 1–6, 2011.

FOBBS, W. C.; BARISELLI, S.; LICHOLAI, J. A.; et al. Continuous representations of speed by striatal medium spiny neurons. **Journal of Neuroscience**, v. 40, n. 8, p. 1679–1688, 2020.

FÜLLGRABE, M. W.; VENGELIENE, V.; SPANAGEL, R. Influence of age at drinking onset on the alcohol deprivation effect and stress-induced drinking in

female rats. **Pharmacology, Biochemistry and Behavior**, v. 86, p. 320–326, 2007.

GALAJ, E.; GUO, C.; HUANG, D.; RANALDI, R.; MA, Y. Contrasting effects of adolescent and early-adult ethanol exposure on prelimbic cortical pyramidal neurons. **Drug and Alcohol Dependence**, v. 216, n. July, 2020.

GHAHREMANI, D. G.; MONTEROSSO, J.; JENTSCH, J. D.; BILDER, R. M.; POLDRACK, R. A. Neural Components Underlying Behavioral Flexibility in Human Reversal Learning. **Cerebral Cortex**, , n. August, p. 1843–1852, 2010.

GOIS, Z. H. T. D.; TORT, A. B. L. Characterizing Speed Cells in the Rat Hippocampus. **Cell Reports**, 2018.

GOLDSTEIN, R. Z.; VOLKOW, N. D. Dysfunction of the prefrontal cortex in addiction : neuroimaging findings and clinical implications. **Nature Reviews Neuroscience**, v. 12, n. November, 2011. Nature Publishing Group.

GREMEL, C. M.; CHANCEY, J. H.; ATWOOD, B. K.; et al. Endocannabinoid Modulation of Orbitostriatal Circuits Gates Habit Formation. **Neuron**, v. 90, n. 6, p. 1312–1324, 2016. Elsevier Inc.

HARDUNG, S.; EPPLE, R.; JÄCKEL, Z.; et al. A Functional Gradient in the Rodent Prefrontal Cortex Supports Behavioral Inhibition. **Current Biology**, v. 27, n. 4, p. 549–555, 2017.

HILLER-STURMHÖFEL, S.; SPEAR, L. P. Binge Drinking's Effects on the Developing Brain — Animal Models. **Alcohol Research: Current Reviews**, p. 77–86, 2018.

IKEMOTO, S. Dopamine reward circuitry: two projection systems from the ventral midbrain to the nucleus accumbens-olfactory tubercle complex. **Journal of Chemical Information and Modeling**, v. 53, n. 9, p. 1689–1699, 2007.

IKEMOTO, S. Brain reward circuitry beyond the mesolimbic dopamine system: A neurobiological theory. **Neuroscience and Biobehavioral Reviews**, v. 35, n. 2, p. 129–150, 2010. Elsevier Ltd.

IKEMOTO, S.; WISE, R. A. Mapping of chemical trigger zones for reward. **Neuropharmacology**, v. 47, n. 1, p. 190–201, 2004.

JAWORSKA, N.; MACQUEEN, G. Adolescence as a unique developmental period. J **Psychiatry Neurosci**, v. 40, n. 5, p. 291–293, 2015.

JIN, X.; COSTA, R. M. Start/Stop Signals Emerge in Nigrostriatal Circuits during Sequence Learning. **Nature**, v. 466, n. 7305, p. 457–462, 2010.

KALIVAS, P.; VOLKOW, N. D. The Neural Basis of Addiction : A Pathology of Motivation and Choice. **American Journal of Psychiatry**, , n. September 2005, 2005.

KALIVAS, P. W. Addiction as a Pathology in Prefrontal Cortical Regulation of Corticostriatal Habit Circuitry. **Neurotoxicity Research**, v. 14, p. 185–189, 2008.

KALIVAS, P. W.; HU, X. Exciting inhibition in psychostimulant addiction. Trends in **Neurosciences**, v. 29, n. 11, 2006.

KOOB, G. F. Alcoholism : Allostasis and Beyond. **Alcohol Clin Exp Res**, v. 27, n. 2, p. 232–243, 2003.

KOOB, G. F.; VOLKOW, N. D. Neurocircuitry of Addiction. **Neuropsychopharmacology**, v. 35, n. 1, p. 217–238, 2009.

KOOB, G. F.; VOLKOW, N. D. Neurobiology of addiction : a neurocircuitry analysis. **Lancet Psychiatry**, v. 3, n. 8, p. 760–773, 2016.

KRAVITZ, A. V.; TYE, L. D.; KREITZER, A. C. Distinct roles for direct and indirect pathway striatal neurons in reinforcement. **Nature Neuroscience**, v. 15, n. 6, p. 816–818, 2012.

KROPFF, E.; CARMICHAEL, J. E.; MOSER, M. B.; MOSER, E. I. Speed cells in the medial entorhinal cortex. **Nature**, v. 523, n. 7561, p. 419–424, 2015.

LANDIN, J. D.; GORE-LANGTON, J. K.; VARLINSKAYA, E. I.; WERNER, D. F.; SPEAR, L. P. General Anesthetic Exposure During Early Adolescence Persistently Alters Ethanol Responses. **Alcoholism: Clinical and Experimental Research**, v. 44, n. 3, p. 611–619, 2020.

LIU, W.; CREWS, F. T. Adolescent intermittent ethanol exposure enhances ethanol activation of the nucleus accumbens while blunting the prefrontal cortex responses in adult rat. **Neuroscience**, p. 92–108, 2015.

LOVINGER, D. M.; ROBERTO, M. Synaptic Effects Induced by Alcohol David. **Curr Top Behav Neurosci**, , n. November 2011, p. 289–320, 2013.

LUNA, B.; MAREK, S.; LARSEN, B.; TERVO-CLEMMENS, B. An Integrative Model of the Maturation of Cognitive Control. **Annu Rev Neurosci**., v. 08, p. 151–170, 2015.

MADAYAG, A. C.; STRINGFIELD, S. J.; REISSNER, K. J.; BOETTIGER, C. A.; ROBINSON, D. L. Sex and Adolescent Ethanol Exposure Influence Pavlovian Conditioned Approach. **Alcohol Clin Exp Res**., v. 41, n. 4, p. 846–856, 2017.

MCGINTY, V. B.; LARDEUX, S.; TAHA, S. A.; KIM, J. J.; NICOLA, S. M. Invigoration of Reward Seeking by Cue and Proximity Encoding in the Nucleus Accumbens. **Neuron**, v. 78, n. 5, p. 910–922, 2013.

MCKIM, T. H.; SHNITKO, T. A.; ROBINSON, D. L.; BOETTIGER, C. A. Translational Research on Habit and Alcohol. **Current Addiction Reports**, v. 3, n. 1, p. 37–49, 2016.

MIZUMORI, S. J. Y.; PRATT, W. E.; RAGOZZINO, K. E. Function of the nucleus accumbens within the context of the larger striatal system. **Psychobiology**, v. 27, n. 2, p. 214–224, 1999.

MOGENSON, G. J.; JONES, D. L.; YIM, C. Y. From motivation to action: Functional interface between the limbic system and the motor system. **Progress in Neurobiology**, v. 14, n. 2–3, p. 69–97, 1980.

MOHEBI, A.; PETTIBONE, J. R.; HAMID, A. A.; et al. Dissociable dopamine dynamics for learning and motivation. **Nature**, v. 570, n. 7759, p. 65–70, 2019.

MOLINA, P. E.; NELSON, S. Binge Drinking's Effects on the Body. **ALCOHOL RESEARCH: Current R**eviews, v. 39, p. 99–109, 2018.

MORRISON, S. E.; MCGINTY, V. B.; HOFFMANN, J.; NICOLA, S. M. Limbic-motor integration by neural excitations and inhibitions in the nucleus accumbens. **J Neurophysiol**, p. 2549–2567, 2017.

NESTLER, E. J. Is there a common molecular pathway for addiction? **NATURE NEUROSCIENCE,** v. 8, n. 11, 2005.

NESTLER, E. J.; LUSCHER, C. The Molecular Basis of Drug Addiction: Linking Epigenetic to Synaptic and Circuit Mechanisms. **Neuron**, v. 102, n. 1, p. 48–59, 2019.

NICOLA, S. M. The nucleus accumbens as part of a basal ganglia action selection circuit. **Psychopharmacology**, p. 521–550, 2007.

NICOLA, S. M. The flexible approach hypothesis: Unification of effort and cue-responding hypotheses for the role of nucleus accumbens dopamine in the activation of reward-seeking behavior. **Journal of Neuroscience**, v. 30, n. 49, p. 16585–16600, 2010.

NICOLA, S. M.; YUN, I. A.; WAKABAYASHI, K. T.; FIELDS, H. L. Cue-Evoked Firing of Nucleus Accumbens Neurons Encodes Motivational Significance during a Discriminative Stimulus Task. **Journal of Neurophysiology**, v. 91, n. 4, p. 1840–1865, 2004.

NIEOULLON, A. Dopamine and the regulation of cognition and attention. **Progress in Neurobiology,** v. 67, n. 1, p. 53–83, 2002.

NOGUEIRA, R.; ABOLAFIA, J. M.; DRUGOWITSCH, J.; et al. Lateral orbitofrontal cortex anticipates choices and integrates prior with current information. **Nature Communications**, v. 8, 2017.

O'KEEFE, J. Place units in the hippocampus of the freely moving rat. Experimental **Neurology**, v. 51, n. 1, p. 78–109, 1976.

OBESO, J. A; RODRÍGUEZ-OROZ, M. C.; RODRÍGUEZ, M.; et al. Pathophysiology of the basal ganglia in Parkinson's disease. **Trends in neurosciences**, v. 23, n. 10 Suppl, p. S8–S19, 2000.

ORNELAS, L. C.; NOVIER, A.; SKIKE, C. E. VAN; DIAZ-GRANADOS, J. L.; MATTHEWS, D. B. The Effects of Acute Alcohol on Motor Impairments in Adolescent, Adult, and Aged Rats. **Alcohol**, 2014. Elsevier Ltd.

PANIGRAHI, B.; MARTIN, K. A.; LI, Y.; et al. Dopamine Is Required for the Neural Representation and Control of Movement Vigor. **Cell**, p. 1418–1430, 2015.

PASCOLI, V.; HIVER, A.; ZESSEN, R. VAN; et al. Stochastic synaptic plasticity underlying compulsion in a model of addiction. **Nature**, 2018.

PASCUAL, M.; BOIX, J.; FELIPO, VI.; GUERRI, C. Repeated alcohol administration during adolescence causes changes in the mesolimbic dopaminergic and glutamatergic systems and promotes alcohol intake in the adult rat. **Journal of Neurochemistry**, v. 108, p. 920–931, 2009.

QIN, L.; LIU, Y.; HONG, J.-S.; CREWS, F. T. NADPH oxidase and aging drive microglial activation, oxidative stress and dopaminergic neurodegeneration following systemic LPS administration. **Glia**, v. 23, n. 1, p. 1–7, 2013.

REMIJNSE, P. L.; NIELEN, T. M. M. A.; UYLINGS, H. B. M.; VELTMAN, D. J. Neural correlates of a reversal learning task with an affectively neutral baseline : An event-related fMRI study. **NeuroImage**, v. 26, p. 609–618, 2005.

RENTERIA, R.; BALTZ, E. T.; GREMEL, C. M. Chronic alcohol exposure disrupts top-down control over basal ganglia action selection to produce habits. **Nature Communications**, v. 9, n. 1, p. 1–11, 2018.

REYNOLDS, S. M.; ZAHM, D. S. Specificity in the projections of prefrontal and insular cortex to ventral striatopallidum and the extended amygdala. **Journal of Neuroscience**, v. 25, n. 50, p. 11757–11767, 2005.

RICEBERG, J. S.; SHAPIRO, M. L. Orbitofrontal cortex signals expected outcomes with predictive codes when stable contingencies promote the integration of reward history. **Journal of Neuroscience**, v. 37, n. 8, p. 2010–2021, 2017.

RISHER, M.; FLEMING, R. L.; BOUTROS, N.; et al. Long-Term Effects of Chronic Intermittent Ethanol Exposure in Adolescent and Adult Rats : Radial-Arm Maze Performance and Operant Food Reinforced Responding. **PloS one**, v. 8, n. 5, 2013.

ROBINSON, D. L.; CARELLI, R. M. Distinct subsets of nucleus accumbens neurons encode operant responding for ethanol versus water. **Eur J Neurosci**, v. 28, n. 1, p. 1887–1894, 2008.

ROBINSON, T. E.; KENT, C. The neural basis of drug craving: an incetive-sensitization theory of addiction. **Brain Research Reviews**, v. 8, p. 247–291, 1993.

ROITMAN, M. F.; WHEELER, R. A.; CARELLI, R. M.; HILL, C.; CAROLINA, N. Nucleus Accumbens Neurons Are Innately Tuned for Rewarding and Aversive Taste Stimuli , Encode Their Predictors , and Are Linked to Motor Output. **Neuron**, v. 45, p. 587–597, 2005.

ROLLS, E. T. The functions of the orbitofrontal cortex. **Brain and Cognition**, v. 55, n. 1, p. 11–29, 2004.

ROWLAND, D. C.; ROUDI, Y.; MOSER, M. B.; MOSER, E. I. Ten Years of Grid Cells. **Annual Review of Neuroscience**, v. 39, n. February, p. 19–40, 2016.

RUDEBECK, P. H.; RICH, E. L. Orbitofrontal cortex. **Current Biology**, v. 28, n. 18, p. R1083–R1088, 2018.

SADDORIS, M. P.; GALLAGHER, M.; SCHOENBAUM, G. Rapid associative encoding in basolateral amygdala depends on connections with orbitofrontal cortex. **Neuron**, v. 46, n. 2, p. 321–331, 2005.

SADDORIS, M. P.; SUGAM, J. A.; CACCIAPAGLIA, F.; CARELLI, R. M. Rapid dopamine dynamics in the accumbens core and shell: Learning and action. **Frontiers in Bioscience - Elite,** v. 5 E, n. 1, p. 273–288, 2013.

SANCHEZ-ROIGE, S.; PEÑA-OLIVER, Y.; RIPLEY, T. L.; STEPHENS, D. N. Repeated Ethanol Exposure During Early and Late Adolescence: Double Dissociation of Effects on Waiting and Choice Impulsivity. Alco**holism: Clinical and Experimental Research**, v. 38, n. 10, p. 2579–2589, 2014.

SAUNDERS, B. T.; RICHARD, J. M.; MARGOLIS, E. B.; JANAK, P. H. Dopamine neurons create Pavlovian conditioned stimuli with circuit-defined motivational properties. **Nature Neuroscience**, v. 21, n. 8, p. 1072–1083, 2018.

SAUNDERS, B. T.; ROBINSON, T. E. Individual Variation in the Motivational Properties of Cocaine. **Neuropsychopharmacology**, p. 1668–1676, 2011.

SAUNDERS, B. T.; YAGER, L. M.; ROBINSON, T. E. Preclinical Studies Shed Light on Individual Variation in Addiction Vulnerability Fractionating the Impulsivity Construct in Adolescence. **Neuropsychopharmacology**, 2013.

SCHOENBAUM, G.; CHANG, C. Y.; LUCANTONIO, F.; TAKAHASHI, Y. K. Thinking Outside the Box: Orbitofrontal Cortex, Imagination, and How We Can Treat Addiction. **Neuropsychopharmacology**, v. 41, n. 13, p. 2966–2976, 2016.

SCHOENBAUM, G.; ROESCH, M. R.; STALNAKER, T. A. Orbitofrontal cortex, decision-making and drug addiction. **Trends in Neurosciences**, v. 29, n. 2, p. 116–124, 2006.

SCHOENBAUM, G.; SHAHAM, Y. The Role of Orbitofrontal Cortex in Drug Addiction : A Review of Preclinical Studies. **Biological Psychiatry**, 2008.

SCHULTZ, W. Predictive reward signal of dopamine neurons. **Journal of Neurophysiology**, v. 80, n. 1, p. 1–27, 1998.

SCHULTZ, W. Behavioral dopamine signals. **Trends in Neurosciences**, v. 30, n. 5, p. 203–210, 2007.

SCUDDER, S. L.; BAIMEL, C.; MACDONALD, E. E.; CARTER, A. G. Hippocampal-Evoked Feedforward Inhibition in the Nucleus Accumbens. **The Journal of neuroscience**, v. 38, n. 42, p. 9091–9104, 2018.

SESACK, S. R.; GRACE, A. A. Cortico-basal ganglia reward network: Microcircuitry. **Neuropsychopharmacology**, v. 35, n. 1, p. 27–47, 2010.

SEY, N. Y. A.; GÓMEZ-A, A.; MADAYAG, A. C.; BOETTIGER, C. A. Adolescent intermittent ethanol impairs behavioral fl exibility in a rat foraging task in adulthood. **Behavioural Brain Research**, v. 373, n. March, p. 112085, 2019.

SHAN, L.; GALAJ, E.; MA, Y. Y. Nucleus accumbens shell small conductance potassium channels underlie adolescent ethanol exposure-induced anxiety. **Neuropsychopharmacology**, v. 44, n. 11, p. 1886–1895, 2019.

SHNITKO, T. A.; SPEAR, L. P.; ROBINSON, D. L. Adolescent binge-like alcohol alters sensitivity to acute alcohol effects on dopamine release in the nucleus accumbens of adult rats. **Psychopharmacology**, p. 361–371, 2016.

SOMMER, W. H.; COSTA, R. M.; HANSSON, A. C. Dopamine systems adaptation during acquisition and consolidation of a skill. **Frontiers in Integrative Neuroscience**, v. 8, n. November, p. 1–8, 2014.

SPEAR, L. P. Effects of adolescent alcohol consumption on the brain and behaviour. **Nature Reviews Neuroscience**, 2018.

SPOELDER, M.; TSUTSUI, K. T.; LESSCHER, H. M. B.; VANDERSCHUREN, L. J. M. J.; CLARK, J. J. Adolescent Alcohol Exposure Amplifies the Incentive Value of Reward-Predictive Cues Through Potentiation of Phasic Dopamine Signaling. **Neuropsychopharmacology**, v. 40, n. 13, p. 2873–2885, 2015.

SWARTZWELDER, H. S.; ACHESON, S. K.; MILLER, K. M.; et al. Adolescent Intermittent Alcohol Exposure : Deficits in Object Recognition Memory and Forebrain Cholinergic Markers. **PloS one**, p. 1–13, 2015.

TAKAHASHI, Y. K.; ROESCH, M. R.; WILSON, R. C.; et al. Expectancy-related changes in firing of dopamine neurons depend on orbitofrontal cortex. **Nature Neuroscience**, v. 14, n. 12, p. 1590–1597, 2011.

TOMIE, A.; GRIMESA, K. L.; POHORECKY, L. A. Behavioral Characteristics and Neurobiological Substrates Shared by Pavlovian Sign-Tracking and Drug Abuse**. Brain Res Rev**, v. 58, n. 1, p. 121–135, 2008.

TOWNER, T. T.; VARLINSKAYA, E. I. Adolescent Ethanol Exposure: Anxiety-Like Behavioral Alterations, Ethanol Intake, and Sensitivity. **Frontiers in Behavioral Neuroscience**, v. 14, n. March, 2020.

VARLINSKAYA, E. I.; KIM, E. U.; SPEAR, L. P. Chronic intermittent ethanol exposure during adolescence: effects on stress-induced social alterations and social drinking in adulthood. **Brain Research**, v. 1654, p. 145–156, 2017.

VARLINSKAYA, E. I.; SPEAR, L. P. Social consequences of ethanol: Impact of age, stress, and prior history of ethanol exposure. **Physiol Behav**., v. 1, n. 607, p. 145–150, 2015.

VETRENO, R. P.; CREWS, F. T. Adolescent binge ethanol-induced loss of basal forebrain cholinergic neurons and neuroimmune activation are prevented by exercise and indomethacin. **PloS one**, p. 1–22, 2018..

VOLKOW, N. D.; FOWLER, J. S. Addiction , a Disease of Compulsion and Drive : Involvement of the Orbitofrontal Cortex. **Cerebral Cortex Mar** , p. 318–325, 2000.

VOLKOW, N. D.; WANG, G.; TELANG, F.; et al. Cocaine Cues and Dopamine in Dorsal Striatum : Mechanism of Craving in Cocaine Addiction. **The Journal of Neuroscience**, v. 26, n. 24, p. 6583–6588, 2006.

WHEELER, R. A.; TWINING, R. C.; JONES, J. L.; et al. Behavioral and Electrophysiological Indices of Negative Affect Predict Cocaine Self-Administration. **Neuron**, v. 57, n. 5, p. 774–785, 2008.

WHITE, H. R.; MARMORSTEIN, N. R.; CREWS, F. T.; et al. Associations between Heavy Drinking and Changes in Impulsive Behavior among Adolescent Males. **Alcohol Clin Exp Res**, v. 23, n. 1, p. 1–7, 2011. .

WITTER, M. P.; OSTENDORF, R. H.; GROENEWEGEN, H. J. Heterogeneity in the Dorsal Subiculum of the Rat. Distinct Neuronal Zones Project to Different Cortical and Subcortical Targets. **European Journal of Neuroscience**, v. 2, n. 8, p. 718–725, 1990.

YAPO, C.; NAIR, A. G.; CLEMENT, L.; et al. Detection of phasic dopamine by D1 and D2 striatal medium spiny neurons. **Journal of Physiology**, v. 595, n. 24, p. 7451–7475, 2017.

YURGELUN-TODD, D. Emotional and cognitive changes during adolescence. **Current Opinion in Neurobiology,** 2007.

ZEEB, F. D.; FLORESCO, S. B.; WINSTANLEY, C. A. Contributions of the orbitofrontal cortex to impulsive choice: Interactions with basal levels of impulsivity, dopamine signalling, and reward-related cues. **Psychopharmacology**, v. 211, n. 1, p. 87–98, 2010.